From Biogeochemistry to Fisheries and Back Again

Modelling the Upwelling Ecosystem off Peru

Dissertation

ZUR ERLANGUNG DES DOKTORGRADES

DER MATHEMATISCH - NATURWISSENSCHAFTLICHEN FAKULTÄT

DER CHRISTIAN–ALBRECHTS–UNIVERSITÄT ZU KIEL

VORGELEGT VON

MARIANA HILL CRUZ
KIEL, MAI 2022

a mi mamá
por darme alas

Zusammenfassung

Meeresökosysteme sind Top–down (von oben nach unten) und Bottom–up (von unten nach oben) anthropogenen Drücken ausgesetzt. Top–down Drücke betreffen höhere trophische Ebenen (HTL) z.B. die Reduktion der Fischpopulation durch die Fischereiwirtschaft.

Bottom–up Drücke beeinflussen das Ökosystem durch Veränderungen der Umwelt, die wiederum niedere trophische Ebenen (LTL) wie z.B. Plankton betreffen. Obwohl der weltweite Ozean meisten als ein Bottom–up getriebenes Ökosystem angesehen wird, gibt es immer mehr Belege für die Bedeutung von Top–down Treibern. Deshalb sollte der anthropogene Einfluss auf den Ozean mit einem ganzeinheitlichen Ansatz verstanden werden, einschließlich der Bottom-up und der Top–down Treiber über das gesamte Nahrungsnetz. Hierfür sind im besonderen End–to–end Modelle besonders hilfreich. Dieser Art von Modellen simulieren das gesamte Ökosystem vom Plankton, was von Umweltfaktoren beeinflusst wird, bis zu marinen Raubtieren.

Das nördliche Humboldt-Stromsystem (NHCS), im östlichen tropischen Südpazifik (ETSP) gelegen, ist das produktivste östliche Grenzauftriebssystem in Bezug auf den Fischfang. Hohe Primärproduktion und eine schlechte Belüftung von tieferen Wasserschichten erzeugen eine ausgeprägte Sauerstoffminimumzone (OMZ), in der Verlustprozesse von bioverfügbaren Stickstoff stattfinden. Die OMZ ist auch starken zwischenjährlichen Schwankungen ausgesetzt, die aufgrund seiner Nähe zum Äquator insbesondere mit der El Niño Southern Oscillation assoziiert sind.

In diesem Projekt wollte ich verstehen, wie der NHCS von Top–Down- und Bottom–Up-Treibern beeinflusst wird. Ich habe das gesamte Ökosystem des NHCS studiert, von der Biogeochemie bis zu HTL, einschließlich Fischen und Makroinvertebraten. Dazu habe ich zwei End–to–end HTL Modelle angewendet, die jeweils mit einem physikalisch-biogeochemischen Modell gekoppelt sind. In vier Studien bin ich zwei Schlüsselfragen nachgegangen: Wie wirkt sich eine Variabilität in der Biogeochemie

auf die Fischbestände aus? Und wie wirkt sich der Druck durch die Fischerei auf die Fischbestände aus und wie wirkt sich die Variabilität in den Fischbeständen auf die Biogeochemie aus?

Für die erste Studie folgten wir einem Top-Down-Ansatz und untersuchten welche Auswirkungen die Fischvariabilität auf die Planktongemeinschaft des ETSP haben könnten. Wir verwendeten das physikalisch-biogeochemische (bgc) Modell CROCO-BioEBUS. Diese ist speziell zur Simulation des Stickstoffkreislaufs in sauerstoffarmen Umgebungen wie der OMZ des NHCS entwickelt worden. Das Modell hat je zwei Arten von Phyto- und Zooplankton. Wir modifizierten die Sterblichkeit von Zooplankton, um Änderung in der Biomasse von Fischen implizit zu simulieren, die auf das Zooplankton Jagd machen würden. Wir kamen zu dem Schluss, dass großes Zooplankton als Top-Predator im bgc Modell der Hauptgrund für die Variabilität in den Planktongruppen ist. Darüber hinaus führt eine höhere Sterblichkeit von Zooplankton zu einer kürzeren Nahrungskette und zu einer höheren Primärproduktion aufgrund einer impliziten Zunahme von Fisch.

Zweitens haben wir ein End-to-End-Modell des NHCS entwickelt, um die Auswirkungen von interjährlicher Variabilität in Plankton auf die HTL des Systems zu untersuchen. Das Modell besteht aus dem physikalisch-biogeochemischen Modell CROCO-BioEBUS gekoppelt mit dem Multispezies-HTL Modell OSMOSE. Der Aufbau simuliert vier Planktongruppen und neun HTL-Gruppen, darunter kleine pelagische Fische, Makroinvertebraten, eine Bodenfischart und mesopelagischen Fisch. Wir untersuchten die Auswirkungen der interjährlichen versus klimatologischen Variabilität in Plankton auf die HTL. Wir beobachteten einen Einfluss der interjährlichen Variabilität auf Fischbiomassen. Dieser war jedoch gering im Vergleich zu der hohen natürlichen Variabilität von Fischbeständen in den Beobachtungen. Wir beobachteten auch eine starke Sensivität des Modells gegenüber Änderungen des Parameters für die Larvenmortalität von Sardellen. Dies kann ein Anhaltspunkt für die Simulation der starken Variabilität von Sardellen in zukünftigen Studien sein.

Ich untersuchte die Auswirkungen des Fischfangs als Top–down Treiber auf zwei Fischarten mit unterschiedlichen Überlebensstrategien. Eine davon ist die kleine pelagische Fischsardelle, die vor der Küste Perus riesige Fischpopulationen aufbaut und damit die größte Einzelfisch Fischerei der Welt versorgt. Eine andere Fischart ist der peruanische Seehecht, ein größerer Jagdfisch, der besonders beliebt ist als schmackhafter Speisefisch. Ich beobachtete eine höhere Resilienz von Sardellen als Seehecht gegenüber dem erhöhten Fischereidruck. Auf der anderen Seite wirkte sich

ein abnehmender Fischereidruck als positiv auf die Seehechtpopulation aus, die dann dem Fischereifang zur Verfügung stand. Daher könnte die gesamte Fischerei von einer geringeren Fangquote von Seehecht profitieren.

Die letzte Studie dieses Projekts besteht aus einem Vergleich des Multispezies-Modells OSMOSE, das LTL als Antrieb nimmt, mit dem Anderson-Modell, einem einfachen Nahrungsnetzmodell, das die Biomasse mesopelagischer Fische auf Grundlage der Primärproduktion abschätzt. Wir haben die Biomasse mesopelagischer Fische in beiden Modellen sowie dessen zeitliche Variabilität analysiert. Wir beobachteten, dass OSMOSE im Vergleich mit dem Anderson-Modell einen gedämpften saisonalen Zyklus hat, aber aufgrund seines LTL-Antriebs eine stärkere interannuale Variabilität besitzt. Im Gegensatz dazu reagiert die zeitliche Variabilität im Anderson Modell linear, dem Trend der Primärproduktion folgend. Wir kamen zu dem Schluss, dass der Lebenszyklus und die trophische Interaktionen in OSMOSE das Reaktionsverhalten von mesopelagischen Fisch auf Änderungen in der LTL beeinflusst. Studien, die sich mit mesopelagischen Fischen befassen, können von den unterschiedlichen Ansätzen und Informationen profitieren, die von den unterschiedlichen Arten von Modellen bereitgestellt werden. Daher sind vergleichende Studien wie diese sehr wertvoll, um eine weiteren Blickwinkel von dem mesopelagischen Ökosystem zu erhalten.

Diese Arbeit ist ein einzigartig Beitrag zu unserem Verständnis der Treiber der Variabilität im NHCS und des Verhaltens des Ökosystems unter sich ändernden Bedingungen. Ich schloss die Arbeit mit einer Reflexion über mögliche nächste Schritte zur Verbesserung der Repräsentation des Ökosystems im NHCS ab; genauer, wie die starke interjährliche Variabilität im NHCS-Ökosystem besser repräsentiert werden könnte und weitere Schritte zur besseren Modellierung der mesopelagischen Fischgemeinschaften. Schließlich ermöglicht uns das Verständnis der individuellen Top-Down-Effekte und Bottom-up-Treiber in dem komplexen System, die Auswirkungen aller Einflüsse getrennt zu verstehen. Der nächste Schritt wäre es, die Rückkopplungen zwischen beiden Arten von Treibern in einem bidirektional gekoppelten System explizit zu modellieren.

Summary

Marine ecosystems are subjected to increasing top–down and bottom–up anthropogenic pressures. Top–down pressures affect higher trophic levels (HTL) such as fish, for instance, through their active removal by the fishing industry. Bottom–up pressures affect the ecosystem by changing the environment, which in turn affects lower trophic levels (LTL), such as plankton. Although the global ocean has been considered mainly a bottom–up driven ecosystem, there is increasing evidence of the importance of top–down drivers. Therefore, understanding the anthropogenic impacts on the ocean should be done in a holistic perspective, considering both top–down and bottom–up drivers across the food-web. For this, end-to-end models are especially useful. This type of models simulates the whole ecosystem, from plankton, which is affected by environmental drivers, to top predators.

The northern Humboldt Current System (NHCS), located in the eastern tropical South Pacific (ETSP), is the most productive eastern boundary upwelling system in terms of fish catches. High primary production and poor ventilation generate an intense oxygen minimum zone (OMZ) where bio-available nitrogen loss processes take place. It is also subjected to strong interannual variability, especially associated to El Niño Southern Oscillation due to its proximity to the Equator.

In this project, I set out to understand how the NHCS is affected by top–down and bottom–up drivers. I studied the whole ecosystem of the NHCS, from the biogeochemistry to HTL, including fish and macroinvertebrates. To do so, I applied two end-to-end models consisting of a physical–biogeochemical model coupled to two different HTL models. Over four studies, I explored two key questions: How does variability in the biogeochemistry affect fish? And how does fishing pressure affect fish and how does variability in fish affect the biogeochemistry?

For the first study, the co-authors and I followed a top–down perspective, looking at the impact that fish variability may have on the plankton community of the ETSP.

We employed the physical–biogeochemical (bgc) model CROCO-BioEBUS, which is especially designed to simulate the nitrogen cycle in low oxygen environments such as the OMZ of the NHCS. The model has two compartments of phyto- and zooplankton each. We modified the zooplankton mortality to implicitly simulate a change in the biomass of fish which would prey on it. We concluded that large zooplankton, as top predator in the bgc model, is the main driver of the community response. In addition, higher mortality due to an implicit increase in fish promotes a shorter food chain and higher primary production.

Secondly, we employed an end-to-end model of the NHCS to study the impacts of plankton variability on the HTL of the system. The model consists of the physical–biogeochemical model CROCO-BioEBUS coupled with the multispecies HTL model OSMOSE. The set-up simulates four plankton groups, and nine HTL groups including small pelagic fish, macroinvertebrates, a demersal fish species and mesopelagic fish. We explored the impact of interannual versus climatological variability in plankton on HTL. We observed an impact of the interannual variability on fish biomasses. However, this is small compared to the high variability of fish in observations. We also observed a strong sensitivity of the model to larval mortality of anchovy. This may be a clue for simulating the strong variability in anchovies in future studies.

In the next study, I explored the top–down impact of fishing on two fish species with contrasting life strategies. One is the small pelagic fish anchovy, which builds up massive congregations off the coast of Peru and is the biggest single-species fishery of the planet. The other one is the Peruvian hake, a larger demersal predatory fish which is valued for direct human consumption. I observed a higher resilience of anchovy to increased fishing pressure than hake. On the other hand, decreasing fishing pressure has a positive impact on the amount of hake available for harvesting. Therefore, the whole hake fishery could benefit from lower fishing rates.

The last study of this project consists of a comparison of the multispecies model OS-MOSE, which takes LTL as forcing, with the Anderson model, which is a simple food-web model that estimates the biomass of mesopelagic fish based on primary production. We compared the biomass of mesopelagic fish in both models as well as the temporal variability. We observed that OSMOSE has a muted seasonal cycle compared with the Anderson model and with its LTL forcing, but a stronger interannual variability. In contrast, the temporal variability in Anderson responds in a linear way, following the trend of the primary production input. We concluded that the life-cycle and trophic interactions in OSMOSE affect the response of simulated mesopelagic fish

to changes in LTL. Studies addressing mesopelagic fish may benefit from the different approaches and information provided by each type of model. Hence, comparative studies like this one are valuable to provide a broader perspective on the mesopelagic ecosystem.

This thesis is an original contribution to our understanding of the drivers of variability in the NHCS and the behaviour of the ecosystem under changing conditions. I concluded the thesis with a reflection on possible next steps for improving the representation of the ecosystem in the NHCS; in concrete, how the representation of the strong interannual variability in the NHCS ecosystem could be improved and further steps for modelling the mesopelagic community. Finally, exploring separate top–down and bottom–up drivers in the system allows us to understand the impact of each driver separately. The next step is to explore the feedbacks between both kinds of drivers in a two-way coupled modelling system.

Acknowledgements

Contents

General introduction

1.1 Motivation and objectives
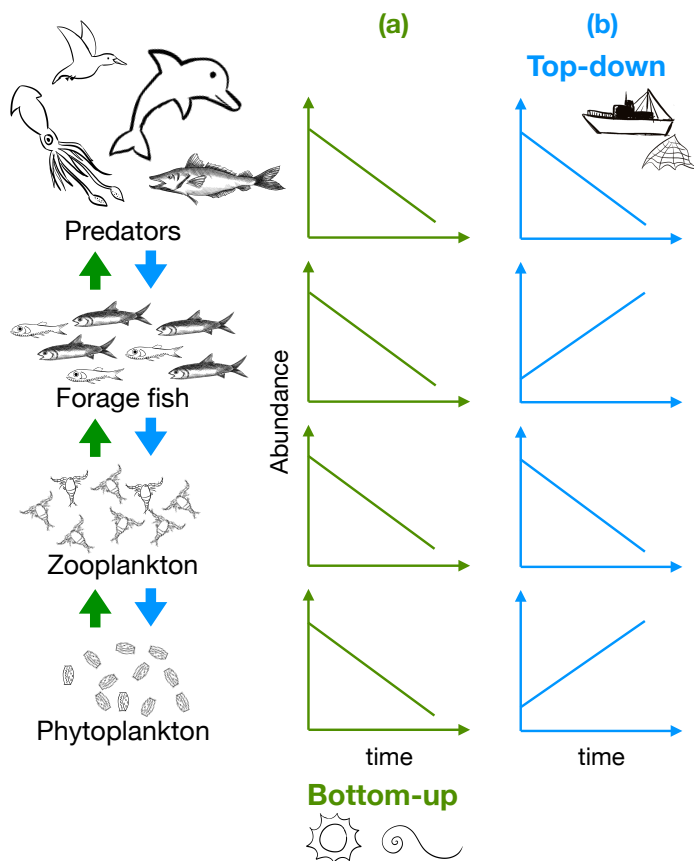
Figure 1.1. Sample marine trophic chain response to bottom–up (environmental change, a) and top–down (harvesting, b) pressures. Note that, in the bottom–up case (a), predators follow the same abundance change in time as their prey and, in the top–down case (b), prey respond inversely to predators abundance change. Modified and adapted from Cury, Shannon, and Shin (2003).

The ocean ecosystems are subjected to increasing anthropogenic pressures, presented in both top–down and bottom–up directions (Figure 1.1). Bottom–up anthropogenic pressures affect the ecosystem by changing the environment. Prominent pressures of this type are climate change and ocean acidification impacts on the ocean due to release of fossil fuels (Behrenfeld et al., 2006; Doney et al., 2009; Kwiatkowski et al., 2020). In coastal systems, cultural eutrophication due to nutrient discharge into water bodies is also a major problem that, among other impacts, affects the food-webs and contributes to ocean acidification and oxygen loss (Smith and Schindler, 2009; Cai et al., 2011). Anthropogenic pressures can also act in a top–down manner through the active removal of marine organisms (Baum and Worm,

2009). While overfishing is a primary concern due the potential collapse of the targeted species (e.g., Kirby, 2004), scientists have now realised the impact that removal of single species can have on other trophic levels (Worm and Myers, 2003; Scheffer, Carpenter, and Young, 2005; Möllmann et al., 2008; Baum and Worm, 2009).

Understanding the development of the marine ecosystems during the Anthropocene requires careful exploration of both top–down and bottom–up drivers, and their impact on the marine ecosystems as a whole, from the environmental conditions (e.i., ocean circulation and physical conditions such as temperature) to the top predators (e.g., large fish). The study of the oceans has traditionally focused on either the physical–biogeochemical components, exploring fluxes of elements, such as carbon and nitrogen, or on the fisheries management field (Travers et al., 2007). While in a global scale, the ocean as a whole has been considered a bottom–up driven system, there is increasing evidence of the importance of top–down drivers (Lynam et al., 2017). Hence, in the last two decades, the concept of end-to-end models has gained popularity as a tool to understand the marine ecosystems, from the environmental forcings on lower trophic levels (LTL), or plankton, to higher trophic levels (HTL) such as fish and top predators, and even the human component (see Travers et al., 2007; Fulton, 2010; Tittensor et al., 2018, for reviews).

For this doctoral project, I set out to study the response of marine ecosystems to bottom–up and top–down drivers, with a special interest in the interactions between HTL, mainly fishes, and the environment. I focused on the northern Humboldt Current System (NHCS) located in the eastern tropical South Pacific (ETSP) off the coast of Peru due to its importance as a hotspot of fish production and of nitrogen loss processes (see Section 1.2). With this project, I aimed at addressing two key questions regarding 1. bottom–up and 2. top–down drivers:

1. How does variability in the biogeochemistry affect fish?

2. How does fishing pressure affect fish and how does variability in fish affect the biogeochemistry?

To answer these questions, I employed a series of dynamic models, namely a single physical–biogeochemical model and two end-to-end ecosystem models. This is an original research project that advances the understanding of the NHCS as a bottom–up and top–down driven coastal marine ecosystem. In addition, it provides insights on the state of the art of the dynamic modelling of this ecosystem and opportunities for future research and model development.

1.2 The northern Humboldt Current System

1.2.1 Physics and biogeochemistry

The northern Humboldt Current System (NHCS) is located in the eastern tropical South Pacific (ETSP) Ocean off the coast of Peru and northern Chile in South America (Figure 1.2). It is composed of the Peru Coastal Current that flows near the coast northwards and the Peru Current flowing offshore also northwards. Between these two currents, the southward Peru–Chile Countercurrent is located. Finally, the Peru–Chile Undercurrent flows sowthawrds along the shelf (see Karstensen and Ulloa, 2009). Steady winds blowing equatorward generate Ekman transport and divergence that result in upwelling of waters deeper

Figure 1.2. Main currents of the northern Humboldt Current System. Modified and adapted from Karstensen and Ulloa (2009).

than 150 m (see Karstensen and Ulloa, 2009). The upwelled waters are rich in nutrients and have a low N:P ratio that supports high primary production of large cells such as diatoms (Franz et al., 2012). The physics and bigoeochemistry in the transition between nutrient–rich coastal waters and the oligotrophic region offshore are affected by mesoscale and sub-mesoscale processes including eddies, filaments and fronts (Rossi et al., 2009; Thomsen et al., 2016).

Underneath the productive euphotic zone, sinking organic matter is remineralised generating, in combination with a poor ventilation, an intense oxygen minimum zone (OMZ) (Karstensen, Stramma, and Visbeck, 2008). Denitrification and anammox occurring in the OMZ are responsible for the loss of bioavailable nitrogen to N_2 and the greenhouse gas N_2O (Hamersley et al., 2007; Farías et al., 2009; Kalvelage et al., 2013).

Therefore, the NHCS plays an important role not only in the global food security (see next section) but also in the nitrogen cycle.

Primary production is not only spatially (see Sect. 1.2.2) but also temporally dynamic. Although the wind strength and upwelling intensity increase in austral winter, the primary production peaks in summer (Bakun and Nelson, 1991; Echevin et al., 2008; Messié and Chavez, 2015). Modelling evidence suggests that this seasonal paradox is due to a shoaling of the mix layer depth in summer which concentrates phytoplankton in the euphotic zone and improves light conditions (Echevin et al., 2008; Xue et al., 2021).

The NHCS is affected by strong interannual variability. This includes interdecadal periods of cold and warm water named "La Vieja" and "El Viejo", respectively (Chavez et al., 2003), as well as the two-to-seven-years cycle of El Niño–Southern Oscillation (ENSO) due to its proximity to the Equator (Penven et al., 2005). During La Niña conditions, the thermocline becomes shallower and sea surface temperature (SST) decreases (see Tarazona and Arntz, 2001; Fiedler, 2002). El Niño conditions are characterised by a deeper thermocline, higher SST and less nutrients at the surface, resulting in lower primary production (see Tarazona and Arntz, 2001; Fiedler, 2002). Strong El Niño events have been associated with fisheries collapses and population declines of seabirds and marine mammals (Barber and Chavez, 1983; Duffy, 1983; Fiedler, 2002; Alheit and Niquen, 2004), evidencing their strong bottom–up impact on the system.

1.2.2 The marine ecosystem

The nutrient-rich coastal waters of the NHCS support a proliferating ecosystem with complex trophic interactions that are affected by both bottom–up and top–down pressures. At the bottom of the trophic chain, the phytoplankton community is rich in large diatoms near the coast (Franz et al., 2012). These are replaced by smaller phytoplankton offshore (Franz et al., 2012). The most abundant copepod species on the continental shelf are *Acartia tonsa* and *Centropages brachiatus* (Ayón et al., 2008a). Squat lobster (*Pleuroncodes monodon*) has been increasingly found over the continental shelf since the mid 1990s (Ayón et al., 2008a; Gutiérrez et al., 2008). This commonly benthic (living at the bottom of the water column) species performs migrations to the pelagic environment at the surface, possibly to avoid the intense OMZ present off Peru (Gutiérrez et al., 2008; Kiko et al., 2015). It shares a similar ecological niche as the commercially exploited anchovies (see below), being preys for larger animals such as seabirds and

predatory fishes (Gutiérrez et al., 2008). Euphausiids are considered the most important prey for anchovies (Espinoza and Bertrand, 2008). The main euphausiid species in the NHCS is *Euphausia mucronata* (Antezana, 2010). This species performs vertical migrations to the OMZ and forages at the surface during night (Antezana, 2010; Kiko and Hauss, 2019).

Vertically migrating mesopelagic fish are dominated by the Panama light fish *Vinciguerria lucetia* (Cornejo Urbina and Koppelmann, 2006). Light fish abundance off Peru has been estimated between 2.9 and 11.1 Mt (Castillo Valderrama et al., 1998; Castillo Valderrama et al., 1999). The Humboldt squid, also known as jumbo flying squid (*Dosidicus gigas*), preys mainly on mesopelagic fish (Markaida and Sosa-Nishizaki, 2003). However, it has also been considered an important predator for Peruvian and Chilean hake (Alarcón-Muñoz, Cubillos, and Gatica, 2008; Guevara-Carrasco and Lleonart, 2008). This is the main invertebrate fishery in Peru (see PRODUCE, 2013).

The NHCS marine ecosystem is dominated by a few species of small pelagic fish with very high biomass. Despite primary production in the NHCS being comparable to other eastern boundary upwelling systems, its fish production is ten times higher (Chavez et al., 2008). This has been associated with a high trophic transfer efficiency and strong interannual variability (see Sect. 1.2.1) that maintains the system in a successional stage that favours small fast-growing fish rather than their predators (Chavez and Messié, 2009). Currently, the most abundant species is the Peruvian anchovy (*Engraulis ringens*) which in the 1960s became the biggest single-species fishery of the planet (Ñiquen Carranza et al., 2000). In 1971, anchovy landings reached a record of 12.3 Mt (Aranda, 2009). However, this species varies strongly every few years and the NHCS has presented periods dominated by anchovies and others where Pacific sardines (*Sardinops sagax*) were more abundant (Chavez et al., 2003; Alheit and Niquen, 2004). Anchovy landings decreased throughout the 1970s and sardines became more abundant. Since the mid 1980s, sardines started to decline and anchovies to increase again until anchovy dominance was reached in the 1990s (Chavez et al., 2003; Alheit and Niquen, 2004). Sardines have been associated with warm periods and anchovies with cold periods in the interannual record (Chavez et al., 2003). The chub mackerel (*Scomber japonicus*) and the jack mackerel (*Trachurus murphyi*) are other small pelagic fishes of commercial importance in Peru (see PRODUCE, 2013). The bonito (*Sarda chiliensis chiliensis*) is a larger species found off the coast of Peru and Chile (Yoshida, 1980). The dolphinfish (*Coryphaena hippurus*) is a predatory pelagic fish that has a global distribution in tropical and sub-tropical waters (Maguire et al., 2006). It is an artisanal fishery in Peru (Torrejón-Magallanes, Grados, and Lau-Medrano, 2019).

5

In the case of demersal species, the Peruvian hake (*Merluccius gayi*) is amongst the most important demersal fisheries in Peru (see PRODUCE, 2013). It is industrially exploited since the 1960s (Guevara-Carrasco and Lleonart, 2008). In 2002, a moratorium on the hake fishery was implemented for 20 months due to the low abundance of hake (Guevara-Carrasco and Lleonart, 2008).

On top of the food chain lie the seabirds and marine mammals. Seabirds include the Humboldt penguin (*Spheniscus humboldti*) and a range of tubenosed birds including the giant petrel (*Macronectes giganteus*) and the Galapagos albatross (*Phoebastria irrorata*), among others (Sueyoshi et al., 2016). There are also the "guano birds", composed mainly by the Guanay cormorant (*Phalacrocorax bougainvillii*), Peruvian booby (*Sula variegata*) and Peruvian pelican (*Pelecanus thagus*) (Tovar, Guillen, and Nakama, 1987; Duffy, 1994). In the XIX century, large scale extraction of guano for exportation negatively affected the population of birds (Tovar, Guillen, and Nakama, 1987). Then, in 1909, the Guano Administration Company was created to regulate the exploitation of this resource (Tovar, Guillen, and Nakama, 1987; Duffy, 1994). Since 1950, the growing fishery of anchovies, prey of seabirds, along with their collapses during El Niño events, was correlated with a decline in guano birds (Tovar, Guillen, and Nakama, 1987; Duffy, 1994).

Marine mammals off Peru include cetaceans, pinnipeds and the marine otter (*Lutra felina*) (Majluf and Reyes, 1989). Species of pinnipeds include the South American (*Arctocephalus australis*) and Juan Fernandez (*Arctocephalus philippii*) fur seals, and the South American sea lion (*Otaria byronia*). More than 20 genera of cetaceans have been found off Peru (Arias-Schreiber, 1996). Large cetacean species include baleen whales such as the blue whale (*Balaenoptera musculus*), fin whale (*Balaenoptera physalus*), Byrde's whale (*Balaenoptera edeni*), sei whale (*Balaenoptera boreali*) and humpback whale (*Megaptera novaeangliae*) (Majluf and Reyes, 1989). In the case of toothed cetaceans, killers whales (*Orcinus orca*), sperm whales (*Physeter macrocephalus*), short-finned pilot whale (*Globicephala macrorhynchus*) and beaked whales have also been reported off Peru (Majluf and Reyes, 1989; Reyes, Mead, and Waerebeek, 1991). Several species of dolphins and porpoises inhabit the coastal waters. These include common dolphin (*Delphinus delphis*) and bottlenose dolphin (*Tursiops truncatus*), among others (Majluf and Reyes, 1989). Whale–watching is a relatively new but growing industry in Peru (Guidino et al., 2020). On the contrary, whaling was stopped in Peru by 1985 (Majluf and Reyes, 1989) and small cetaceans are protected since 1990 (Reyes, Mead, and Waerebeek, 1991). However, intentional and non-intentional (e.g., entanglement in nets) capture of pinnipeds and small cetaceans continues (Reyes, Mead, and Waerebeek, 1991; Pizarro, 2015).

In summary, the NHCS is a highly productive region of the Pacific Ocean characterised by a high trophic transfer efficiency, higher fish yield than any other eastern boundary upwelling systems, a shallow and intense OMZ and a strong interannual variability. The marine ecosystem is composed by huge amounts of small pelagic fish that feed a range of apex predators including marine mammals and seabirds. Evidence shows that most components of the ecosystem have been affected to some extent by top–down anthropogenic pressure or by bottom–up environmental pressure.

1.3   End-to-end marine ecosystem models

End-to-end models are dynamic models that represent the ecosystem from the plankton and environmental drivers to the higher trophic levels (HTL), such as fish, marine mammals and macro-invertebrates, and usually including several species or functional groups. These are valuable tools for simulating marine ecosystems and aiding ecosystem based fisheries management (Pikitch et al., 2004). There is a rich range of end-to-end models in the literature (see Fulton, 2010; Tittensor et al., 2018, for reviews). Some of these include lower trophic levels (LTL) (e.g., Field, Francis, and Aydin, 2006) and even environmental components (e.g., Fulton et al., 2011) as part of a single modelling package. There are also combined models where a HTL model is coupled to an independent physical–biogeochemical model that provides plankton biomass or primary production as forcing. These can be coupled one-way (e.g., Christensen et al., 2015) or two-way (e.g., Travers-Trolet et al., 2014). I used this type of modelling system for my thesis. Therefore, the components of typical combined models are presented in the remaining of this section.

1.3.1   Physical–biogeochemical sub-models

Physical–biogeochemical models simulate LTL, or plankton, in the modelling system. The physical component is an ocean circulation model that describes the movement of water between grid-cells by solving physical equations that describe momentum, mass and energy conservation. Because there are no analytical solutions, numerical methods are used to solve the equations. Biogeochemical models (bgc) usually simulate nutrients, organic matter and living organisms including phyto- and zooplankton based on empirical functions, such as the nutrient uptake by phytoplankton. Plankton organisms are assumed to be transported by the water advection rather than actively

swimming on their own. The currency of biogeochemical models may be based on one or many elements, depending on which element is considered to be the major limiting nutrient in the system. Typically, such limiting element is nitrogen (e.g., Gutknecht et al., 2013a) and any inferences derived from these models with regards to other elements are based on standard ratios such as Redfield. Some other models (e.g., Keller, Oschlies, and Eby, 2012; Stock, Dunne, and John, 2014; Aumont et al., 2015; Kriest and Oschlies, 2015) include additional elements, like phosphorus, iron and silicate, to explicitly simulate their potential limiting effects.

Physical-biogeochemical models can be regional or global. Global models have typical horizontal resolutions around 1° (e.g, Kriest and Oschlies, 2015). These can be integrated over hundreds of years to make long-term predictions. These models have been used by the Intergovernmental Panel on Climate Change (IPCC) to make climate projections (IPCC, 2013). Regional models cover only a small part of the ocean, with the advantage that they can have a higher resolution in order to represent smaller scale spatial variability such as mesoscale and sub-mesoscale processes with coastal upwelling and narrow shelves (e.g., Penven et al., 2001; José, Dietze, and Oschlies, 2017). These models are forced at the boundaries and at the surface with, either data derived from satellites and ocean physical and biogeochemical conditions based on observations, or with another model of coarser resolution in a nesting procedure (e.g., José, Dietze, and Oschlies, 2017). Due to their high computing demand, usually these models are integrated for a shorter period of time such as a few decades.

Models can be used, for instance, for realistic simulations over the past years to decades, so called hindcasts (e.g., José et al., 2019), or to simulate a climatology (e.g., José, Dietze, and Oschlies, 2017). A hindcast tends to simulate both seasonal and interannual variability while a climatology aims at reproducing the daily or monthly conditions averaged for several years. Hence, interannual variability is removed in climatological simulations. Sensitivity studies consist of slightly changing the model set-up to test how it responds, for instance, to changes in boundary conditions, surface forcing, or to changes in the model parameters (e.g., Travers-Trolet et al., 2014). In this project, I worked with hindcast as well climatological simulations using a regional bgc model which is described in Sect. 1.4. In Chapter 3, the differences between forcing a HTL model with a bgc climatology or hindcast are explored. In Chapter 2, the sensitivity of a bgc model to zooplankton mortality is evaluated in a climatological set-up.

1.3.2 Higher trophic levels sub-models

In recent years, fisheries management has started to transition from a single-species-based approach to an ecosystem based fisheries management (see Marasco et al., 2007). Multispecies models are necessary for understanding the impacts of fishing not only on the target species but on the surrounding ecosystem (Pikitch et al., 2004). Hence, most fish models focus on fish groups of commercial importance and coastal regions (e.g., Megrey et al., 2007; Halouani et al., 2016; Xing et al., 2017). Some studies have attempted to model large marine regions or the whole globe by integrating fishes into large groups such as size classes (e.g., Watson, Stock, and Sarmiento, 2015; Carozza, Bianchi, and Galbraith, 2016), and focusing on a few targeted species (e.g., Lehodey, Chai, and Hampton, 2003; Maury, 2010).

The multispecies models that are coupled to physical–biogeochemical models usually do this through feeding HTL with plankton, which is provided by the bgc model. Examples of HTL models that have plankton as input include the individual-based models (Shin and Cury, 2001; Rose et al., 2015). These kinds of models simulate groups of fish with identical characteristics denominated "super-individuals" in the ecosystem. Fiechter et al. (2016) also included sea lions as single individuals in their model. A few models do not perform the coupling through plankton food but some other biogeochemical variable. For instance, the simple food-web model by Anderson et al. (2019) uses primary production as forcing and includes the representation of zooplankton groups already in the HTL model component. This has the advantage that it can be derived directly from satellite observations rather than a bgc model. More details on this specific model, as well as the individual-based model OSMOSE, will be provided in the following section as these are the primary tools utilised in this project.

1.4 Modelling set-ups

In this project, I used the physical–biogechemical model CROCO–BioEBUS as stand-alone (Chapter 2) and also coupled with two different higher trophic level models: OSMOSE (Chapters 3 to 4) and Anderson (Chapter 5). An overview of the full coupling system is provided in Fig. 1.3. In the following sections, I explain each component of the system.

Model system CROCO-BioEBUS-OSMOSE

OSMOSE/Anderson

Higher trophic levels:
Fish and large invertebrates
Shin & Cury, 2001
http://www.osmose-model.org/
Anderson et al., 2019

mortality   **food**

BioEBUS

Biogeochemistry:
Nutrients (e.g., nitrate), oxygen,
organic nitrogen (e.g., detritus)
and lower trophic levels
(phytoplankton and zooplankton)
Gutknecht et al., 2013

transport & mixing
temperature
light

CROCO (ROMS)

Ocean physics and circulation
Shchepetkin & McWilliams, 2005
http://www.croco-ocean.org/

upwelling

Figure 1.3. End-to-end modelling system with the physical (CROCO), biogeochemical (BioEBUS) and higher trophic levels (OSMOSE and Anderson) components, as well as the interactions between them. BioEBUS forces OSMOSE and Anderson in a one-way fashion (blue arrow) in the set-ups used for Chapters 3 to 5. Note that the two-way coupling fashion of forcing BioEBUS with mortality derived form higher trophic levels was not implemented in this project. However, in Chapter 2, an implicit impact of higher trophic levels on BioEBUS was implemented by modifying the mortality of zooplankton. Therefore, the mortality forcing (red arrow) was also included in the diagram. Also note that, while the physical component (CROCO) mostly drives the biogeochemistry (BioEBUS) in a one-way fashion (grey arrow), high plankton abundance has an impact on light limitation through shading.

1.4.1 CROCO-BioEBUS

The physical-biogeochemical component of this project is the Coastal and Regional Ocean COmmunity model (CROCO, formerly ROMS; Shchepetkin and McWilliams, 2005) coupled online to the Biogeochemical model developed for Eastern Boundary Upwelling Systems (BioEBUS; Gutknecht et al., 2013a). CROCO is a free–surface, terrain–following coordinate regional physical ocean model (Shchepetkin and McWilliams, 2005). Two set-ups of the model were used across the different chapters of this project. First, we used a climatological version when the name was still ROMS–BioEBUS and, secondly, an interannual set-up of CROCO–BioEBUS from 1990 to 2010. The domains span from 18° N to 40° S and 69° to 120° W (Chapter 2), and from 33° S to 10° N and 118° to 69° W (Chapters 3 to 5). Both domains have 32 sigma layers and are divided in a horizontal grid of $\frac{1}{12}$° resolution. CROCO describes the mixing and transport of chemical tracers (C_i) between each of the grid cells. These are represented by advection ($-\nabla \cdot (uC_i)$ where u is the velocity vector), horizontal diffusion ($K_h \nabla^2 C_i$ with K_h as the horizontal diffusion coefficient) and vertical diffusion ($\frac{\partial}{\partial z}(K_z \frac{\partial C_i}{\partial z})$ with the vertical diffusion coefficient K_z):

$$\frac{\partial C_i}{\partial t} = -\nabla \cdot (uC_i) + K_h \nabla^2 C_i + \frac{\partial}{\partial z}(K_z \frac{\partial C_i}{\partial z}) + SMS(C_i) \tag{1.1}$$

In addition, the sources minus sinks due to biological activity term (SMS) is the result of reactions that change biogeochemical tracers, such as nutrient uptake that is associated with growth of phytoplankton.

BioEBUS is a nitrogen–based NPZD–type model that represents the biogeochemistry of a system up to zooplankton. It represents oxygen dependent processes which is useful for the NHCS because it can simulate the nitrogen losses that occur in the OMZ. It has a nitrogen currency and simulates two size classes of detritus, zooplankton and phytoplankton, as well as three nutrients: nitrate, nitrite and ammonium, and dissolved organic nitrogen (DON; Figure 1.4).

Phytoplankton cells perform primary production and are grazed upon by zooplankton. In addition to grazing losses, phytoplankton cells are subjected to a linear mortality. On the other hand, zooplankton losses are represented by a linear and a quadratic mortality term ($\gamma_Z \cdot [Z]$ and $\mu_Z \cdot [Z]^2$, where γ_Z and μ_Z are mortality rates). The linear term represents metabolic losses while the quadratic term includes the predation by higher trophic levels which is more dynamic.

Although there is not a size parameter in BioEBUS, the two size classes of plankton are meant to simulate communities of different sizes. Small phytoplankton represents cells that survive in low nutrient conditions and are smaller than 2 μm such as flagellates, while large phytoplankton represents larger cells such as diatoms. Small zooplankton are organisms roughly between 20 and 200 μm such as ciliates and large zooplankton lies between 0.2 and 2 mm such as copepods. More details about BioEBUS are available in Gutknecht et al. (2013a).
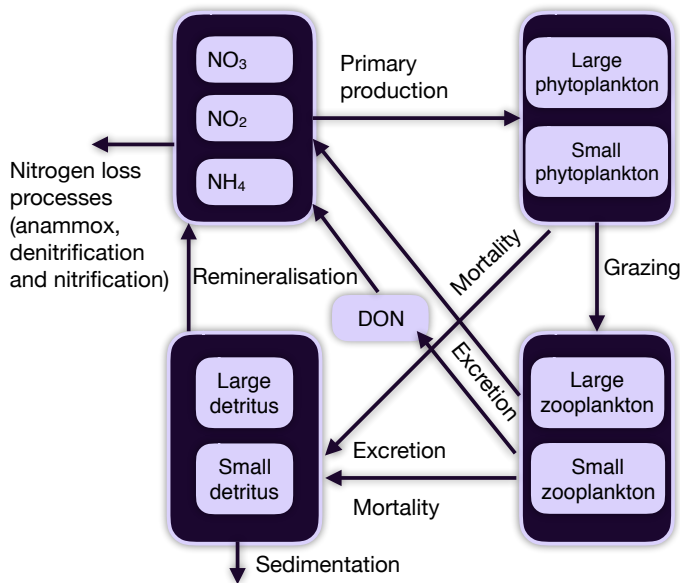
Figure 1.4. Main nitrogen fluxes among the prognostic variables in the BioEBUS model. Modified and adapted from Gutknecht et al. (2013a)

In a first study, the ROMS–BioEBUS model was applied to understand the changes in the biogeochemistry that may arise from a top–down pressure by the fish. This was implicitly simulated by changing the mortality of zooplankton (Chapter 2). CROCO–BioEBUS was also coupled to two HTL models to explore the interactions with fish and other marine organisms, particularly to understand bottom–up drivers of the bgc model on the fish (Chapter 3 and 5). A more detailed explanation of CROCO(ROMS)–BioEBUS, including the boundary conditions and model evaluation, is provided in Chapters 2 and 3.

1.4.2 OSMOSE

The Object-oriented Simulator of Marine Ecosystems (OSMOSE) is an individual-based model developed in the early 2000s by Shin and Cury (2001, 2004). It simulates schools of fish that move randomly over a grid, feed, grow and reproduce. Predation is possible when a school overlaps spatially with a prey that falls within certain predator–prey minimum and maximum size ratios. The life cycle of the fish, from eggs until adults, is simulated (Figure 1.5). Therefore, each life stage of fish can prey on different organisms depending on their specific size, regardless of the species. Furthermore, this allows the trophic chain to evolve in a mechanistic way rather than

being set *a priori*.

In the version of OSMOSE used for this project, the environmental limitations on fish are driven implicitly by how environmental factors affect plankton availability. Plankton groups such as small and large phyto- and zooplankton are extracted from the output of BioEBUS. Since CROCO–BioEBUS is a tri-dimensional model and OSMOSE a bi-dimensional model –missing a the depth dimension–, the plankton has to be vertically integrated to obtain horizontal fields. These are provided as forcing for OSMOSE and size ranges are assigned to each plankton group. Fish whose prey range

Figure 1.5. Representation of a school of fish in OSMOSE. Every school has an age, size and number of fish attribute. As the simulation progresses, fish in the school grow up. Adult fish reproduce and generate new schools of eggs which become larvae. Schools consume food and are subjected to several sources of mortality. They move randomly on every time-step over the region defined by distribution maps.

covers certain plankton group forages on it. More information on the plankton–fish link in OSMOSE is provided by Travers and Shin (2010). The OSMOSE domain used in this project spans from 90° to 73° W and from 20° S to 6° N. It has a $\frac{1}{6}$° resolution; the plankton from BioEBUS was cropped and regridded to match the grid of OSMOSE.

The spatial distribution of fish schools in OSMOSE is constrained by distribution maps. The maps used in this project were developed using habitat niche models by Oliveros-Ramos (2014). These statistical models relate the occurrence of fish with oceanographic data, including sea surface temperature, surface water masses, depth of the oxycline and surface chlorophyll, that were obtained from remote sensing and *in situ* observations, as well as output of a physical-biogeochemical model. More details are available in Oliveros-Ramos (2014). At the beginning of every season, the fish schools of every species are randomly distributed over their respective, species–specific, distribution map. Each distribution map prescribes the probability of a fish school to fall on each of the grid cells of the map with the sum of all grid cells equalling one.

OSMOSE is calibrated using an evolutionary algorithm. This type of algorithm is inspired on the evolution of species through mutations and natural selection. This con-

sists of running the model several times with different sets of parameters, which in the real world would be "genotypes". The sets for parameters for which the model better matches observations (the "better genotypes") are selected. The parameters of these sets are then recombined (the best "genes" are passed to the next generation by "reproduction") and a few new parameters added ("mutations"). In this way, the "genotypes" or sets of parameters "evolve" until the algorithm ("natural selection") produces a group of "genotypes" that generate the model output (or "fenotype") that has the best match to observations (that are "well adapted"). For this project, I used the package *calibrar* (Oliveros-Ramos, 2014; Oliveros-Ramos and Shin, 2016) to calibrate OSMOSE. A detailed explanation of the OSMOSE configuration, as well as its calibration and evaluation is provided in Chapter 3.

The CROCO–BioEBUS–OSMOSE system was used in Chapter 3 to assess the bottom–up effect of variability in plankton on fish. In addition, OSMOSE has the capability of simulating explicit fishing pressure as a mortality term for the fish and to calculate landings. Therefore, I employed the same system in Chapter 4 to explore the top–down impact of different fishing pressures on two species of commercial importance.

1.4.3 Anderson

The second HTL model that I used in this project was developed by Anderson et al. (2019). This model represents the community of mesopelagic fish taking primary production as forcing. For this project, the primary production was obtained from CROCO–BioEBUS. It then assumes that the production can be exported to detritus or consumed by zooplankton in the surface of the ocean. Some zooplankton live in the epipelagic region permanently and graze all the time. Other zooplankton can live permanently in the deep water and feed on sinking detritus and other types of zooplankton perform vertical migrations and feed at the surface at night. All these groups are then consumed by carnivorous zooplankton such as amphipods (see Anderson et al., 2019). Finally all previously mentioned zooplankton groups are eaten by mesopelagic fish. Just as with the zooplankton, mesopelagic fish is also divided into migrating and non-migrating fish. Migrating fish can feed in the epipelagic layer during the night and non-migrating feed exclusively in the deep water. A linear mortality term parameterises all losses of mesopelagic fish, from metabolic losses to predation. All components of the model are provided in Fig. 1.6.
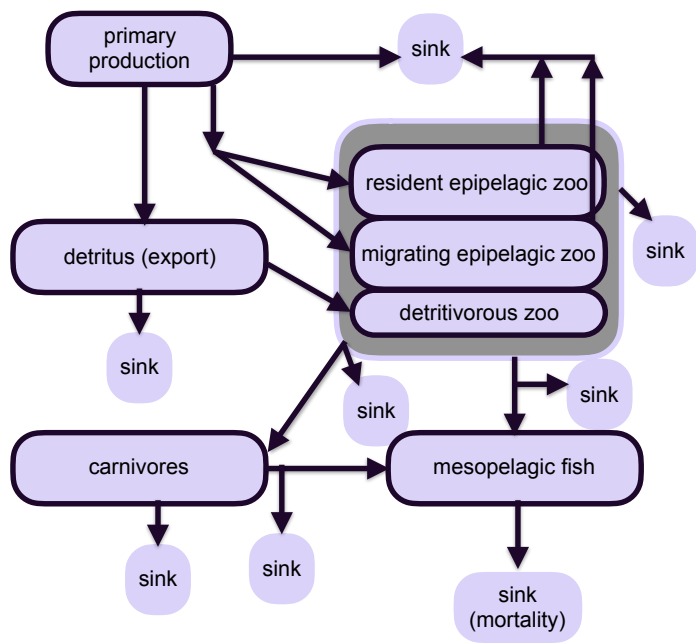
Figure 1.6. Components of the Anderson model and biomass fluxes amongst them. Every compartment is subjected to specific sink processes, for instance, mesopelagic fish are affected by mortality. Modified and adapted from Anderson et al. (2019)

The Anderson model does not have an explicit spatial component but only the parameterisation of the vertical movement of fish. The output takes the dimension of the primary production forcing which can be a single value or a bi-dimensional field. Therefore, it does not represent any kind of horizontal spatial interactions between model cells. More information on how this model was implement in my project and how it compares with OSMOSE is provided in Chapter 5.

Anderson is a simple flow model that calculates mesopelagic fish biomass from primary production forcing. It can be easily coupled to forcing derived from observations, for instance satellite data, or from bgc models. On the other hand, OSMOSE is a more complex model that simulates life cycle and an explicit trophic-web. In Chapter 5, both models were coupled to the same bgc model, CROCO–BioEBUS, to evaluate the strengths, weaknesses and advantages of using each type of model and, particularly, in relation to how they both respond to bottom–up variability prescribed by the bgc model.

1.5   Outline and author contribution

This thesis is a contribution to the scientific understanding of the interactions between biogeochemistry and higher trophic levels in the eastern tropical South Pacific Ocean and the northern Humboldt Current System (NHCS). The interplay of top–down, such as fishing pressure, and bottom–up, or environmental drivers, is explored throughout four studies:

Chapter 2 examines the potential effect of top–down pressures, for instance coming from variability in small pelagic fishes, on the biogeochemistry component of the

ecosystem with an emphasis on the plankton community. This chapter is based on a paper that is already published in Biogeosciences. Mariana Hill Cruz, Iris Kriest and Anderas Oschlies designed the study. Yonss Saranga José carried out the simulations. Mariana Hill Cruz performed the analysis. Rainer Kiko and Helena Hauss provided zooplankton observations and expertise on zooplankton dynamics in the NHCS. All authors discussed the results and wrote the manuscript.

Chapter 3 describes the end-to-end model system CROCO–BioEBUS–OSMOSE (physical, biogeochemical and higher trophic levels, respectively) and the calibration of the higher trophic levels (HTL) component, OSMOSE. This chapter contains a paper that has been submitted to Ecological Modelling and is currently under review. It also explores the effect of plankton temporal interannual variability on the HTL. Mariana Hill Cruz, Iris Kriest and Julia Getzlaff designed the experiments. Mariana Hill Cruz calibrated the OSMOSE climatological configuration, ran and analysed the experiments, and led the writing of the paper. Tianfei Xue tuned and ran the interannual hindcast of the CROCO-BioEBUS model. Iris Kriest, Julia Getzlaff, Ivy Frenger and Yunne-Jai Shin provided guidance and scientific expertise. All authors contributed to the discussion of results and writing of the paper.

Chapter 4 explores the impact of different fishing management scenarios on anchovy and hake using the same end-to-end model as described in Chapter 3. The experiment was designed by Mariana Hill Cruz based on a suggestion by Yunne-Jai Shin. The technical set-up, data analysis and writing was done by Mariana Hill Cruz.

Chapter 5 compares the mesopelagic fish in two end-to-end models and how they are affected by temporal variability in plankton and primary production. We are planning to submit the paper to the ICES Journal of Marine Science. Mariana Hill Cruz and Iris Kriest designed the experiments. Iris Kriest set up the Anderson model. Mariana Hill Cruz set up OSMOSE which had been used in Chapter 3, carried out the simulations with both fish models coupled to the physical–biogeochemical model and analysed the data. All authors discussed the results and wrote the manuscript.

Zooplankton mortality effects on the plankton community of the northern Humboldt Current System: sensitivity of a regional biogeochemical model

Mariana Hill Cruz, Iris Kriest, Yonss Saranga José, Rainer Kiko, Helena Hauss, and Andreas Oschlies

This chapter contains an already-published article. I adjusted the text and page numbering of the article to fit with the format of the overall thesis document. Please refer to the original paper published by Biogeosciences.

2.1   Abstract

Small pelagic fish off the coast of Peru in the eastern tropical South Pacific (ETSP) support around 10 % of global fish catches. Their stocks fluctuate interannually due to environmental variability which can be exacerbated by fishing pressure. Because these fish are planktivorous, any change in fish abundance may directly affect the plankton and the biogeochemical system.

To investigate the potential effects of variability in small pelagic fish populations on lower trophic levels, we used a coupled physical–biogeochemical model to build scenarios for the ETSP and compare these against an already-published reference simulation. The scenarios mimic changes in fish predation by either increasing or decreasing

mortality of the model's large and small zooplankton compartments.

The results revealed that large zooplankton was the main driver of the response of the community. Its concentration increased under low mortality conditions and its prey, small zooplankton and large phytoplankton, decreased. The response was opposite, but weaker, in the high mortality scenarios. This asymmetric behaviour can be explained by the different ecological roles of large, omnivorous zooplankton and small zooplankton, which in the model is strictly herbivorous. The response of small zooplankton depended on the antagonistic effects of mortality changes as well as on the grazing pressure by large zooplankton. The results of this study provide a first insight into how the plankton ecosystem might respond if variations in fish populations were modelled explicitly.

2.2   Introduction

Eastern boundary upwelling systems (EBUSs) are among the most productive regions in the ocean. Despite their small size, they support a large fraction of the world's fisheries (Chavez and Messié, 2009). The northern Humboldt Current System (NHCS) in the eastern tropical South Pacific (ETSP) Ocean is the most productive EBUS, producing 10% of global fish catches (Chavez et al., 2008) and supporting the fishery of the Peruvian anchovy *Engraulis ringens*, which is the biggest single-species fishery on the planet (Chavez et al., 2003). The ETSP is also characterised by substantial interannual variability (i.e. El Niño–Southern Oscillation; Holbrook et al., 2012), and an intense midwater oxygen minimum zone (OMZ), resulting in high denitrification rates (Farías et al., 2009).

As in other EBUSs, small pelagic fish are highly abundant (Cury et al., 2000) in the NHCS, building up large populations that are severely affected by climate fluctuations. For example, anchovy biomass in the NHCS fluctuated between 10×10^6 and 16×10^6 t in the 1960s (Alheit and Niquen, 2004). Its area of distribution spans from northern Peru to northern Chile and the Talcahuano region off central Chile (Figure 1 in Alheit and Niquen, 2004). During the El Niño event of 1972, it dropped to 6×10^6 t (Alheit and Niquen, 2004), presumably caused by warming and the resulting decrease in upwelling and production. These unfavourable growth conditions for anchovy might have been exacerbated by fishing pressure (Beddington and May, 1977; Hsieh et al., 2006). From 1992 to 2008, the population of anchovy off the Peruvian coast fluctuated between 3×10^6 and 12×10^6 t (Figure 13 in Oliveros-Ramos et al., 2017).

The Peruvian anchovy is a planktivorous fish whose diet changes over its ontogenic development. Anchovy first-feeding larvae consume mainly phytoplankton and when they reach a length of 4 mm their diet gradually switches to zooplankton, especially nauplii of copepods (Muck, Mendiola, and Antonietti, 1989). Adult anchovies' main sources of energy are euphausiids and copepods although phytoplankton is still found in their diet (Espinoza and Bertrand, 2008). The other prominent small planktivorous fish species in the NHCS is the Pacific sardine *Sardinops sagax*, which feeds on smaller particles than anchovy, including phytoplankton and small zooplankton (Ayón et al., 2008a). These two species can therefore be expected to impose a direct top-down control on plankton; at the same time, they may be bottom-up affected by changes in plankton abundance caused by variations in physical forcing.

Pauly et al. (1989) estimated that the total population of anchovy off Peru consumes 12.1 times its own biomass in 1 year. Assuming an area of $6x10^{10}$ m^2 (Ryther, 1969) and a conversion factor of zooplankton wet weight to nitrogen of 1000 mg ww (mmol N)$^{-1}$ (Travers-Trolet, Shin, and Field, 2014), a fluctuation in anchovy population of 9×10^6 t would result in a change in zooplankton mortality of 5 mmol N m^{-2} d^{-1} from anchovy predation alone, in a top-down-driven ecosystem assuming no non-linearities. The assumption that anchovy can exacerbate a top-down control on zooplankton is supported by a decline in zooplankton concentration in dense aggregations of anchovies (Ayón et al., 2008a; Ayón et al., 2008b). On the other hand, co-occurring long-term fluctuations of zooplankton and anchovies at the population scale also indicate a relevant bottom-up control in the NHCS (Alheit and Niquen, 2004; Ayón et al., 2008b).

Numerical models are valuable tools to examine the potential tight coupling across a large range of trophic levels and the mutual interactions among the different components, including top-down and bottom-up effects. Rose et al. (2010) pointed out the increasing need for so-called end-to-end models of the marine food webs; these set-ups couple models including physical and biogeochemical processes with models for higher trophic levels. When lower-trophic-level (biogeochemical) and higher-trophic-level (fish) models are coupled, the link is typically made at the plankton level, with the former models providing food for the latter (e.g. Travers-Trolet et al., 2014).

In stand-alone biogeochemical models that do not include higher trophic levels, zooplankton mortality is a closure term, used to return the additional biomass to detritus. It represents all processes that reduce the concentration of zooplankton and are not explicitly included in the model (for instance, predation by gelatinous organisms, predation by higher trophic levels and non-consumptive mortality). For example, Getzlaff

and Oschlies (2017) used it to mimic predation and immediate egestion or mortality by higher trophic levels. Zooplankton mortality may also form the link to fish models, when these are explicitly considered in the context of biogeochemical models (e.g. Travers-Trolet et al., 2014).

However, there is no consensus on the form of the mortality term, linear ($\mu \cdot [Z]$, where [Z] is the zooplankton concentration and μ is a mortality rate) and quadratic ($\mu \cdot [Z]^2$) being two common forms (e.g. Evans and Parslow, 1985; Fasham, Ducklow, and McKelvie, 1990; Koné et al., 2005; Kishi et al., 2007; Aumont et al., 2015). A common argument for preferring quadratic to linear mortality is the reduction in unforced short-term oscillations (Steele and Henderson, 1992), although Edwards and Yool (2000) argue that quadratic mortality does not always remove such oscillations. A quadratic mortality term may also be interpreted as an increase in diseases because of high population densities, cannibalism, or increased predation due to high densities of prey. Because it is very difficult to determine zooplankton mortality in the field, there is also no agreement on the exact value of mortality (either linear or quadratic), and this term, in practice, is often adjusted to tune the model. However, not using mortality rates based on observations may limit the capability of the model to accurately represent the zooplankton compartment (Daewel et al., 2014), and to draw predictions about the state and dynamics of the marine ecosystem (Anderson, Gentleman, and Sinha, 2010). Hirst and Kiørboe (2002) predicted a global mortality of copepods of 0.062 d^{-1} at 5°C and 0.19 d^{-1} at 25°C in the field. Two-thirds of such mortality is due to predation. In models, the values of the quadratic mortality rate (hereafter called μ_Z) in the literature vary over a large range, from 0.025 (mmol N m^{-3})$^{-1}$ d^{-1} (Fennel et al., 2006) up to 0.25 (mmol N m^{-3})$^{-1}$ d^{-1} (Lima and Doney, 2004).

For the NHCS, the high variability in forcing, biogeochemistry and plankton and the high abundance of planktivorous fish, together with its economic importance, indicate the need for end-to-end models that include details of all components. However, developing such a model is challenging, and studies in this area have so far focused on either fish (Oliveros-Ramos et al., 2017) or physics and biogeochemistry (José, Dietze, and Oschlies, 2017). Given the large importance of zooplankton mortality as a link between these two model systems (Mitra et al., 2014) and the uncertainty associated with it, in this study we focus on the effects of this parameter on the biogeochemical system of the ETSP as a first step towards a fully coupled system.

In order to model the highly dynamic nature of both physical and biogeochemical processes in the ETSP, we employed a biogeochemical model specifically designed for

EBUSs, coupled to a finely resolved regional circulation model. The coupled model has already been validated against oxygen, nitrate and chlorophyll (José, Dietze, and Oschlies, 2017); this configuration serves as a starting point and reference for the sensitivity experiments. In this study, we focus on the four plankton groups of the model: small and large phytoplankton and small and large zooplankton. Large phytoplankton is highly abundant near the coast of Peru in the nutrient-rich upwelling region. Towards the open ocean it is grazed down by its predator, large zooplankton; and further offshore, as conditions become oligotrophic, small zooplankton and phytoplankton take over.

In this study, we first extend the model validation by José, Dietze, and Oschlies (2017) and assess the reliability of the large zooplankton compartment in the model by comparing it against mesozooplankton observations obtained by net hauls. Note that in this paper we always refer to simulated phyto- and zooplankton by their size class (small or large), while observations are referred to as mesozooplankton. We then present two sensitivity experiments in which we varied the mortality rate of quadratic zooplankton mortality by ± 50 %. Model sensitivity is examined with regard to concentrations of model components and inter-compartmental fluxes. Besides the overall response of the prognostic variables to an increase or decrease in zooplankton mortality, we describe how changing zooplankton mortality affects the trophic structure of plankton, with focus on the highly productive coastal domain. Finally we discuss the implications of our study for the plankton community and for modelling higher trophic levels.

2.3 Methods

2.3.1 ROMS–BioEBUS model set-up

The Regional Oceanic Modeling System (ROMS; Shchepetkin and McWilliams, 2005) is a high-resolution, free-surface, terrain-following coordinate ocean model that solves the primitive equations considering the Boussinesq and hydrostatic assumptions. The Biogeochemical model for Eastern Boundary Upwelling Systems (BioEBUS), which was derived from a $N_2P_2Z_2D_2$ model from Koné et al. (2005), is coupled online to the physical part (Gutknecht et al., 2013a; Gutknecht et al., 2013b).

In this study the coupled ROMS–BioEBUS model has the same configuration as in

José, Dietze, and Oschlies (2017). It contains a small, high-resolution domain forced by a larger coarse-resolution domain, using the AGRIF (adaptive grid refinement in Fortran) 2-way nesting procedure. The small inner grid has a horizontal resolution of 1/12° spanning from about 69° W to 102° W and from 5° N to 31° S (Figure 2.1). The large outer grid spans from 69° W to 120° W and from 18° N to 40° S with a resolution of 1/4°. The biological processes occur in three time steps of 900 seconds for each physical time step of 2700 seconds in both domains. The two domains have 32 sigma layers with a vertical resolution of less than 5 m at the surface and decreasing to around 500 m at a maximum depth of 4500 m.
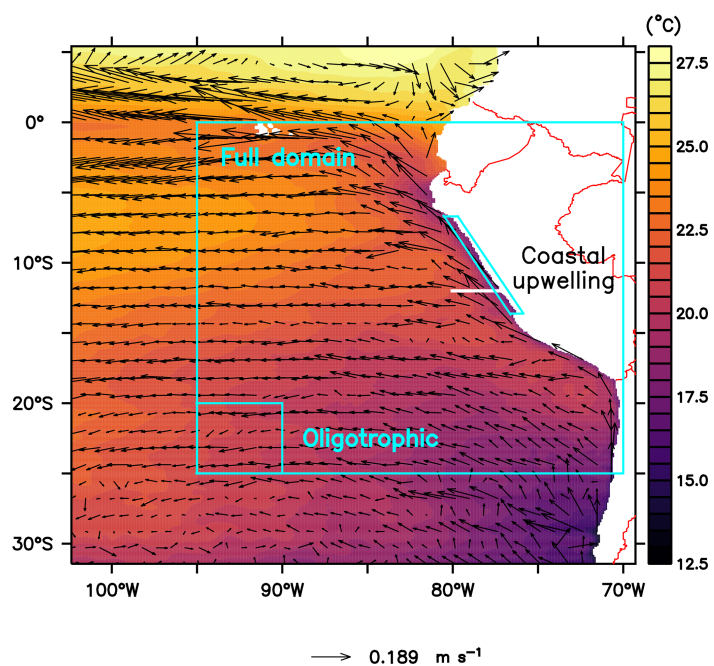
Figure 2.1. Annually averaged sea surface temperature (° C) and horizontal advection vectors (m s^{-1}), and location of the analysed regions (see labels), and of a vertical section for analysing plankton spatial succession (white line at 12° S). The coastal upwelling region (see Section 2.3.5) spans from the coast to about 40 to 50 km offshore.

The coarse-resolution domain temperature, salinity and horizontal velocity are forced at the lateral boundaries with monthly climatological (1990-2010) SODA reanalysis (Carton and Giese, 2008). Both domains are forced at the surface with 1/4° resolution wind velocity fields from QuikSCAT (Liu, Tang, and Polito, 1998) and monthly heat and freshwater fluxes from COADS (Worley et al., 2005). At the lateral boundaries of the coarse-resolution domain, the biogeochemical model is forced with monthly nitrate and oxygen values from CARS (Ridgway, Dunn, and Wilkin, 2002) and surface chlorophyll from SeaWiFs (O'Reilly et al., 1998). Phytoplankton and zooplankton boundary conditions are derived from a vertical extrapolation of the chlorophyll data. Detailed information about the boundary and initial conditions, and validation of the model is available in José, Dietze, and Oschlies (2017).

2.3.2 Biogeochemical model description

The evolution of a biological tracer in time is represented by Eq. (2.1). On the right-hand side of the equation, the first term represents the advection with the velocity vector u. The eddy and molecular diffusion is represented by the second and third terms, where K_h is the horizontal diffusion coefficient and K_z the vertical diffusion coefficient. The last term is a source-minus-sink (SMS) term due to biological processes. The full set of equations and detailed explanation about each process are available in Gutknecht et al. (2013a).

$$\frac{\partial C_i}{\partial t} = -\nabla \cdot (uC_i) + K_h \nabla^2 C_i + \frac{\partial}{\partial z}(K_z \frac{\partial C_i}{\partial z}) + SMS(C_i) \qquad (2.1)$$

The BioEBUS model is adapted for the biogeochemical processes specific to the low-oxygen conditions of EBUSs, with some processes being oxygen dependent (see Gutknecht et al., 2013a). It has two compartments of phytoplankton, two compartments of zooplankton and two compartments of detritus. The zooplankton and phytoplankton groups are divided into two size classes (small and large). There is not an explicit size parameter in the model; however, the compartments aim at representing the main ecological functions of the plankton community falling within each group. Hence, small phytoplankton (P_S) represents organisms smaller than about 20 μm that require low nutrients such as flagellates, while large phytoplankton (P_L) represents larger organisms such as diatoms. Similarly, small zooplankton (Z_S) simulates the role of a zooplankton community smaller than about 200 μm, such as ciliates, and large zooplankton (Z_L) represents a community larger than 200 μm, such as copepods. The two size classes of detritus (small D_S and large D_L) are produced from phytoplankton and zooplankton mortality and by release of unassimilated grazing material. The model also contains three compartments of dissolved inorganic nitrogen (NH_4^+, NO_2^- and NO_3^-), dissolved organic nitrogen (DON), oxygen (O_2) and nitrous oxide (N_2O).

The BioEBUS model (Gutknecht et al., 2013a) includes oxygen-dependant-remineralisation processes, which are divided into ammonification, nitrification and denitrification, as well as anammox, and are based on the formulations by Yakushev et al. (2007). N_2O is a diagnostic variable for model output and its production does not affect the concentration of the other variables. It is based on the parameterisation of Suntharalingam, Sarmiento, and Toggweiler (2000) and Suntharalingam et al. (2012), which relates the production of N_2O to the consumption of O_2 from decomposition of organic matter

in oxic and suboxic conditions. O_2 concentrations depend on primary production, zooplankton respiration, nitrification and remineralisation. This model includes gas exchange of O_2 and N_2O with the atmosphere.

Phytoplankton

The SMS terms in the small and large phytoplankton compartments are determined by Eq. (2.2) and (2.3), respectively:

$$SMS(\mathrm{P_S}) = (1 - \varepsilon_{\mathrm{P_S}}) \cdot J_{\mathrm{P_S}}(\mathrm{PAR}, T, \mathrm{N}) \cdot [\mathrm{P_S}] - G_{\mathrm{Z_S}}^{\mathrm{P_S}} \cdot [\mathrm{Z_S}] - G_{\mathrm{Z_L}}^{\mathrm{P_S}} \cdot [\mathrm{Z_L}] - \mu_{\mathrm{P_S}} \cdot [\mathrm{P_S}] \quad (2.2)$$

$$SMS(\mathrm{P_L}) = (1 - \varepsilon_{\mathrm{P_L}}) \cdot J_{\mathrm{P_L}}(\mathrm{PAR}, T, \mathrm{N}) \cdot [\mathrm{P_L}] - G_{\mathrm{Z_S}}^{\mathrm{P_L}} \cdot [\mathrm{Z_S}] - G_{\mathrm{Z_L}}^{\mathrm{P_L}} \cdot [\mathrm{Z_L}] - \mu_{\mathrm{P_L}} \cdot [\mathrm{P_L}] - w_{\mathrm{P_L}} \cdot \frac{\mathrm{d}}{\mathrm{d}z}[\mathrm{P_L}].$$
$$(2.3)$$

Here $G_{\mathrm{Z}_j}^{\mathrm{X}_i}$ represents feeding rates by zooplankton (see Section 2.3.2), $\mu_{\mathrm{P}_i} \cdot [\mathrm{P}_i]$ is the mortality term, representing all not explicitly modelled phytoplankton losses; $w_{\mathrm{P_L}}$ is the sinking speed of large phytoplankton sedimentation, which is an additional loss term for this compartment; $\varepsilon_{\mathrm{P}_i}$ is the exudation fraction of primary production, and $J_{\mathrm{P}_i}(\mathrm{PAR}, T, \mathrm{N})$ is the growth rate limited by light, temperature, and nutrients:

$$J_{\mathrm{P}_i}(\mathrm{PAR}, T, \mathrm{N}) = \frac{J\mathrm{max}_{\mathrm{P}_i} \cdot \alpha \mathrm{P}_i \cdot \mathrm{PAR}}{\sqrt{J\mathrm{max}_{\mathrm{P}_i}^2 + (\alpha \mathrm{P}_i \cdot \mathrm{PAR})^2}} \cdot f_{\mathrm{P}_i}(\mathrm{NO_3^-}, \mathrm{NO_2^-}, \mathrm{NH_4^+}) \quad (2.4)$$

where $f_{\mathrm{P}_i}(\mathrm{NO_3^-}, \mathrm{NO_2^-}, \mathrm{NH_4^+})$ is the growth limitation by nutrients, PAR is the photosynthetically available radiation (see Koné et al., 2005), $J\mathrm{max}_{\mathrm{P}_i}$ is the maximal light-saturated growth rate which is a function of temperature, and $\alpha \mathrm{P}_i$ is the initial slope of the photosynthesis-irradiance (P-I) curve (Gutknecht et al., 2013a). Large phytoplankton is characterised by a steeper initial slope of the P-I curve and by larger half-saturation constants for nutrient uptake (see Table 2.2). Therefore, it grows better than small phytoplankton under low-light conditions, but its nutrient uptake increases more slowly as nutrient concentrations increase.

Zooplankton

Zooplankton increases its biomass through grazing on phytoplankton and in the case of large zooplankton also on small zooplankton. Metabolism; mortality; and, in the case of small zooplankton, predation by large zooplankton are sink terms. Predation by fish and other higher trophic levels is implicit in the quadratic mortality term. The biomass lost by metabolism and mortality is assumed to become detritus which may sink to the sediments or become remineralised, and a small fraction of zooplankton losses become ammonium and dissolved organic nitrogen, which is also subjected to remineralisation.

The SMS terms of the small and large zooplankton compartment are determined by Eq. (2.5) and (2.6), respectively:

$$SMS(\mathrm{Z_S}) = f1_{\mathrm{Z_S}} \cdot (G_{\mathrm{Z_S}}^{\mathrm{P_S}} + G_{\mathrm{Z_S}}^{\mathrm{P_L}}) \cdot [\mathrm{Z_S}] - G_{\mathrm{Z_L}}^{\mathrm{Z_S}} \cdot [\mathrm{Z_L}] - \gamma_{\mathrm{Z_S}} \cdot [\mathrm{Z_S}] - \mu_{\mathrm{Z_S}} \cdot [\mathrm{Z_S}]^2 \qquad (2.5)$$

$$SMS(\mathrm{Z_L}) = f1_{\mathrm{Z_L}} \cdot (G_{\mathrm{Z_L}}^{\mathrm{P_S}} + G_{\mathrm{Z_L}}^{\mathrm{P_L}} + G_{\mathrm{Z_L}}^{\mathrm{Z_S}}) \cdot [\mathrm{Z_L}] - \gamma_{\mathrm{Z_L}} \cdot [\mathrm{Z_L}] - \mu_{\mathrm{Z_L}} \cdot [\mathrm{Z_L}]^2. \qquad (2.6)$$

Here $f1_{\mathrm{Z_S}}$ and $f1_{\mathrm{Z_L}}$ are assimilation coefficients (see also Table 2.2). $G_{\mathrm{Z_j}}^{\mathrm{X_i}}$ is feeding rates of predator $\mathrm{Z_j}$ (either large or small zooplankton) on prey $\mathrm{X_i}$ (small and large phytoplankton, and small zooplankton) calculated with the formulation by Tian et al. (2000) and Tian et al. (2001). There is a linear loss rate accounting for basic metabolism ($\gamma_{\mathrm{Z_i}}$), and a quadratic loss rate also referred to as mortality. The mortality parameters $\mu_{\mathrm{Z_S}}$ and $\mu_{\mathrm{Z_L}}$ of the reference simulation are 0.025 and 0.05 (mmol N m^{-3})$^{-1}$ d^{-1} for small and large zooplankton, respectively, as in José, Dietze, and Oschlies (2017) and Gutknecht et al. (2013a).

The feeding rate follows the formulation from Tian et al. (2000) and Tian et al. (2001):

$$G_{\mathrm{Z_j}}^{\mathrm{X_i}} = g_{\mathrm{max}_{\mathrm{Z_j}}} \cdot \frac{e_{\mathrm{Z_j X_i}} \cdot [\mathrm{X_i}]}{k_{\mathrm{Z_j}} + F_t} \qquad (2.7)$$

where $g_{\mathrm{max}_{\mathrm{Z_j}}}$ is the maximum grazing rate of predator $\mathrm{Z_j}$, $e_{\mathrm{Z_j X_i}}$ is the preference of predator $\mathrm{Z_j}$ for prey $\mathrm{X_i}$, $k_{\mathrm{Z_j}}$ is the half-saturation constant and F_t is the total availability of food for predator $\mathrm{Z_j}$. Large zooplankton responds more slowly to changes in food due to the high $k_{\mathrm{Z_L}}$. In the case of large zooplankton $F_t = e_{\mathrm{Z_L P_S}} \cdot [\mathrm{P_S}] + e_{\mathrm{Z_L P_L}} \cdot [\mathrm{P_L}] +$

$e_{Z_L Z_S} \cdot [Z_S]$ and in the case of small zooplankton $F_t = e_{Z_S P_S} \cdot [P_S] + e_{Z_S P_L} \cdot [P_L]$ (Gutknecht et al., 2013a).

2.3.3 Zooplankton evaluation

As noted above, this model was already validated against oxygen, nitrate and chloro-phyll (José, Dietze, and Oschlies, 2017). As a complement, we here compare the large zooplankton compartment of the model, averaged from January to March, with ob-servational data collected on RV *Meteor* cruise M93. The samples obtained during this cruise include day- and nighttime hauls with a Hydro-Bios multinet (nine nets, 333 µm mesh) between February 10 and March 3, 2013 on a transect off the Peruvian coast ($\approx 12°$S; see Fig. 2.2f), capturing the vertical and horizontal gradient in zooplankton concentration. Samples were size-fractionated by sieving and processed according to the ZooScan method (Gorsky et al., 2010). Observations included crustaceans, chaetog-naths and annelids greater than 500 μm. For model comparison we converted the ob-servation from nighttime hauls to dry biomass according to Lehette and Hernández-León (2009), and further to nitrogen units as suggested by Kiørboe (2013). A detailed description of the zooplankton processing is provided by Kiko and Hauss (2019). Only night observations were compared since our model does not include diel vertical mi-gration.

In both the model and observations, concentration of large zooplankton is greatest in the surface and decreases with depth (Figure 2.2). At the surface, modelled concentra-tions are 1 order of magnitude larger than observations at almost all stations (Figure 2.2). Only at station d do observations reach 1 mmol N m^{-3}, while the model exhibits maximum values close to 4 mmol N m^{-3}. At most stations, the distribution of mod-elled concentrations is similar to that of observed concentrations in the surface layer (upper 100 m), although model estimates are consistently higher. This is also the case when comparing against a different dataset of observations (see Supplement). Below 100 m, however, model estimates are consistently lower than the observations, which is in particular evident at the deep offshore stations (Appendix 2.8, Figure 2.8 a) and b)). Zooplankton in our model does not consume detritus or bacteria; small zooplank-ton feeds on phytoplankton, and large zooplankton feeds on small zooplankton and on phytoplankton. Therefore, in contrast to observations, its presence is not expected in deep water. In summary, the model matches the observed spatial pattern of zooplank-ton distribution, but tends to overestimate zooplankton concentration in the surface layer and to underestimate it in the mesopelagic depths. Possible reasons for this mis-

match will be discussed in Sect. 2.5.1.
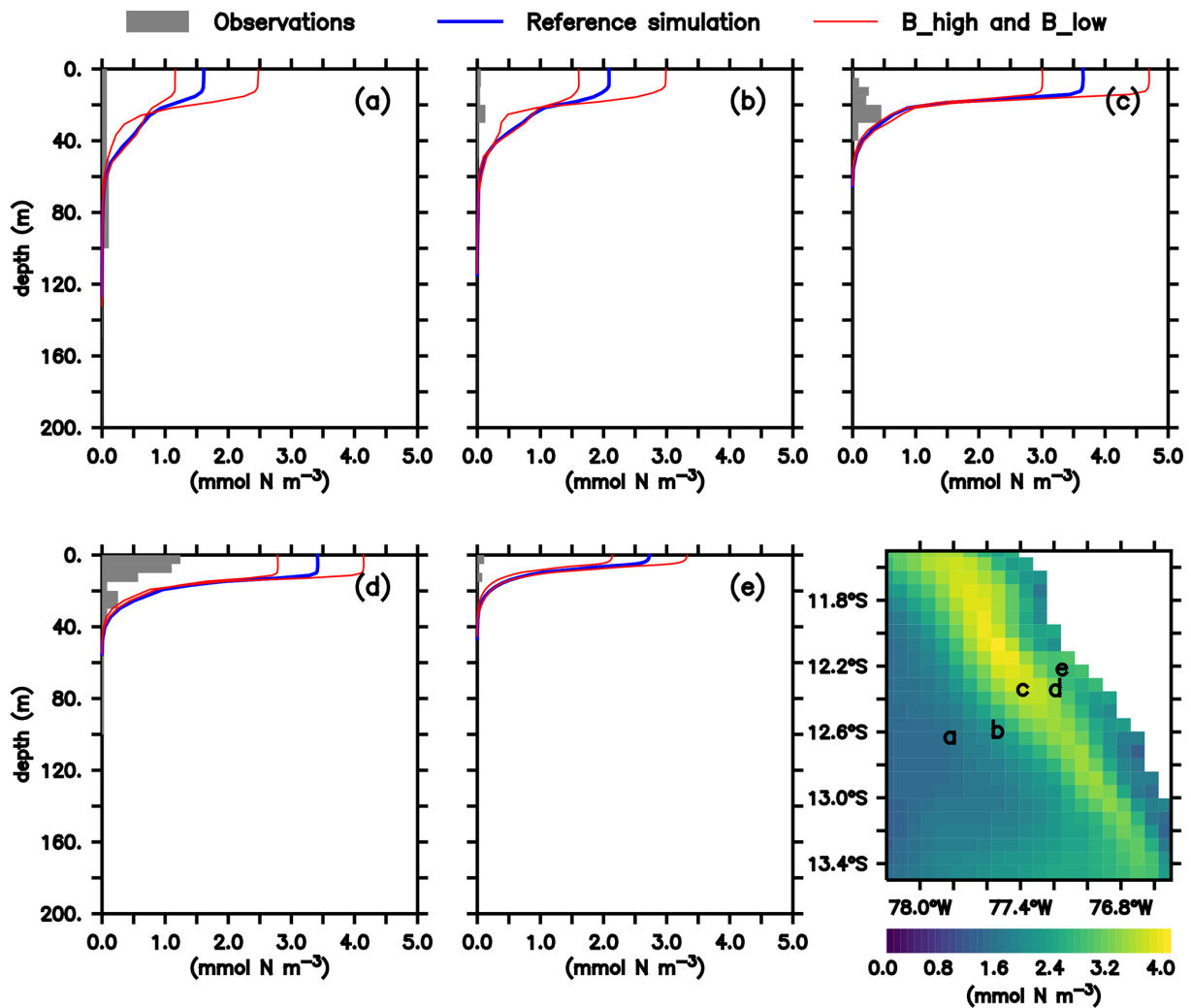
Figure 2.2. a) to e) Zooplankton concentrations (mmol N m^{-3}). Lines indicate modelled large zooplankton concentrations in the reference scenario and experiments B_high and B_low averaged from January to March. Shaded area shows observed nighttime mesozooplankton biomass concentrations over the sampled depth intervals (m). Observations are lower than 0.1 mmol N m^{-3} below 200 m, thus they have not been included. For a plot including deep-water observations, please see Appendix 2.8, Fig. 2.8 and Fig. 4 in Kiko and Hauss (2019). Bottom right: Modelled large zooplankton biomass concentration at the surface in the reference scenario (mmol N m^{-3}) and locations where observations were collected.

2.3.4   Experimental design

To mimic changes in grazing pressure on zooplankton due to small-pelagic-fish biomass fluctuations, we followed the approach by Getzlaff and Oschlies (2017), and varied the mortality rate of each zooplankton compartment by ± 50 % in comparison to the reference scenario described by José, Dietze, and Oschlies (2017). Thereby, an increase in mortality assumes a large consumption of zooplankton by fish, while a

decrease in mortality assumes fewer fish. Because the model does not include an explicit compartment for fish, it is assumed that all zooplankton biomass consumed by fish becomes part of the detritus pool via immediate fish mortality and defecation. In reality, a fraction of the biomass is extracted from the system by the fishing industry, predation by sea birds that defecate over land, and migrations.

Our model has two zooplankton compartments. In order to explore the different roles of large zooplankton as top predator and small zooplankton as grazer and prey, we performed four experiments, in which we varied the respective mortality rate of large and small zooplankton (0.05 and 0.025 $[\text{mmol N m}^{-3}]^{-1} \text{ d}^{-1}$, respectively) by ± 50 %:

- A_high with $1.5 \times \mu_{Z_L}$

- A_low with $0.5 \times \mu_{Z_L}$

- B_high with $1.5 \times \mu_{Z_L}$ and $1.5 \times \mu_{Z_S}$

- B_low with $0.5 \times \mu_{Z_L}$ and $0.5 \times \mu_{Z_S}$

where μ_{Z_i} is the mortality rates of large and small zooplankton. The average nitrogen flux to detritus due to large zooplankton mortality over the upper 100 m depth near the coast of Peru (coastal upwelling region, see Section 2.3.5 and Figure 2.3) in the reference scenario is 3.1 mmol N m^{-2} d^{-1} ($\mu_{Z_L} \cdot [Z_L]^2$, Figure 2.3). Neglecting any non-linear and feedback effects within the model, a 50 % change in the mortality rate would result in a change in zooplankton loss due to mortality of 1.55

Figure 2.3. Nitrogen flux from large (left) and small (right) zooplankton to detritus due to zooplankton mortality, integrated over the upper 100 m of the water column in the reference scenario (mmol N m^{-2} d^{-1}).

mmol N m^{-2} d^{-1}. It is thus a conservative value, compared to a change of 5 mmol N m^{-2} d^{-1} that anchovy population fluctuations could theoretically exert, as estimated in Sect. 2.2.

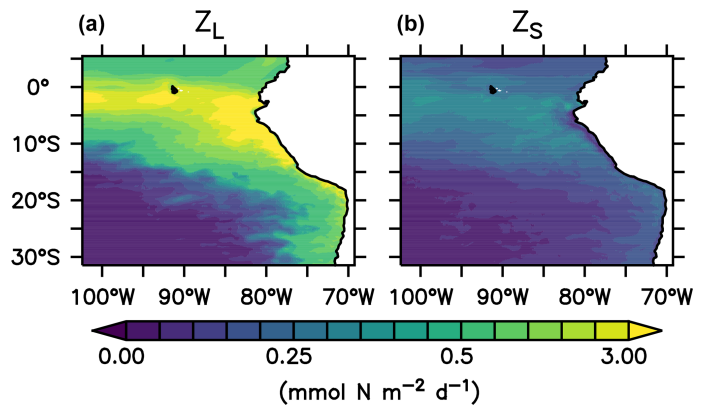All model experiments and the reference scenario were spun up for 30 climatological years. Annual means of the state variables and nitrogen fluxes from the last climatological year of the high-resolution domain were analysed.

2.3.5 Model analysis

The ETSP is highly dynamic at temporal and spatial scales, with nutrient-rich cold water near the coast of Peru, and oligotrophic regions offshore. Therefore, we analysed four different regions: the "full domain" without boundaries (F), an "oligotrophic" region (O) offshore, and the "coastal upwelling" region (C) near the Peruvian coast (Figure 2.1). Since the upwelling system of Peru is quite heterogeneous with lots of mesoscale processes, we restricted the C region to the very coastal upwelling area, where the concentration of large phytoplankton is high, up to about 40 to 50 km offshore. Region O was picked to be as far as possible from the nutrient-rich areas along the Equator and along the coast, but apart from the domain boundary to avoid boundary effects. For most of our analysis, percentage relative differences between the reference scenario and the other scenarios were calculated. In addition, we analyse the development of plankton succession from the coast of Peru towards the open ocean at 12° S (Figure 2.1, white line). Because plankton concentrations are negligible below 100 m depth and we are mainly interested in the plankton community, we focus most of our analysis on the upper water layers. For our analysis we therefore integrate or average plankton concentrations over the upper 100 m or, in the case of shallower waters, down to the seafloor. Also, all analyses in our study take into account only annual averages. However, we recognise that there is high temporal variability in the NHCS (see Appendix 2.9 and Supplement).

2.4 Results

We first provide an overview of the general performance of the reference scenario, with respect to the different model components and biogeochemical provinces (Section 2.4.1). We then investigate their response to changes in zooplankton mortality, and the response of the plankton ecosystem structure (Section 2.4.2). The coastal upwelling region (C) is especially productive and the habitat of the largest aggregations of small pelagic fish, whose temporal variability inspired this study. Therefore, in Sect. 2.4.3 we place special emphasis on this region. Finally, we investigate the response of the zooplankton losses due to mortality in the experiments, in order to understand whether the model structure buffers or increases the effect of varying the zooplankton mortality rate on such a term (Section 2.4.4). This would give us an insight into potential feedbacks to higher trophic levels.

2.4.1 Biogeochemistry and plankton distribution in the reference scenario
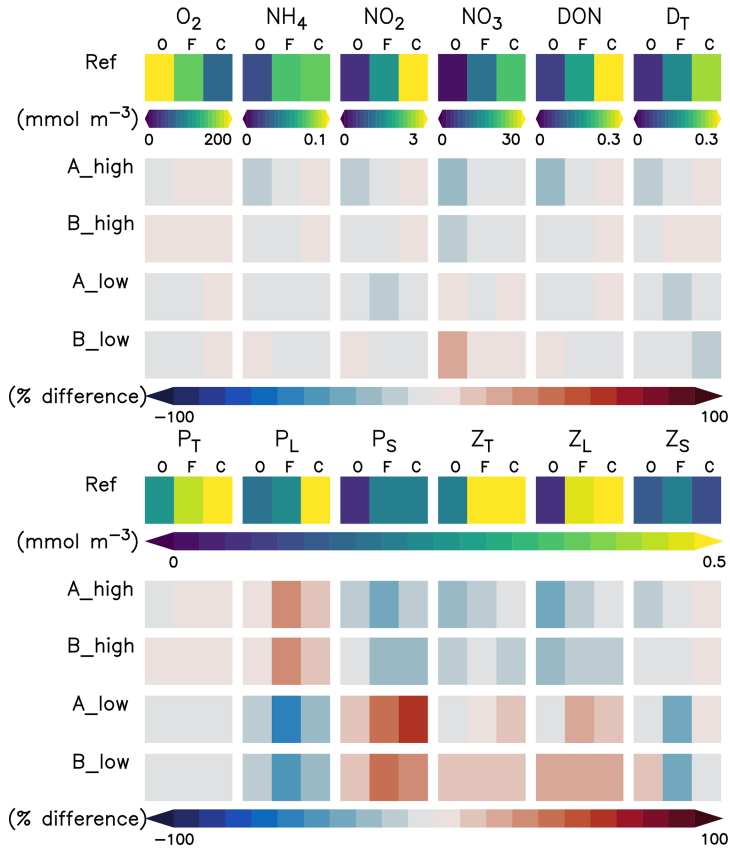

Figure 2.4. Annually, spatially (oligotrophic (O) region, full domain (F) and coastal upwelling (C) region; see Figure 2.1 for further reference) and depth-averaged (0-100 m) concentrations (mmol N m^{-3} or mmol O$_2$ m^{-3}) of the biogeochemical prognostic variables in the model reference scenario and normalised percent difference between the reference scenario and experiments. P is phytoplankton, Z is zooplankton, D is detritus, DON is dissolved inorganic nitrogen, T is total, L is large and S is small.

In this section we describe the concentrations of the inorganic and organic compartments in our model reference scenario, averaged between a 0 and 100 m depth (Figure 2.4) unless otherwise specified. Oxygen concentrations increase offshore, with an average of 226.6 mmol O$_2$ m^{-3} in the oligotrophic region (O) compared to 69.7 mmol O$_2$ m^{-3} in the coastal upwelling region (Figure 2.4). The concentration decreases further below 100 m, reaching an average of 5.3 mmol O$_2$ m^{-3} between 100 and 1000 m in the coastal upwelling region (C). Nitrate is the most abundant nutrient all over the domain, ranging from 0.6 in O to 21.7 mmol N m^{-3} in C. On the other hand, ammonium and nitrite are only 0.8 and 3.2 mmol N m^{-3} in C respectively (Figure 2.4). Please refer to José, Dietze, and Oschlies (2017) for a further in-depth analysis of biogeochemical tracers in the reference scenario.

Phyto- and zooplankton are generally absent in the deep water. In the surface layer between 0 and 100 m depth (Figure 2.4), phytoplankton is clearly favoured by nutrient-rich coastal upwelling, where total phytoplankton reaches 0.93 mmol N m^{-3} on average, compared to 0.25 mmol N m^{-3} in the oligotrophic region (Figure 2.4). Total detritus follow the concentration trend of plankton, with 0.26 in C and only 0.03 in O.

When zooming into the coastal region (Figure 2.5), large phytoplankton exhibits a sharp peak near the coast which drops offshore. Moving further offshore, large zooplankton peaks at the decline in the large phytoplankton peak, followed by increased concentrations of small phytoplankton. Given the (Ekman-driven) transport of surface waters (Figure 2.1) this spatial pattern might be interpreted as a form of succession as the water is advected offshore. In general, modelled concentrations of large zooplankton are high not only in the coastal upwelling region (Section 2.3.3) but also in large parts of the domain (Figure 2.4), except for in the oligotrophic south-western region (Figure 2.4).

The growth rate of phytoplankton is limited by temperature, nutrients and light (see Eq. 2.4). Hence, the spatial pattern of plankton near the coast can be explained by the competitive advantage of large phytoplankton in deep water due to its steeper initial slope of the P-I curve (see Appendix 2.7, Table 2.2), eutrophic conditions in the nutrient-rich upwelling water, and relatively low predation due to the lack of large zooplankton. This opens a loophole for large phytoplankton to grow in the upwelling waters. As water is transported offshore (Figure 2.1), large zooplankton starts to grow and grazes on large phytoplankton. More oligotrophic sunlit conditions even further offshore favour small phytoplankton growth at the surface. Therefore, this first analysis reveals spatial segregation and succession from the coast to offshore waters. These patterns are caused by the model's parameterisation of plankton groups, and their mutual interactions.

2.4.2 Response to zooplankton mortality

When changing zooplankton mortality, the inorganic variables (Figure 2.4) are not noticeably affected by the experiments.

Plankton responds very similarly to changes in mortality in experiments A and B (Figure 2.4 and Appendix 2.10, Figure 2.10). Phytoplankton and large zooplankton follow the same direction of response in all regions: concentrations of large zooplankton decrease in the high mortality scenario and increase in the low mortality scenario, as could be expected. Large phytoplankton responds inversely to large zooplankton, evidencing a top-down control of its main grazer. On the other hand, the response of small phytoplankton is inverse to that of large phytoplankton. In contrast, small zooplankton shows an asymmetric response to changes in mortality, as it mainly decreases in the low mortality scenarios but responds only weakly in the high mortality scenarios

(Figure 2.4 and Appendix 2.10, Figure 2.10).

The spatial plankton distribution along the transect (Figure 2.5) remains the same when zooplankton mortality changes, but the absolute concentrations of each compartment change. In all scenarios large phytoplankton peaks close to the coast. When large zooplankton concentrations are reduced because of its higher mortality in experiment B_high, the large phytoplankton peak increases (Figure 2.5, right). Similarly, large phytoplankton decreases with lower zooplankton mortality, due to higher grazing of zooplankton on phytoplankton (Figure 2.5, left). This pattern is also similar in experiments A. Because the largest effects occur in the very productive coastal region (C), in the following section we narrow our analysis to this domain.
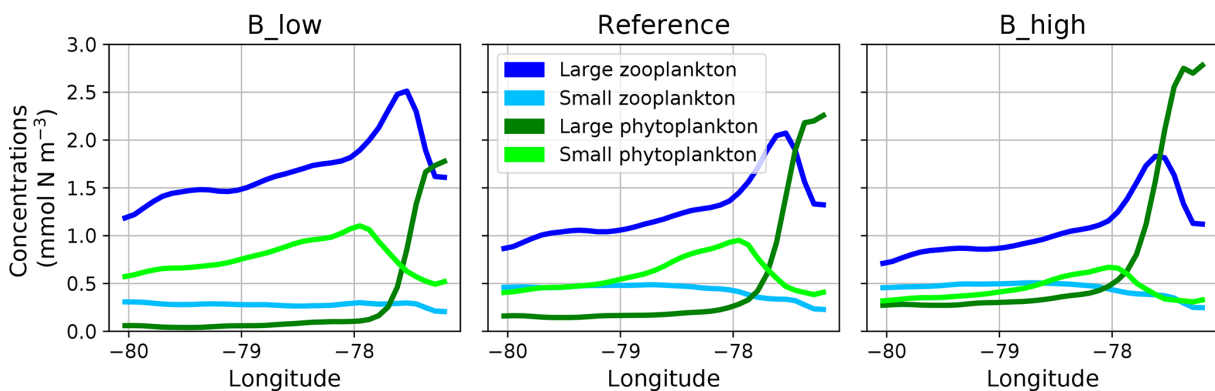
Figure 2.5. Zonal distribution of surface plankton concentrations at 12° S annually averaged in the reference and the two B scenarios, respectively. The location of this section is indicated as a white line in Fig. 2.1.

2.4.3 Effects on the food web in the coastal domain

An increase in zooplankton mortality causes only small changes in total primary production in the coastal upwelling region (C) , but the partitioning between the two phytoplankton groups changes (Figure 2.6). In particular, total primary productivity of the system is increased by 3.9 % in B_high and reduced by 5.5 % in B_low. Large phytoplankton is the dominant group. However, its productivity increases by about 19 % in B_high and decreases by 22 % in B_low, i.e. its changes are much more pronounced than the overall phytoplankton response. Because small phytoplankton shows an inverse response in production, this dampens the change in total primary production. Thus, a low zooplankton mortality favours small phytoplankton and its growth, and a high mortality favours large phytoplankton; changes in both phytoplankton groups result in a weak response of total primary production.
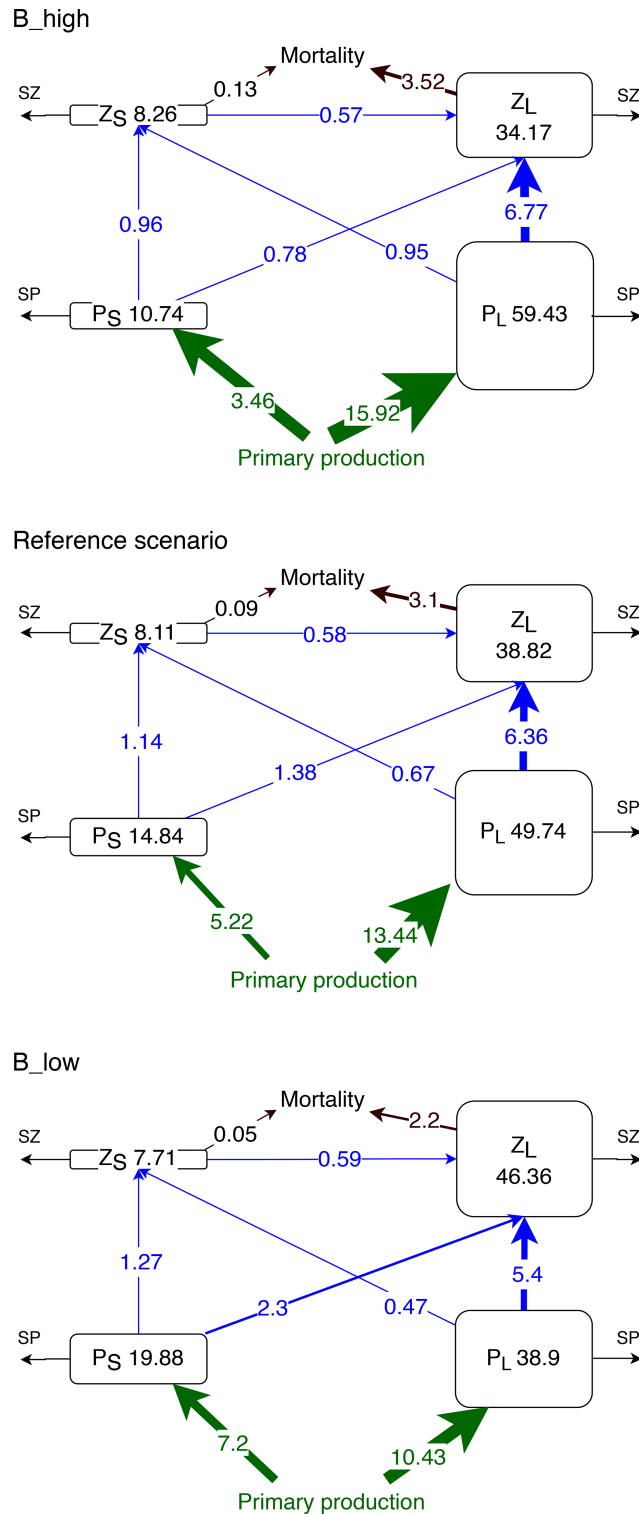
Figure 2.6. Concentrations (mmol N m^{-2}) and nitrogen fluxes (mmol N m^{-2} d^{-1}) between plankton compartments (small and large phytoplankton P_S and P_L and small and large zooplankton Z_S and Z_L, respectively) integrated over the upper 100 m or up to the seafloor if shallower than 100 m and averaged over latitude and longitude in the coastal upwelling region (see Figure 2.1). SZ and SP indicate the sinks which include phytoplankton mortality, zooplankton metabolism, large phytoplankton sedimentation, unassimilated primary production and unassimilated grazing (Gutknecht et al., 2013a).

33

Experiment B_high exhibits the highest total plankton biomass in the upper 100 m of the upwelling system (112.6 mmol N m^{-2}, Figure 2.6), which is mostly concentrated in the large phytoplankton compartment (59.43 mmol N m^{-2}). In this experiment the main pathway of nitrogen transfer to large zooplankton is via its grazing on large phytoplankton (6.77 mmol N m^{-2} d^{-1}). As mortality decreases, small phytoplankton and large zooplankton gain biomass. Large phytoplankton grazing remains the main nitrogen source for large zooplankton. However, large zooplankton consumption of small phytoplankton is almost 3 times higher in B_low than in B_high (Figure 2.6). Thus, a reduction in mortality causes a switch in the diet of large zooplankton, from mainly large phytoplankton to a diet that consists of more than one-quarter small phytoplankton.

Small zooplankton biomass decreases by ~0.4 mmol N m^{-2} (about 5 % of the reference value) in B_low but it only increases by 0.15 mmol N m^{-2} (about 2 %) in B_high (Figure 2.6). Despite the changes in small zooplankton biomass, the consumption of its biomass by large zooplankton remains approximately the same in all experiments, resulting in a higher proportional biomass loss of small zooplankton in scenario B_low. Hence, predation by large zooplankton as well as competition for food negatively affects small zooplankton. Under high mortality conditions, the availability of large phytoplankton as food increases (Figure 2.6). However, small phytoplankton, the preferred prey of small zooplankton, declines as explained above. Such antagonistic effects on small zooplankton buffer its response in this scenario.
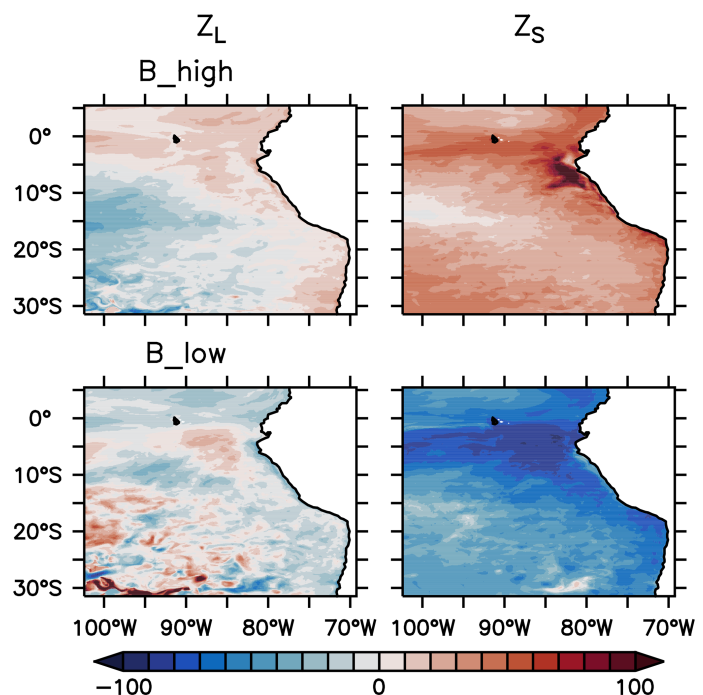

Figure 2.7. Percentage normalised difference in the nitrogen flux from large and small zooplankton to detritus due to zooplankton mortality, integrated over the upper 100 m of the water column, between experiment B_high and experiment B_low, and the reference scenario (see Figure 2.3 for the reference scenario).

2.4.4 Zooplankton losses due to mortality response

In this section, we describe the response of the nitrogen loss due to mortality, also referred as the quadratic mortality term ($\mu_{Z_i} \cdot [Z_i]^2$, see Eq. (2.5) and (2.6)). The integrated $\mu_{Z_i} \cdot [Z_i]^2$ in the reference scenario was provided in Sect. 2.3.4, Fig. 2.3. In experiment B, $\mu_{Z_S} \cdot [Z_S]^2$ and $\mu_{Z_L} \cdot [Z_L]^2$ exhibit different behaviours. In the coastal upwelling region, both $\mu_{Z_S} \cdot [Z_S]^2$ and $\mu_{Z_L} \cdot [Z_L]^2$ increase in B_high and decrease in B_low (Figure 2.6). However, the relative response of $\mu_{Z_L} \cdot [Z_L]^2$ is mild and fluctuates between ± 30 % outside the oligotrophic area (Figure 2.7). In contrast, $\mu_{Z_S} \cdot [Z_S]^2$ exhibits a clear relative increase all over the domain in B_high, and a decrease in B_low. The moderate response of large zooplankton loss can be attributed to the combined effects of changes in zooplankton concentration ($[Z_L]$) and changes in the mortality parameter (μ_{Z_L}), which we varied by ± 50 % in this study. Large zooplankton concentration increases when μ_{Z_L} is decreased, and vice versa. This opposite trend buffers the effect of a change in μ_{Z_L}. On the other hand, small zooplankton concentration ($[Z_S]$) changes in the same direction as μ_{Z_S}, due to the combined effects of changes in its concentration, due to grazing pressure exerted by large zooplankton and competition for food with this group, and changes in μ_{Z_S}.

To summarise, increasing and decreasing zooplankton mortality by 50 % generates a rearrangement of the plankton ecosystem; however, the overall changes in the large zooplankton loss are not as high as would be expected from a change in the mortality rate alone. This might buffer the system once the biogeochemical model is coupled to a model of higher trophic levels.

2.5 Discussion

2.5.1 Constraining the zooplankton compartment

An increasing need for the development of end-to-end models has generated interest in using results of biogeochemical models as forcing for higher-trophic-level models (fish, macroinvertebrates and apex predators) (see Tittensor et al., 2018, for a review). In a one-way coupling set-up, the biomass of plankton available as food for higher trophic levels has been adjusted during calibration of the latter, reducing the amount of plankton that is available for fish consumption (e.g. Oliveros-Ramos et al., 2017;

Travers-Trolet et al., 2014). However, for two-way coupling set-ups, this adjustment of the available plankton biomass could buffer the effect of higher trophic levels on lower trophic levels (e.g. Travers-Trolet et al., 2014). Biogeochemical models can produce a wide range of output depending on their parameter values (Baklouti et al., 2006) and their non-linearity. For example, a quadratic zooplankton mortality exacerbates the reduction in zooplankton biomass when concentrations are very high, and prevents its extinction at very low concentrations. In addition, the multiple-resources form of the Holling type-II grazing function allows the predator to modify its grazing preference towards the most abundant prey (Fasham, Boyd, and Savidge, 1999). Finally, Lima, Olson, and Doney (2002) noted that coupled physical and food web models can transition from equilibrium to chaotic states under even small changes in their parameters. Few studies have aimed to understand such behaviour (Baklouti et al., 2006) and examined the sensitivity of the model to parameters (Arhonditsis and Brett, 2004; Shimoda and Arhonditsis, 2016). Our model study was partly motivated by the uncertainty associated with the zooplankton mortality. Indeed our model showed that a small alteration in the mortality parameter (small compared to the wide range of values that have been used for this parameter in different biogeochemical models) can strongly affect the mass flux within the simulated ecosystem. Hence, there is an increasing need for accurate plankton representation in biogeochemical models without dismissing other compartments, such as nutrients or oxygen. Nevertheless, lack of data for validation especially of higher trophic levels is a common problem for biogeochemical models of the northern Humboldt Upwelling System (Chavez et al., 2008). Oxygen, chlorophyll and nitrate in our model have been evaluated previously (José, Dietze, and Oschlies, 2017). Here we presented the first attempt to compare the large zooplankton compartment of the ROMS–BioEBUS ETSP configuration with mesozooplankton observations.

At the surface, zooplankton concentrations simulated by our model in the reference scenario are 1 order of magnitude higher than observations at most stations. However, sampling in the upper 10 m depth may be impacted by water disturbance by the ship adding additional errors to the measurements. The match to observations improves with depth. Modifying the mortality rate by +50 % (-50 %) produced only a change of -12 % (+19 %) in large zooplankton concentration, indicating that either the induced changes in mortality rate were not large enough, or this parameter is not overly influential in improving the model fit to observations. Systems with a non-density-dependent, or linear, mortality rate respond to perturbations in a "reactive" way, as defined by Neubert, Klanjscek, and Caswell (2004), drifting away from equilibrium, in contrast to systems with density-dependent closure terms which tend to buffer the perturbations (Neubert, Klanjscek, and Caswell, 2004). Therefore, we might have

expected a stronger impact if we had manipulated the linear closure term of the model, or metabolic losses (see Section 2.3.2), rather than the quadratic term. For an average nitrogen flux due to large zooplankton mortality of 2.2, 3.1 and 3.52 mmol N m^{-2} d^{-1} and large zooplankton integrated concentrations of 46.36, 38.82 and 34.17 mmol N m^{-2} in the coastal upwelling region (see Section 2.4.3), the mortality rate would be 0.04, 0.08 and 0.1 d^{-1} in scenarios B_low, reference and B_high respectively. In all cases the values are lower than the 0.19 d^{-1} estimated by Hirst and Kiørboe (2002) for copepods in the field at 25° C. The closest scenario to observations is B_high where the mortality rate is only about half of the estimate by Hirst and Kiørboe (2002). This is also the scenario that better resembles mesozooplankton observations, since it exhibits the lowest concentrations. On the other hand, the mortality rate estimated for the reference scenario (0.08 d^{-1}) is closer to the 0.065 d^{-1} estimation by Hirst and Kiørboe (2002) at 5° C. This is considerably lower than the temperature in our modelled region (see Figure 2.1). Note, however, that zooplankton mortality in our model does not depend on temperature.

Some part of the mismatch between model and observations might be related to how both data types are generated. Therefore, a direct comparison between model and observations has to be viewed with some caution. In our model, large zooplankton acts as a closure term which is adjusted to balance the biomass and nitrogen flux to other compartments, and does not resemble a specific set of species. Its parameters (maximum grazing rate, feeding preferences, etc.) are meant to represent larger, slow-growing species with a preference for diatoms. As such, they might not be directly comparable to the observed groups. The observations, on the other hand, are susceptible to sampling errors such as net avoidance, and do not cover the whole taxonomic and size spectrum of mesozooplankton. For instance, no gelatinous organisms are accounted for, which may account for an important fraction of the wet biomass (Remsen, Hopkins, and Samson, 2004), only mesozooplankton greater than 500 μm is considered in the sampling (Kiko and Hauss, 2019); and fragile organisms, such as Rhizaria, are not quantitatively sampled by nets (Biard et al., 2016). Therefore, the observations might be biased low in comparison to the model. Furthermore, a lack of an explicit size term in the model limits a direct comparison with observations because these depend on the mesh size of the sampling net. Finally, given the above-mentioned rather pragmatic parameterisation especially of zooplankton growth and loss rates, it is very likely that the model could be improved by a tuning or calibration exercise that targets a good match between observed and simulated zooplankton concentrations. Both the mortality estimation by Hirst and Kiørboe (2002) and the zooplankton observations in the field suggest that further tuning of the model should lean towards higher mortality

rates. Nevertheless, this may require the further tuning of other parameters. Despite the complexity of the model, the considerable uncertainty in model parameters and the sparsity of observations that can constrain these parameters, this is a complex task (see, e.g. Kriest et al., 2017). Therefore, we have refrained from this effort for the present but aim at providing a better-calibrated model in the future.

The spatial variability between different profiles of zooplankton is greater in the observations than in the model, and the variability in concentrations within each single profile is much larger than the differences between the modelled mortality scenarios (Figure 2.2). Several sources of variability are not accounted for in the model as it only simulates the most relevant processes in the system. We employ a climatological model which aims at simulating the average dynamics over several years, dismissing interannual variability. Furthermore, we here compare a 3-month average from January to March while observations provide only a snapshot of a highly dynamical system. In addition, we only compared our simulated zooplankton against night observations because in our model zooplankton is always active at the surface. In reality, zooplankton is known to perform diel vertical migrations (DVMs), which could increase the export flux to the deep ocean (Aumont et al., 2018; Archibald, Siegel, and Doney, 2019; Kiko and Hauss, 2019; Kiko et al., 2020). The lack of DVM could affect the export of organic matter to greater depths, and therefore the biogeochemical turnover at the surface. Zooplankton likely also experiences lower mortality at depth (Ohman, 1990); however, off Peru these benefits might be counterbalanced by reduced oxygen availability and the concurrent metabolic costs. These obstacles for comparing zooplankton models with observations had already been described by Mullin (1975) more than 4 decades ago: a) "the zooplankton is a very heterogeneous group, defined operationally by the gear used for capture rather than by a discrete position in the food web" (Mullin, 1975). b) Zooplankton is irregularly distributed in space, not necessarily following physical features. c) Adult stages of some zooplankton groups perform vertical migrations (Mullin, 1975).

To summarise, some biases and mismatches between model and observations remain; given the uncertainties and episodic nature associated with the observations, and their correspondence to their model counterparts, further studies will be necessary to more precisely calibrate the model. For a complete model evaluation, however, the small zooplankton compartment should also be evaluated against microzooplankton samples. The high mortality scenario, B_high, is the one that is closest to the observations, due to producing the smallest concentrations of large zooplankton at the surface. However, changing this parameter was obviously not enough to match the observations.

In fact, in our model an increase of 50 % in the mortality rate produced only an increase of 14 % (0.4 mmol N m^{-2} d^{-1}) in large zooplankton mortality loss (see Section 2.4) because of the high non-linearity of the model. Indeed, potential changes in zooplankton losses of 5 mmol N m^{-2} d^{-1}, derived by fluctuations in anchovy stocks and grazing pressure (see Section 2.2) point towards much larger values for the mortality rate. An even stronger increase in the zooplankton mortality rate (e.g. Lima and Doney, 2004, applied a 5-times-larger value), along with a subsequent adjustment of other parameters may be necessary to approach observed values. In addition, complementary observations with other sampling methods, could provide a better estimation of mesozooplankton concentrations for tuning the model.

2.5.2 Zooplankton mortality and the response of the pelagic ecosystem

Our model study showed the strongest response of the ecosystem to changes in the mortality rate in the highly productive coastal upwelling. Here, the response of the model ecosystem was mainly driven by large zooplankton. This can be concluded from the close similarity of model solutions A_high and B_high, as well as of A_low and B_low (see Appendix 2.10). The mortality term for small zooplankton played a lesser role; in addition to the direct effect of the mortality rate, this compartment was also affected by grazing by, and competition with, large zooplankton. Large zooplankton fluctuations due to mortality directly affected large phytoplankton through grazing. Small phytoplankton, on the other hand, was affected by grazing but also by competition with large phytoplankton. Changing the mortality rate produced little effect on the mass loss of large zooplankton due to mortality; however, it altered the nitrogen pathways along the trophic chain and ultimately the concentrations of most plankton groups, albeit in different ways, depending on the direction of change. Under conditions of high zooplankton mortality the food chain is dominated by nitrogen transfer from large phytoplankton to large zooplankton, the classical food web attributed to highly productive upwelling systems (Ryther, 1969). When zooplankton mortality is reduced, large zooplankton increases its consumption of small phytoplankton, taking over the role of small zooplankton.

In our model, large zooplankton has a competitive advantage by feeding on its competitor, small zooplankton, a strategy that was also found to evolve in simple ecosystem models as an advantageous alternative to direct competition (Cropp and Norbury, 2020). We find that under low mortality conditions, this advantage increases. The im-

portance of competition is further evidenced in the changes in small phytoplankton concentrations in the coastal upwelling region. These were partly driven by changes in the availability of resources arising from fluctuations in large phytoplankton concentrations, which constitute the dominant group in the coastal upwelling. Natural selection, competitive exclusion and different resource utilisation strategies, together with bottom-up forcing by the physical processes in the environment, can shape the plankton community in global models (Follows et al., 2007; Dutkiewicz, Follows, and Bragg, 2009; Barton et al., 2010) and indicate bottom-up effects on the phytoplankton community. On the other hand, Prowe et al. (2012) showed that variable zooplankton predation can increase phytoplankton diversity by opening refuges for less competitive phytoplankton groups, and thus exert top-down effects. In our study, the biological interactions between two phytoplankton groups, mainly competition for resources (bottom-up), are additionally affected in a top-down manner by changes in zooplankton concentrations.

The processes driving the ecosystem response in our regional study are dominated by trophic interactions among the size classes of phytoplankton and zooplankton. We found a top-down-driven response affecting mainly the plankton compartments of the model. The direction of the total zooplankton and total phytoplankton change is determined by the large zoo- and phytoplankton groups. Small zoo- and phytoplankton buffer the response when they present opposite trends to their larger counterparts (Table 2.1). In the following, we will compare our results with a similar study by Getzlaff and Oschlies (2017).

Getzlaff and Oschlies (2017), in their sensitivity study, modified the zooplankton mortality by ±50 % in a global biogeochemical model with a spin-up time of 300 years. Their model has only one zooplankton size class with a quadratic mortality term. For their analysis, Getzlaff and Oschlies (2017) evaluated three regions: the whole domain, also referred here as "global"; the region from 20° S to 20° N which in this coarse-resolution model is mainly an oligotrophic region, and is referred to as "tropics"; and the region south of 40° S where nutrient concentrations are high and is named "Southern Ocean". After the model spin-up, global zooplankton biomass changes by about -(+)5 %, and phytoplankton biomass by about +(-)1 % in the high (low) mortality scenario (Getzlaff and Oschlies, 2017, their Fig. 2). In contrast, in our study, total zooplankton averaged over the full domain decreases (increases) by -11 % (10 %), and total phytoplankton changes by about +(-)6 % in the high (low) mortality scenario (Figure 2.4 and Table 2.1). Hence, the effects of changing zooplankton mortality follow the same trend in both studies but they are slightly milder in the study by Getzlaff

and Oschlies (2017). At the regional scale, the responses in the study of Getzlaff and Oschlies (2017) have a feedback from lower trophic levels, either to phytoplankton in the nutrient-repleted region or all the way to nutrients in the oligotrophic region. Therefore, the biomass of both zooplankton and phytoplankton is ultimately bottom-up affected. This is evidenced by a change in zooplankton and phytoplankton concentrations in the same direction (Getzlaff and Oschlies, 2017, their Fig. 3). On the other hand, although our study also exhibits a feedback from phytoplankton to zooplankton, the strongest driver remains the top-down predation of zooplankton on phytoplankton (Table 2.1).

The regional differences between our study and that by Getzlaff and Oschlies (2017) can likely be explained by the different model structures and experimental set-ups, namely the number of phyto- and zooplankton compartments, different timescales considered for model simulation and analysis, and the spatial domain: while Getzlaff and Oschlies (2017) applied a global biogeochemical model with just one size class of phyto- and zooplankton, simulated until near a steady state, our regional model study applies a more complex biogeochemical model with a strong seasonal cycle (see Appendix 2.9), simulated for only 30 years and constantly forced at the boundaries. Further, the short few-year timescale of our model simulations might have prevented the effects of changed zooplankton mortality from propagating to deeper water layers which contain the largest concentrations of nutrients. Finally, the region modelled in our study is spatially already very dynamic at the mesoscale resolution, as evidenced by well-defined plankton spatial succession from the coast of the continent towards the open ocean. The phytoplankton bloom, which develops closest

Table 2.1. Qualitative comparison of the response of total, large and small zooplankton (Z_T, Z_L, Z_S) and phytoplankton (P_T, P_L, P_S) to a 50 % higher and lower zooplankton mortality parameter in our experiments B, with the results from Getzlaff and Oschlies (2017) (Z_{GO}, P_{GO}). Full, oligotrophic and coastal upwelling refer to the regions in our study (see Fig. 2.1) integrated over the upper 100 m, global, Southern Ocean and tropics refer to the study by Getzlaff and Oschlies (2017, their Figs. 2 and 3 at year 300). We grouped together global and full because both refer to the whole model domain in each of the two studies. Similarly, oligotrophic and tropics refer to regions characterised by low nutrient concentrations, and coastal upwelling and Southern Ocean are both regions with high nutrient concentrations.

	Z_T	P_T	Z_L	P_L	Z_S	P_S	Z_{GO}	P_{GO}
Full and global								
High	−	+	−	+	−	−	−	+
Low	+	−	+	−	−	+	+	−
Oligotrophic and tropics								
High	−	+	−	+	−	+	−	−
Low	+	−	+	−	+	+	+	+
Coastal upwelling and Southern Ocean								
High	−	+	−	+	+	−	+	+
Low	+	−	+	−	−	+	−	−

to the coast and then is offset while water is transported offshore, can be explained by an imbalance between sources and sinks, triggered by changing environmental conditions. For example, Irigoien, Flynn, and Harris (2005) applied the concept of 'loopholes' proposed by Bakun and Broad (2003) to explain fish productivity and recruitment success, to phytoplankton: according to their concept, phytoplankton blooms are formed when environmental conditions open a loophole in the plankton community of a mature ecosystem. Then, particularly phytoplankton species that are able to escape microzooplankton predation are those that will take advantage of the loophole and bloom (Irigoien, Flynn, and Harris, 2005). Our model results suggest that similar processes occur. Low concentrations of large zooplankton allow large phytoplankton to bloom near the coast. While the water is advected offshore, zooplankton growth and grazing offset the bloom. Observations by Franz et al. (2012) also reported a spatial succession with large diatoms abundant in the coastal upwelling region being replenished by nanophytoplankton offshore. However, they propose silicate as the limiting nutrient offsetting the diatoms peak, which is not present in our model. Furthermore, such succession is not unique to the NHCS but a characteristic feature of upwelling regions (Hutchings, 1992). We note that in the present configuration the BioEBUS model does not include any temperature-dependent zooplankton grazing rate. We expect that, if this were implemented, the loophole for phytoplankton growth in the cold waters of the coastal upwelling region would even be widened, amplifying the spatial succession we observed. However, temperature might also affect zooplankton metabolism, with colder temperatures decreasing its loss rates, which could in turn mute these effects again. On the other hand, the global model by Getzlaff and Oschlies (2017) does not resolve mesoscale processes. Furthermore, while they divided their study into the tropics, as an oligotrophic region, and the Southern Ocean, as an upwelling region, the upwelling system off Peru in the eastern tropical South Pacific is a nutrient-rich area. For all of this, we based our comparison on similarities in the nutrient concentration (high nutrients, oligotrophic and whole domain), rather than on geographic overlap.

In Getzlaff and Oschlies (2017), the zooplankton loss due to mortality is not provided. However, it can be calculated from the zooplankton concentration and mortality rate. Assuming integrated zooplankton biomasses at year 300 (Getzlaff and Oschlies, 2017, their Fig. 2) of 98, 93 and 89 Tg N in the low, reference and high mortality scenarios, respectively; mortality parameters of 0.03, 0.06 and 0.09 (mmol N m^3)$^{-1}$ d^{-1}, and a quadratic mortality term; then there is a difference of -44.5 % and 37.4 % in the zooplankton loss due to mortality between the low and reference scenario and between the high and reference scenario, respectively. As shown in Sect. 2.4.4, the mortality rate in our study is also smaller than the ±50 % changes that would be expected from

a change in the mortality parameter of ± 50 % (see Section 2.3.4). The non-linearity of both global and regional models seems to reduce the effect of changes in the mortality parameter on zooplankton loss.

In summary both studies show a similar global response to changes in zooplankton mortality, driven by zooplankton preying on phytoplankton. Two zooplankton and phytoplankton size classes present opposite trends in our studies, buffering the overall response. Nevertheless, the relative changes in total zooplankton and total phytoplankton are on the same order of magnitude as in Getzlaff and Oschlies (2017) and even slightly higher. Regionally different feedbacks operated in the two models, possibly due to the specific set-up of each study, spin-up time and resolution. Finally, the relative change in the zooplankton loss due to mortality is smaller than the expected ± 50 % in both studies.

2.5.3   From plankton to higher trophic levels

In our study, we changed the zooplankton quadratic mortality, which could be regarded as the effect of a predator targeting highly aggregated zooplankton populations, or whose concentration closely follows that of zooplankton. This can be viewed as a way to parameterise the effect of changing fish abundance on the biogeochemistry of the system. In this case, a low zooplankton mortality implies fewer small pelagic fish (such as anchovies and sardines), while a high zooplankton mortality implies a higher abundance of such fish. Further, our experiments are based on two different assumptions: one where small pelagic fish feed only on large zooplankton (experiments A) and one where they feed on and affect the mortality of both large and small zooplankton (experiments B).

The diet of anchovy is still under debate. While previous studies had considered that anchovies feed mainly on phytoplankton, Espinoza and Bertrand (2008) concluded that anchovies feed on zooplankton, especially euphausiids and copepods. Furthermore, the diet of anchovy seems to be more flexible than previously considered (Espinoza and Bertrand, 2008). For instance, the anchovy collapse in 1972 was correlated with a shift from a population feeding mostly on phytoplankton to a southern population feeding on zooplankton (Hutchings, 1992). On the other hand, small zooplankton groups such as ciliates have been reported as a minor component of anchovies diet (Table 5 in Espinoza and Bertrand, 2008). Thus, experiments A are more likely to resemble the fluctuations in anchovy populations. On the other hand, sardines, with their finer

gill rakers, obtain most of their nutrition from microzooplankton (Lingen, Hutchings, and Field, 2006). Although currently sardines are not as abundant as anchovies off Peru, historically they have also built up large concentrations and strong fluctuations over time have been observed (Lluch-Belda et al., 1989; Rykaczewski and Checkley, 2008). Thus, when also considering sardine populations and feeding modes, experiments B (simultaneous mortality change in both large and small zooplankton) might be more appropriate to parameterise the effects of changed fishing mortality on lower trophic levels.

Although the quadratic mortality rate is constant over the entire domain, the fractional loss rate by zooplankton mortality ($\mu_{Z_i} \times Z_i$, d^{-1}) varies over the domain because of changes in zooplankton concentration. This might mimic spatially variable grazing pressure by fish. However, our experimental set-up might be too simple to investigate the detailed response of predator–prey relationships. We partly tried to avoid conclusions the are too general by focusing our analysis on the coastal upwelling region off Peru, since anchovies are highly concentrated in this region (Checkley et al., 2009). In addition, we neglected any feedback effects between zooplankton and their predator fish. A more detailed model set-up, as, for example, in coupled biogeochemical–fish models (Oliveros-Ramos et al., 2017), would help to elucidate the specific trophic interactions in this region and their response to environmental changes, and changes in fishing pressure.

Finally, we note that the parameterisation of fish predation in our study implies that all organic matter is transferred from zooplankton straight to the detritus compartment and then remineralised. In the real world, it is stored as fish for some time until the fish defecate or die (Allgeier, Burkepile, and Layman, 2017). In an equilibrium state this would not be a problem since there is a constant turnover of nutrients. In a non-equilibrium state, the time that nutrients spend as part of larger animals' biomass would increase the gap between nutrient consumption by phytoplankton and their replenishment, affecting phytoplankton growth rate and potentially the blooming timing. However, this should not be a problem in the coastal upwelling region because nutrients are highly concentrated here. This is not the case for the oligotrophic region although, in our study, this region presents the weakest response. Furthermore, small pelagic fish concentrate mainly in the highly productive upwelling region rather than in the oligotrophic waters offshore. On the other hand, fish and larger animals are highly mobile and do not constantly drift by advection as nutrients and plankton do. Therefore, migrations transport nutrients and organic matter in and out of the region in a horizontal (McInturf et al., 2019; Varpe, Fiksen, and Slotte, 2005; Williams et al.,

2018) and vertical (Davison et al., 2013; Lavery et al., 2010) fashion. Such nutrient dynamics over time and space driven by higher trophic levels can be further explored either in explicitly coupled end-to-end models or in an implicit way similarly to in our study.

2.6   Conclusions

In summary, our study showed that changes in zooplankton mortality can have a strong impact on the trophic interactions between the plankton compartments of the model. Such changes are meant to mimic variations in the abundance of planktivorous fish in the system. Large zooplankton mortality, as the top predator in the model, is the main driver of the planktonic food web response in the model. Changes in the mortality rate of small zooplankton, which may resemble fluctuations in the sardine populations, are masked when large zooplankton mortality also changes. The zooplankton high mortality scenario, which mimics an increase in planktivorous fish, generates a shorter food web where most of the nutrients are taken up by large phytoplankton. In the low mortality scenario, the biomass of small phytoplankton increases and a longer food chain where nitrogen reaches large zooplankton through consumption of small zooplankton is favoured (Section 2.4.3). Our 50 % mortality changes are small compared to changes expected from the population fluctuations that small pelagic fish have historically experienced in the NHCS (Sections 2.2 and 2.3.4). In this study we were interested in the possible top-down effects of those fluctuations on the biogeochemistry, rather than on their causes. However, in a highly bottom-up-driven system, it is important to be cautious and conservative when evaluating top-down scenarios. A fully coupled end-to-end ecosystem model explicitly including fish (as by, for example, Travers-Trolet et al., 2014) would allow the representation of the effect of temporal and spatial variability of fish. It would also allow for a specialised targeting of fish food and for including the bottom-up effect of changing zooplankton concentration on fish populations, as well as their top-down effect and its potential consequences for the entire ecosystem. However, this would also involve the inclusion of more parameters in the model (up to hundreds of parameters; see Oliveros-Ramos et al., 2017), which are only poorly constrained. Therefore, while explicitly including fish in a model widens the possibilities for controlling the system, it may also increase the sources of uncertainty. Here we utilised an already-validated physical and biogeochemical model, and parameterised the loss of zooplankton due to fluctuations in small pelagic fish, without adding additional complexity to the model. Our results may be a baseline reference for

further studies exploring such an effect.

2.7 Appendix A: Plankton parameters

Our reference simulation has the same configuration as in José, Dietze, and Oschlies (2017) which in turn is based on the parameters used in Gutknecht et al. (2013a), with minor adjustments. Tab. 2.2 provides a list of the most relevant parameters for this study, as well as their descriptions and units. This is not a comprehensive list; for the full list of parameters and their values please see Gutknecht et al. (2013a) and José, Dietze, and Oschlies (2017).

Table 2.2. Plankton parameters in the model. The complete list of biogeochemical parameters is given in Gutknecht et al. (2013a), and the values for the reference simulation are provided in José, Dietze, and Oschlies (2017).

Symbol	Description	Value	Unit
αP_S	Initial slope of P-I curve for P_S	0.025	$(\text{W m}^{-2})^{-1}\,\text{d}^{-1}$
αP_L	Initial slope of P-I curve for P_L	0.04	$(\text{W m}^{-2})^{-1}\,\text{d}^{-1}$
μ_{P_S}	Mortality rate of P_S	0.027	d^{-1}
μ_{P_L}	Mortality rate of P_L	0.03	d^{-1}
$K_{\text{NH4}_{P_S}}$	Half-saturation constant for uptake of NH_4 by P_S	0.5	mmol N m^{-3}
$K_{\text{NH4}_{P_L}}$	Half-saturation constant for uptake of NH_4 by P_L	0.7	mmol N m^{-3}
$K_{\text{NO3}_{P_S}}$	Half-saturation constant for uptake of $NO_3 + NO_2$ by P_S	1.0	mmol N m^{-3}
$K_{\text{NO3}_{P_L}}$	Half-saturation constant for uptake of $NO_3 + NO_2$ by P_L	2	mmol N m^{-3}
w_{P_L}	Sedimentation velocity of P_L	0.5	m d^{-1}
$f1_{Z_S}$	Assimilation efficiency of Z_S	0.75	–
$f1_{Z_L}$	Assimilation efficiency of Z_L	0.7	–
$g_{\text{max}_{Z_S}}$	Maximum grazing rate of Z_S	0.9	d^{-1}
$g_{\text{max}_{Z_L}}$	Maximum grazing rate of Z_L	1.2	d^{-1}
$e_{Z_S P_S}$	Preference of Z_S for P_S	0.75	–
$e_{Z_S P_L}$	Preference of Z_S for P_L	0.25	–
$e_{Z_L P_S}$	Preference of Z_L for P_S	0.26	–
$e_{Z_L P_L}$	Preference of Z_L for P_L	0.5	–
$e_{Z_L Z_S}$	Preference of Z_L for Z_S	0.24	–
k_{Z_S}	Half-saturation constant for ingestion by Z_S	1	mmol N m^{-3}
k_{Z_L}	Half-saturation constant for ingestion by Z_L	2	mmol N m^{-3}
μ_{Z_S}	Mortality rate of Z_S	0.025	$(\text{mmol N m}^{-3})^{-1}\,\text{d}^{-1}$
μ_{Z_L}	Mortality rate of Z_L	0.05	$(\text{mmol N m}^{-3})^{-1}\,\text{d}^{-1}$
γ_{Z_S}	Metabolic rate of Z_S	0.05	d^{-1}
γ_{Z_L}	Metabolic rate of Z_L	0.05	d^{-1}

2.8   Appendix B: Mesozooplankton evaluation

Modelled large zooplankton is higher than observed nighttime mesozooplankton above 100 m (Figure 2.8). Deep-water zooplankton is absent in the model, while observed mesozooplankton is present at depths between 600 and 1000 m. Mesozooplankton below 200 m further increases during the daytime (data not show; please see Fig. 4 in Kiko and Hauss (2019)).
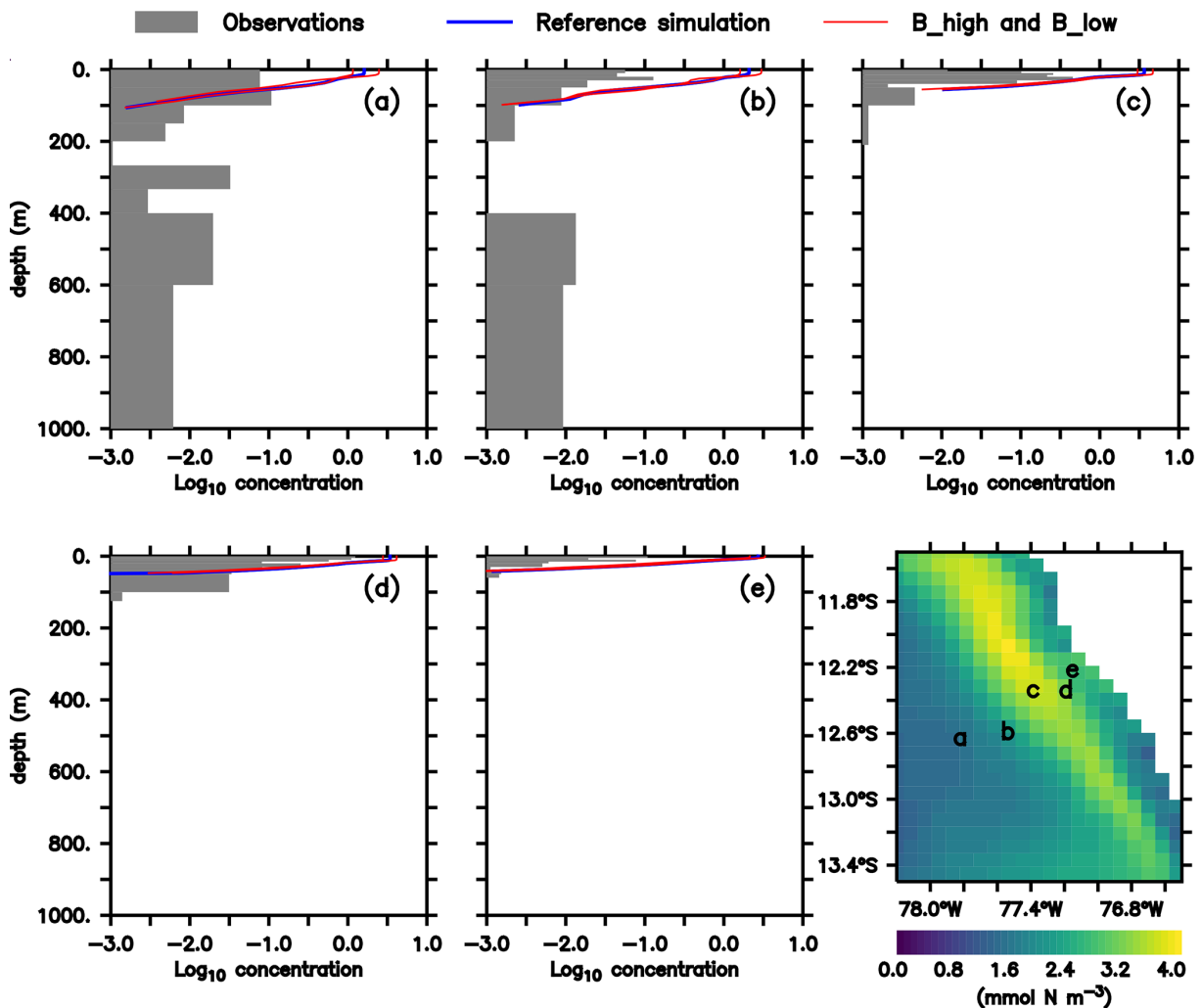

Figure 2.8. Same as Fig. 2.2, but a) to e) show a depth range up to 1000 m and a logarithmic horizontal axis.

2.9   Appendix C: Temporal variability

The NHCS presents high climatological and interannual variability. In our modelled region, small phytoplankton concentrations are relatively stable throughout the year. On the other hand, large phytoplankton production exhibits a clear seasonal pattern, with the largest concentrations presented in austral summer (Figure 2.9). Echevin et al. (2008) discuss a similar seasonal pattern found in their model. Such a pattern has also been identified in satellite-derived primary production (Messié and Chavez, 2015).
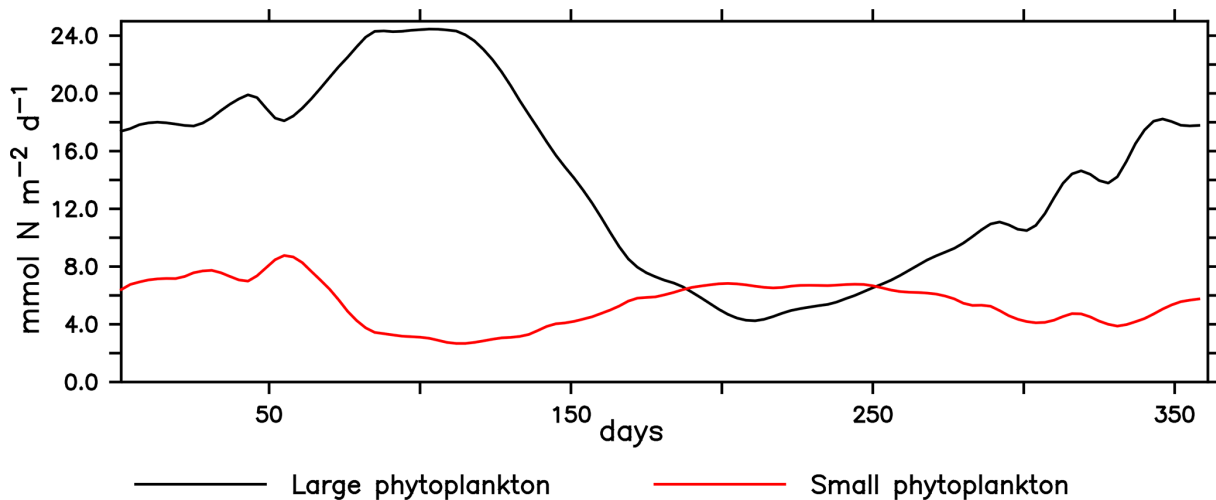
Figure 2.9. Primary production by large and small phytoplankton during the last climatological year of the simulation, averaged over the upwelling region (see Figure 2.1) and integrated over the upper 100 m in the reference scenario.

2.10   Appendix D: Plankton surface concentrations

Experiments A and B exhibit very similar spatial trends. Fig. 2.10 provides an overview of surface plankton concentrations in their reference scenario, and their changes in the experiments. Note that in the two sets of experiments, large zooplankton increased when mortality decreased and vice versa. On the other hand, small zooplankton presents a counter-intuitive response when mortality decreases, responding to the change in the concentration of its predator rather than to changes in mortality, and an ambiguous response in the high mortality cases. Large and small phytoplankton exhibit opposite trends, seemingly driven by the concentration change of their main predator (large and small zooplankton, respectively).
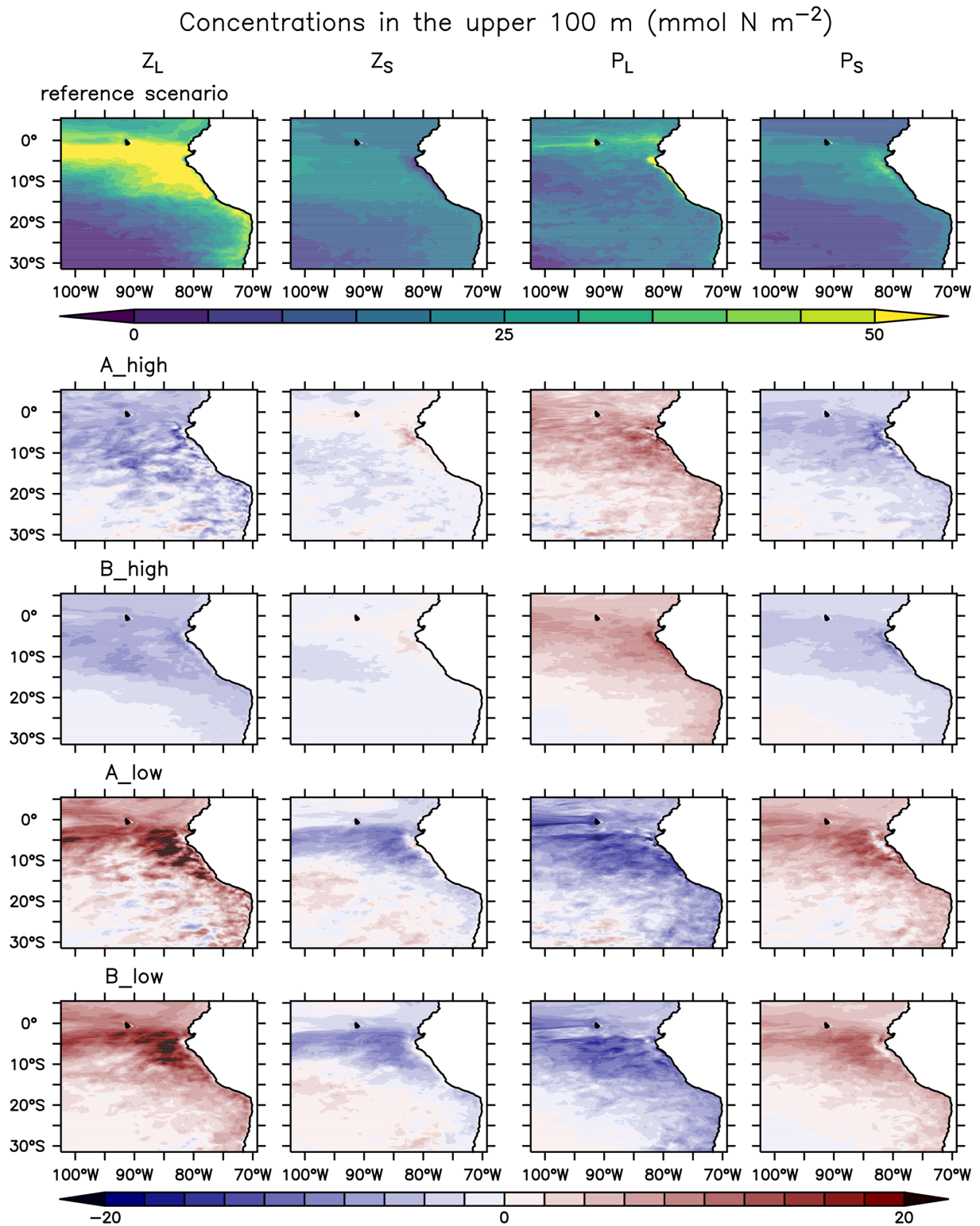
Figure 2.10. Large and small zooplankton (Z_S and Z_L) and large and small phytoplankton (P_L and P_S) integrated over the upper 100 m of the water column (mmol N m^{-2}). Rows from top to bottom: reference scenario and difference between experiments A_high, B_high, A_low and B_low and the reference scenario.

Code and data availability

Code and data used in this study are available upon request. The ROMS model is maintained at https://www.myroms.org (last access: 22 April 2021).

Author contributions

IK and AO designed the study. YSJ carried out the simulations. MHC performed the analysis. RK and HH provided zooplankton observations and expertise on zooplankton dynamics in the NHCS. All authors discussed the results and wrote the manuscript.

Competing interests

The authors declare that they have no conflict of interest.

Acknowledgements

Financial support

Sonderforschungsbereich 754 "Climate-Biogeochemistry Interactions in the Tropical Ocean" project (http://www.sfb754.de, last access: 3 May 2021).

Review statement

This paper was edited by Stefano Ciavatta and reviewed by three anonymous referees.

2.11 Supplement

2.11.1 Abstract

This supplement provides an additional comparison of the model large zooplankton with mesozooplankton observations, and additional information on the model temporal evolution.

2.11.2 Large zooplankton evaluation

Fig. 2.11 shows a comparison between the model (right) and the Eastern Tropical South Pacific region of the global mesozooplankton dataset by Moriarty and O'Brien (2013) and O'Brien and Moriarty (2012) (left). We transformed the observation values provided in the dataset to nitrogen units assuming a carbon to nitrogen ratio by weight of 4.9 (Kiørboe, 2013) and a nitrogen molar mass of 14 g/mol. Both model and observations are averaged over the whole year and over the upper 100 m depth. Model values are generally higher than observations. However, please note that the observations are sparse and in many cases there is only one data point available for the whole water column. Therefore, the averages may not be representative of the whole water column.
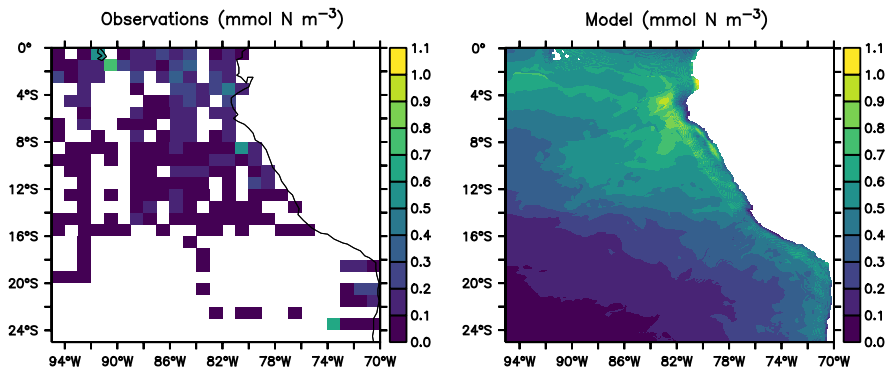
Figure 2.11. Comparison of mesozooplankton observations from the global dataset by O'Brien and Moriarty (2012), and model large zooplankton averaged over the upper 100 m depth (mmol N m^{-3}).

2.11.3 Temporal evolution of experiment A_high

Fig. 2.12 shows the temporal evolution of the four plankton groups of the model in each of the analysed regions (thick lines), as well as the interannual change (thin lines) in experiment A_high. This was calculated by taking the percentage differences between every point in time and the same point one year later. There is no noticeable trend of increase or decrease in the plankton concentrations between year 21 and 30 of the model spin-up. However, there is some variability among the years which is especially high in the coastal upwelling region (bottom), and almost completely muted in the full domain (top). In all cases, the interannual variability is much weaker than the seasonal variability.
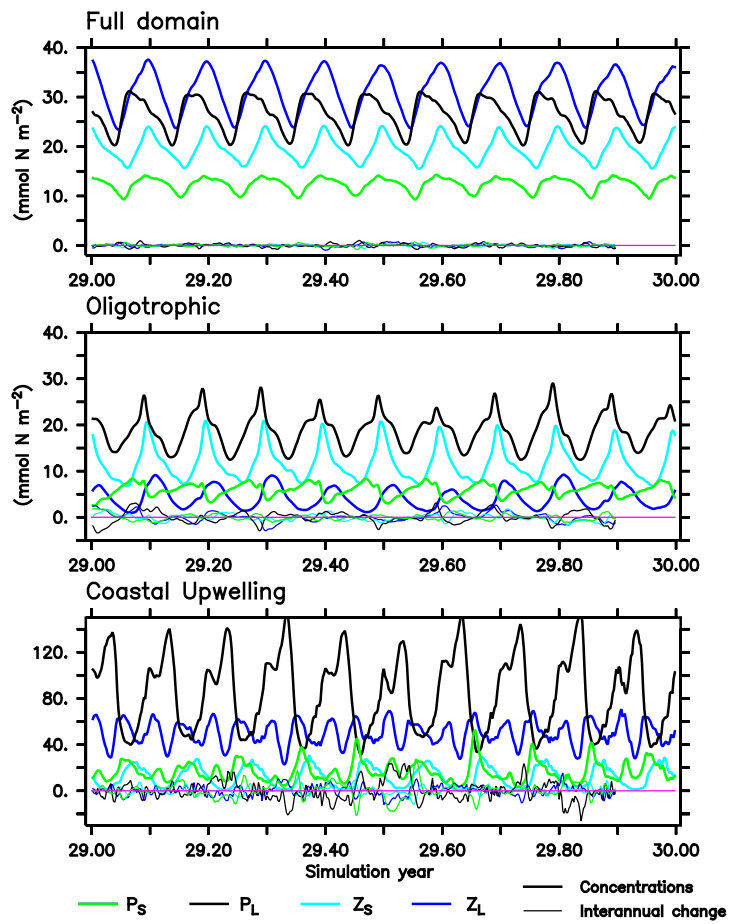
Figure 2.12. Time series from year 21 to year 30 of plankton concentrations (mmol N m^{-2}) integrated over the upper 100 m and averaged over space (thick lines), and percentage difference between every point in time and the same date one year later (thin lines), on each of the analysed regions of the model.

54

Understanding the drivers of fish variability in an end-to-end model of the northern Humboldt Current System

Mariana Hill Cruz, Ivy Frenger, Julia Getzlaff, Iris Kriest, Tianfei Xue and Yunne-Jai Shin

3.1   Abstract

The northern Humboldt Current System is the most productive eastern boundary upwelling system, generating about 10 % of the global fish production, mainly coming from small pelagic fish. It is bottom-up and top-down affected by environmental and anthropogenic variability, such as El Niño–Southern Oscillation and fishing pressure, respectively. The high variability of small pelagic fish in this system, as well as their economic importance, call for a careful management aided by the use of end-to-end models. This type of models represent the ecosystem as a whole, from the physics, through plankton up to fish dynamics. In this study, we utilised an end-to-end model consisting of a physical-biogeochemical model (CROCO-BioEBUS) coupled one-way with an individual-based fish model (OSMOSE). We investigated how time-variability in plankton food production affects fish populations in OSMOSE and contrasted it against the sensitivity of the model to two parameters with high uncertainty: the plankton accessibility to fish and fish larval mortality. The results show a small impact of interannual variability of plankton on the modelled fish in this productive ecosystem. In contrast, changes in larval mortality have a strong effect on anchovies. In OS-

MOSE, it is a common practice to scale plankton food for fish, accounting for processes that may make part of the total plankton in the water column unavailable. We suggest that this scaling should be done constant across all plankton groups when previous knowledge on the different availabilities is lacking. In addition, end-to-end modelling systems should consider environmental impacts on larval mortality in order to better capture the interactions between environmental processes, plankton and fish.

3.2 Introduction

The northern Humboldt Current System (NHCS), located in the eastern tropical south Pacific (ETSP) ocean, is the most productive eastern boundary upwelling system, generating about up to 10 % of the global fish production (Chavez et al., 2008; FAO, 2020). It hosts the largest single-species fishery of the planet, the Peruvian anchovy (*Engraulis ringens*) (Chavez et al., 2003; Aranda, 2009). Along with the Pacific sardine (*Sardinops sagax*), these small pelagic fish feed on plankton and build up huge biomasses that support a large industry of fish meal production. They are also valued by the local communities culturally (Lama et al., 2021) and economically (Christensen et al., 2014), and are consumed by many marine predators such as seabirds (Muck, 1987; Jahncke, Checkley, and Hunt, 2004), marine mammals (Majluf and Reyes, 1989) and larger predatory fish (Pauly et al., 1987). However, they have shown to be prone to collapses related to environmental variability along with overfishing (Boerema and Gulland, 1973), putting at risk the fishing industry (Paredes and Gutierrez, 2008). The drivers behind the disproportionately large fish production of the NHCS compared to other eastern boundary upwelling systems are not fully understood (Carr, 2002). Possible explanations include the reset of the system succession to small pelagic fish during the El Niño periods (Bakun and Broad, 2003), the compression of zooplankton prey for small pelagic fish at the surface by a shallow oxygen minimum zone, and increased trophic transfer efficiency caused by relatively weak winds in combination to high primary production (Chavez and Messié, 2009). The ETSP is affected by strong interannual variability. In addition to El Niño and La Niña events, the ETSP is subjected to regimes of cold ocean temperature, named La Vieja, and warm temperature, called El Viejo (Chavez et al., 2003). Anchovies and sardines also fluctuate interannually with regimes of high anchovy abundance alternating with regimes of high sardine abundance (Schwartzlose et al., 1999; Chavez et al., 2003). Causes for these fluctuations are not completely clear and have been related to interannual variability in water temperature (Chavez et al., 2003). Between the 1970s and 1990s, the ecosystem was under a regime of abundant

sardines. The regime shifted during the 1990s towards an anchovy-dominated ecosystem. Anchovy collapsed during the El Niño of 1998 but managed to recover while sardines continued declining to almost no presence by 2000 (Chavez et al., 2003; Alheit and Niquen, 2004). In addition, red squat lobsters (*Pleuroncodes monodon*), a generally benthic species off central Chile but mostly pelagic off Peru (Gutiérrez et al., 2008), became particularly abundant in the pelagic system after this event (Gutiérrez et al., 2008). Finally, the system is both bottom-up and top-down affected by environmental and anthropogenic drivers, such as changes in temperature and productivity due to El Niño–Southern Oscillation, and fishing pressure, respectively (Boerema and Gulland, 1973; Barrett et al., 1985; Barber and Chavez, 1983). The high and poorly understood temporal variability of fishes in the NHCS, as well as their importance for the economy, food security and the rest of the ecosystem, call for a careful and sustainable fisheries management using an ecosystem-based-management approach supported by end-to-end models (Pikitch et al., 2004).

End-to-end models aim at representing the marine ecosystems as a whole by including environmental components as well as lower (plankton) and higher trophic levels (HTL) such as fish and their utilisation by humans. Common ecosystem models represent functional groups or individual species interacting in a trophic-web (see Fulton, 2010; Tittensor et al., 2018, for reviews). End-to-end models also include primary producers, such as plankton, which are affected by the environment, either already included in the model (e.g., Atlantis; Fulton et al., 2004) or provided by physical-biogeochemical models (e.g., PISCES-APECOSM; Maury, 2010). Among other types of ecosystem models, the multispecies individual-based models are as detailed as simulating the single individuals or schools of fish (e.g., Rose et al., 2015). Belonging to such type of models, the Object-oriented Simulator of Marine Ecosystems (OSMOSE) simulates the whole life cycle of fish (Shin and Cury, 2001; Shin and Cury, 2004, www.osmose-model.org). It is usually one-way coupled with biogeochemical models which provide lower trophic levels, or plankton, as food for some of the fish in the ecosystem (e.g., Halouani et al., 2016; Moullec et al., 2019b). In this study, we simulated the ETSP ecosystem with a one-way coupled model system including a physical-biogeochemical (Coastal and Regional Ocean COmmunity model (CROCO) - (Biogeochemical model developed for the Eastern Boundary Upwelling Systems (BioEBUS) Shchepetkin and McWilliams, 2005; Gutknecht et al., 2013a) model and OSMOSE as HTL model.

To improve the model fit to observations, models have to be calibrated by adjusting model parameters for which no values are available easily or unambiguously from literature. Using optimisation algorithms – here in particular evolutionary algorithms –

provides an automated and objective way for calibration, and can converge to solutions that may not be reached manually or analytically when handling complex models (Duboz et al., 2010; Oliveros-Ramos and Shin, 2016). Yet, the strong variability in physical forcing and in fish abundance observed in the NHCS makes the calibration of OSMOSE for this specific ecosystem challenging. OSMOSE has been implemented in several ecosystems using time-constant parameters to represent a steady ecosystem state (Travers et al., 2006; Fu et al., 2012; Grüss et al., 2015; Halouani et al., 2016; Xing et al., 2017; Bănaru et al., 2019; Moullec et al., 2019b), which can serve as a starting point for evaluating the ecosystem response under changing conditions (e.g., Fu et al., 2012; Moullec et al., 2019a; Diaz et al., 2019; Travers-Trolet et al., 2014). Marzloff et al. (2009) developed a configuration of OSMOSE with time-constant parameters for the pelagic ecosystem off Peru using years 2000 to 2006 as reference for the calibration, just after the regime shift of 1998. On the other hand, Oliveros-Ramos et al. (2017) addressed the interannual variability of the NHCS by calibrating time-varying parameters. The resulting configuration matched the seasonal and interannual fluctuations in observations. This approach implicitly assumes that the observed variability in fish may be caused by processes that need to be accounted for by temporally varying parameter values and it provides an estimation for such parameters. However, it might dampen any variability caused bottom-up by fluctuations in physical forcing and its propagation to plankton biomass. On the other hand, using constant parameters allows to isolate the impact of time-variability in the forcings.

To investigate the potential relevance of bottom-up causes of fluctuations of fish biomass, we decided here to allow for process studies and apply a calibrated configuration of OSMOSE for the ETSP (see Figure 3.1) with constant parameters. We then explored whether interannual variability in a physical–biogeochemical model propagates through plankton to OSMOSE. To do so, we first calibrated OSMOSE against biomass and landings data of nine fish and invertebrate species from the post-El Niño, low-sardine regime between 2000 and 2008, period in which no strong El Niño event occurred. For calibration, OSMOSE was forced with a plankton climatology that we obtained from the biogeochemical model (CROCO-BioEBUS) hindcast over the time-period from 2000 to 2008. We then forced the calibrated OSMOSE configuration with an interannually varying biogeochemical hindcast from 1992 to 2008 to assess whether or not the plankton forcing alone could generate the regime shift after the El Niño of 1998 in OSMOSE. To put the effects of interannual forcing into perspective, we also carried out sensitivity experiments varying two different parameters of the OSMOSE model, which are either directly related to the food availability of the biogeochemical model, or address the larval mortality of fish species, which in previous studies has

often been adjusted to calibrate OSMOSE. The results of this study provide insight on advisable improvements for the connection of OSMOSE with biogeochemical models for a better representation of the effect of environmental variability in end-to-end models.

3.3 Methods

3.3.1 The lower trophic levels model: CROCO-BioEBUS

We used the Coastal and Regional Ocean COmmunity model (CROCO, Shchepetkin and McWilliams, 2005) coupled online with a Biogeochemical model developed for Eastern Boundary Upwelling Systems (BioEBUS, Gutknecht et al., 2013a). The model domain spans from 10°N to 33°S and from 69° to 118°W with a horizontal resolution of $\frac{1}{12}^{\circ}$ and 32 sigma layers. BioEBUS consists of 12 prognostic variables: oxygen, ammonium, nitrate, nitrite, nitrous oxide, dissolved organic nitrogen, small and large detritus, small and large phytoplankton, and small and large zooplankton. Following a spin-up of 30 years with forcing from 1990, the coupled ocean physical-biogeochemical model was simulated from 1990 to 2010 with interannually-varying forcing. The configuration used in this study is described in detail by José et al. (2019) and a list of the parameters that were adjusted for this configuration is available in Xue et al. (2021).

For coupling with OSMOSE, small and large phyto- and zooplankton were integrated above the oxygen minimum zone (OMZ; here defined by an oxygen threshold of 90 μmol O_2 kg^{-1}, Karstensen, Stramma, and Visbeck, 2008) and integrated concentrations were transformed from nitrogen to wet weight (WW, main currency in OSMOSE) by multiplying them by the conversion factors: 720, 720, 675 and 1000 mg WW mmol N^{-1}, respectively (Travers-Trolet, Shin, and Field, 2014, their Tab. 4), regridded from $\frac{1}{12}^{\circ}$ to $\frac{1}{6}^{\circ}$ resolution, and then provided as food forcing for the fish in OSMOSE (see Section 3.3.2).

3.3.2 The higher trophic levels model: OSMOSE

OSMOSE is an object-oriented individual-based model that simulates the whole-life cycle of fish, from eggs to adults. Individual fish are grouped in schools of the same size and age. These are distributed over a 2-dimensional grid (see Figure 3.1) and

within species and life stage specific distribution maps that are produced by statistical climate niche models (Oliveros-Ramos et al., 2017). On every time-step, each school moves randomly to one adjacent grid cell within its distribution map. Predation is opportunistic, based on the spatial overlap of predator and prey. Every species or group feeds on prey that falls within certain minimum and maximum predator-prey size ratios. In consequence, predatory interactions are not set *a priori* by the model user but these emerge from the size structure of the populations. A full description of the model is available in Shin and Cury (2001) and Shin and Cury (2004) and Travers et al. (2009).

Configuration overview

The configuration in this project uses OSMOSE version 3.3.3 and was derived from the configuration by Oliveros-Ramos et al. (2017), which covers the same region, from 20°S to 6°N and from 93° to 70°W (see Figure 3.1), spans from 1992 to 2008 and was calibrated against interannually-varying observations. For our configuration, we averaged the observations from 2000 to 2008, to produce a configuration representative of this period of time, after the strong El Niño of 1998. Observations were available for all groups simulated in the model for this period of time. We also averaged the

Figure 3.1. Spatial distribution of simulated anchovy in the climatological set-up (see Section 3.3.3). All schools averaged over time, after spin-up, and transformed to concentration (g wet weight m^{-2}).

plankton simulated by CROCO-BioEBUS from 2000 to 2008 to produce a plankton climatology as forcing for OSMOSE. This time period is dominated by anchovies while sardines were dominant through the 1980s and decreased during the 1990s until their final collapse after the El Niño event of 1997–1998 (Chavez et al., 2003). We set up a configuration with constant parameters to generate a mechanistic model that can be used to understand the ecosystem response to certain forcings, such as fishing pressure and environmental changes, in sensitivity studies.
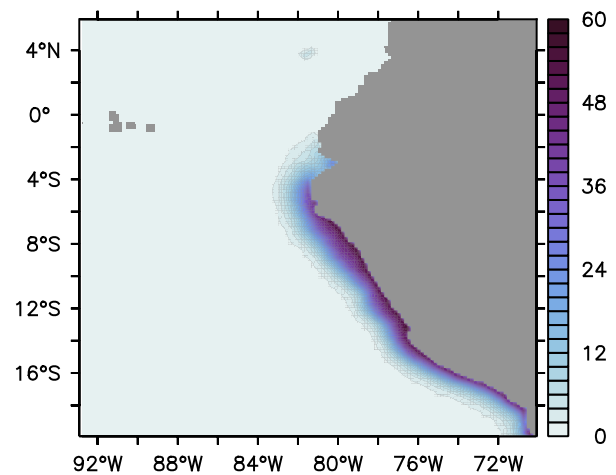
In OSMOSE, fish distribution is constrained by maps defining their habitat. The maps define the probability of a school to occur on each of the grid cells of the domain, with

the sum of all wet grid cells equalling 1. In our study, the distribution maps of each species vary for every season. At the beginning of the season, the schools are randomly located over the new map taking into account the probability given by each grid cell. We averaged the distribution maps of the configuration mentioned above, provided by Oliveros-Ramos and Lujan-Paredes (personal communication), from 2000 to 2008, to produce a climatology.

The configuration for the Northern Humboldt Current System (NHCS) consists of Peruvian anchovy (*Engraulis ringens*), Peruvian hake (*Merluccius gayi*), Pacific sardine (*Sardinops sagax*), Chilean jack mackerel (*Trachurus murphyi*), Pacific chub mackerel (*Scomber japonicus*), mesopelagic fish, squat lobster (*Pleurocondes monodon*), Humboldt squid (*Dosidicus gigas*) and euphausiids. Parameters as well as distribution maps for all groups are provided in Appendix 3.7.1 and in the supplement. The parameters in our configuration are the same as in Oliveros-Ramos et al. (2017), with the exceptions mentioned in Sect. 3.3.2. We applied constant annual fishing rates for each species in our climatological set-up. Because anchovies are only fished during certain seasons, their landings show a marked seasonality. Therefore, a seasonality of fishing rate was derived from the anchovy landings observations (see Figure 3.9 in the Appendix 3.7.1). The fishing rate of all other species was assumed to be constant over the year. The model is initialised through a seeding process that generates schools of fish at the egg and larval stages during several years at the beginning of the model run. After the initial 12 years of the spin-up, the seeding is stopped and all further eggs are only produced by adult fish.

Model calibration

The model was calibrated using the evolutionary algorithm developed by Oliveros-Ramos et al. (2017). Detailed instructions on the calibration are available in the OSMOSE documentation: http://documentation.osmose-model.org/index.html. The calibration ran for 400 hundred generations using a population size of 75 individuals (an individual is a vector of parameter values in this calibration framework) per generation for the evolutionary algorithm. In every iteration, the model was run for 50 years consisting of 25 years of spin-up and evaluating against observations the last 25 years of the simulation. Available observations included biomasses from acoustic surveys integrated over the exclusive economic zone of Peru (EEZ) and averaged from 2000 to 2008, and monthly landings of exploited species (anchovy, hake, sardine, jack mackerel, chub mackerel and Humboldt squid) also averaged from 2000 to 2008.

Because the acoustic indices only cover the EEZ of Peru, we scaled the model output by dividing it by a factor q (see Table 3.4), which represents the proportion of the averaged distribution map of each group that falls within the Peruvian EEZ.

In their configuration, Oliveros-Ramos et al. (2017) calibrated a time-varying larval mortality (LM), constant natural additional mortality, time- and size-class-varying fishing rate, time-varying plankton accessibility coefficient (AC) and time-varying incoming flux of squat lobster. In our climatology, no incoming flux of squat lobster is included, because the squat lobster is present since the beginning of the simulation, and we only calibrated time-constant LM and plankton AC. Time-constant natural additional mortalities and fishing rates (with a seasonality for anchovies, see Section 3.3.2) were obtained from the literature (see Table 3.4). In addition, we manually adjusted the fishing rate of Humboldt squid before the calibration process since our configuration had a tendency to overestimate the landings of this species.

The AC is the fraction of the total plankton that is provided as food for the fish. It parameterises a range of processes that affect the availability of plankton for the fish such as turbulence, stratification and vertical distribution and migrations (see Travers-Trolet, Shin, and Field, 2014). Literature values of this parameter for OSMOSE vary strongly, from very low values of 10^{-5} % (Marzloff et al., 2009) up to 69 % (Grüss et al., 2015). Our calibration suggested optimal values AC of 3.0, 5.0, 2.0 and 0.4 % for small and large phytoplankton and zooplankton, respectively. The larval mortality rate (LM; ts^{-1}) is applied to the first stage of fish in OSMOSE (eggs and larvae) during its first time-step (ts) of life. This parameter is typically calibrated for OSMOSE (e.g., Travers et al., 2009; Marzloff et al., 2009; Halouani et al., 2016; Bănaru et al., 2019) since field observations are scarce. The optimal parameter values are available in Tab. 3.4 in Appendix 3.7.1.

After calibrating the model, we simulated the configuration for 300 years to evaluate its stability. With the calibrated parameters, the sardine population collapses after the initial 50 years of simulation (see Supplement). To avoid this decrease, we adjusted by hand the natural mortality of juvenile and adult sardine, as well as its LM (see Table 3.4 in Appendix 3.7.1).

3.3.3   Experimental design

To evaluate the effect of an interannual versus a climatological plankton forcing on the simulated biomass of fish and macroinvertebrates, we carried out six simulations. First, starting from the calibrated climatological set-up as described in Sect. 3.3.2, we changed the plankton forcing as described below, while keeping the same calibrated parameter sets:

1. Climatological: 25 years spin-up with climatological plankton followed by 21 years of simulation using the same plankton climatology.

2. Interannual: The spin-up consisted of 4 years with climatological plankton forcing and then 21 years with interannual forcing. After the spin-up, we simulated an additional 21 years applying the interannual hindcast of plankton from 1990 to 2010.

3. Hybrid: 25 years of spin-up time with climatological plankton followed by 21 years of simulation using the interannual hindcast of plankton from 1990 to 2010.

Because OSMOSE is a stochastic model (random movement of schools and ordering of mortality events in a time-step), the output varies slightly among simulations. Therefore, we analysed the average of 20 simulations for each scenario. After the 25-year spin-up, the following 21 years of simulation (either interannual or climatological) were used for model analysis.

We contrasted the experiments with time-varying forcing with three further experiments, in which we fixed the plankton forcing to scenario "Hybrid", but changed two parameters of OSMOSE which were calibrated and have a high uncertainty. Firstly, we evaluated the effect of a reduction in the AC by 10% (Hybrid-AC), which translates into less plankton being available as potential food. In reality, this can be interpreted as, for example, zooplankton hiding in a shallower oxygen minimum zone, or a deeper mixed layer that dilutes phytoplankton. However, the specific AC for each plankton group might, to some extent, dampen the effect of the variability of different plankton groups on fish. To investigate this further, in a second parameter experiment, we set the AC to a constant value of 10% for all plankton groups (Hybrid-eqAC). We note that the resulting biomasses of this experiment are not directly comparable to the other scenarios because of the strong increase in AC. In all experiments described so far, we have investigated the effect of changing food, i.e. the gains of fish biomass, either

through the forcing, or through the AC. In a sixth experiment (Hybrid-aLM), we finally investigated how these changes on the "gain", or food, side compare to changes in loss terms of fish, by increasing the LM of anchovies by 10%. We only manipulated the LM of anchovy in order to avoid an effect obscured by trophic interactions when manipulating the LMs of the other groups.

4. Hybrid-AC: Hybrid set-up with AC reduced by 10 %.

5. Hybrid-eqAC: Hybrid set-up with AC of all four plankton groups equal to 10 %.

6. Hybrid-aLM: Hybrid set-up with anchovy LM increased by 10 %.

This study explores the effect of plankton variability on OSMOSE. Therefore, we kept climatological distribution maps in all configurations. Appendix 3.7.3 provides the results of an alternative set-up where interannually-varying distribution maps were applied from 1992 to 2008 in the hybrid configuration.

3.4 Results

3.4.1 CROCO-BioEBUS model evaluation

We evaluated the plankton compartments in the physical-biogeochemical model due to their importance as food (forcing) for the higher trophic levels model. Simulated phytoplankton biomass was converted to chlorophyll *a* using function get_chla.m of the croco_tools package (Penven, 2019) and compared against MODIS remotely sensed chlorophyll *a* (NASA, 2018). The model reproduces the temporal variability in chlorophyll *a* observations generally well, replicating the seasonal pattern with higher chlorophyll *a* in austral summer (Figure 3.2). However, from 2006 onwards it tends to overestimate chlorophyll *a*, especially during the austral summer.
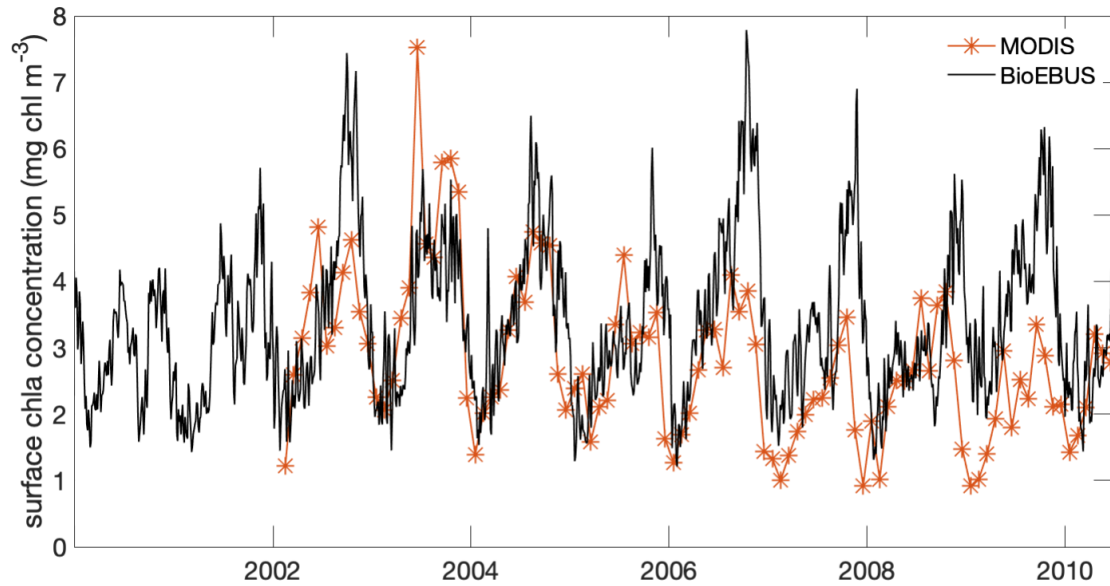
Figure 3.2. Chlorophyll *a* in the model surface layer and in MODIS observations (NASA, 2018), averaged over the closest 2° or about 200 km off the coast of Peru from 15 to 5°S.

Large zooplankton model concentrations were compared against mesozooplankton observations by Moriarty and O'Brien (2013) and O'Brien and Moriarty (2012), which are provided in carbon units. For model comparison we transformed the observations to nitrogen dividing by a carbon to nitrogen ratio of 4.9 gC/gN (Kiørboe, 2013) and by the nitrogen molar mass of 14 g/mol. Because the model does not parameterise diel vertical migrations, simulated zooplankton is only present where food is available, within the upper 100 m. We therefore compared only the averaged zooplankton in the model and observations over the upper 100 m of the water column. An extensive discussion on the possible causes of mismatch between simulated large zooplankton and mesozooplankton observations observed in an earlier version of BioEBUS is provided by Hill Cruz et al. (2021).

A previous version of the model (José, Dietze, and Oschlies, 2017) strongly overestimated zooplankton in comparison to observations (Hill Cruz et al., 2021). Therefore, for the present study, we tuned the model to better match observed concentrations. After tuning the model, large zooplankton is generally of the same order of magnitude as mesozooplankton observations (Figure 3.3). Both, model and observations, show a high concentration of mesozooplankton in the region near the Equator as well as towards the coast of Peru. Within 50 km from the coast, large zooplankton declines in the model. This is not evident in the observations; however, this might be due to the low spatial resolution of samples. Observations show a hotspot of high mesozooplankton

65

concentrations around the Galapagos Islands which is not visible in the model. This could be either a weakness of the model or it could also be an artefact in the observations due to averaging over very few samples for the whole water column.
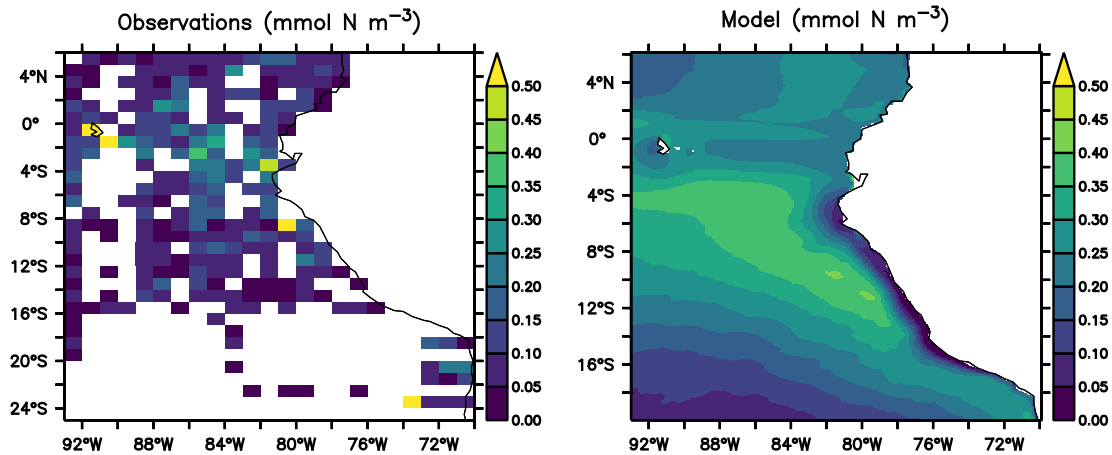

Figure 3.3. Comparison of mesozooplankton observations from the global dataset by O'Brien and Moriarty (2012) and Moriarty and O'Brien (2013) and simulated large zooplankton averaged over the upper 100 m depth (mmol N m^{-3}).

3.4.2   OSMOSE model calibration and evaluation

After calibrating and hand adjusting the parameters, simulated biomass and landings show a good fit to observed estimates for most of the groups and are stable for at least 300 years (Figure 3.4). We also evaluated the model performance by comparing the trophic levels simulated by OSMOSE (Figure 3.5) with literature values (Table 3.1). Generally, trophic levels simulated by our model system are very similar to those simulated with Ecopath models (Guénette, Christensen, and Pauly, 2008; Tam et al., 2008). The trophic structure in OSMOSE agrees with the trophic structure of Ecopath. After plankton, euphausiids are the lowest trophic level in the simulation, followed by the small pelagic fish. Humboldt squid and hake are the top predators (Figure 3.5 and Table 3.1). For anchovy, Pizarro, Docmac, and Harrod (2019) observed a trophic level of 3.23 while, in our model, the trophic level of anchovies lies between 3.1 and 3.4. Pizarro, Docmac, and Harrod (2019) point out the presence of two groups of anchovies with different diet preferences. One of them, with a mean trophic level of 2.91, prefers to graze on phytoplankton and another carnivorous group has a mean trophic level as high as 3.79 (Pizarro, Docmac, and Harrod, 2019). The smaller trophic level range of

anchovy in our study is likely due to having a single feeding preference (predator-prey size ratio range) for all schools of the same age class. We could not find trophic level estimations for squat lobster. However, given that it occupies a similar niche to anchovy (Gutiérrez et al., 2008) we may also expect a trophic level around 3. In OSMOSE we observe that it lies between about 2.5 and 3 (Figure 3.5).
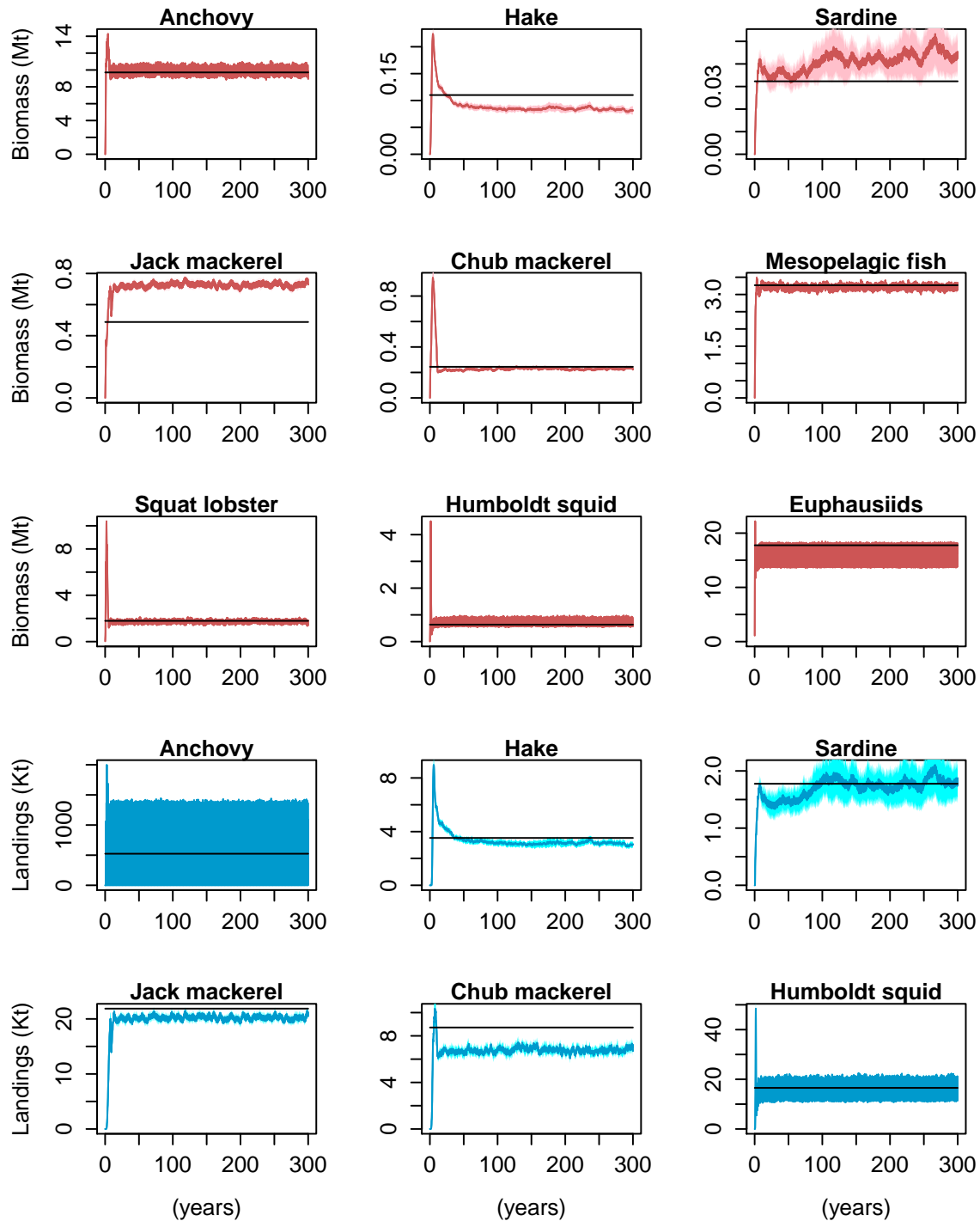

Figure 3.4. Simulated biomass (red) and monthly landings (blue) over 300 years of climatological simulation and observations averaged from 2000 to 2008 (black). These were the observations used to calibrate the model and the model output with the final set of calibrated and adjusted parameters.

3.4.3 Effect of plankton temporal variability, accessibility coefficient and larval mortality on fish biomass

Table 3.1. Trophic levels reported in the literature in Ecopath models of the NHCS (1a, 1b and 2) and observations. Sources: 1a,b Tam et al. (2008). 1a refers to a model of the ecosystem state between 1995–1996, during La Niña conditions and 1b between 1997–1998 during El Niño conditions. 2 Guénette, Christensen, and Pauly (2008). 3 Pizarro, Docmac, and Harrod (2019).

	(1a)	(1b)	(2)	obs
Anchovy	2.35	3.17	2.22	3.23 (3)
Hake	3.66-4.32	3.59-4.51	3.33	
Sardine	3.16	2.99	2.98	
Jack mackerel	2.6	3.57	3.3	
Chub mackerel	3.74	3.59	3.18	
Mesopelagics	3.49	3.12		
Squat lobster				
Humboldt squid	4.18	4.14		
Euphausiids	2.50	2.12	2.12	

The climatological calibration replicates well the time-averaged biomass of fish and macroinvertebrates for the averaged time period 2000-2008 (Figure 3.4). For most scenarios and groups, simulated biomass lies within the large variability in the observations (Figure 3.6). The hybrid and the interannual configurations show similar results (Figure 3.6), pointing out that the different spin-ups do not have a considerable impact on the simulation. This is especially evident for the eup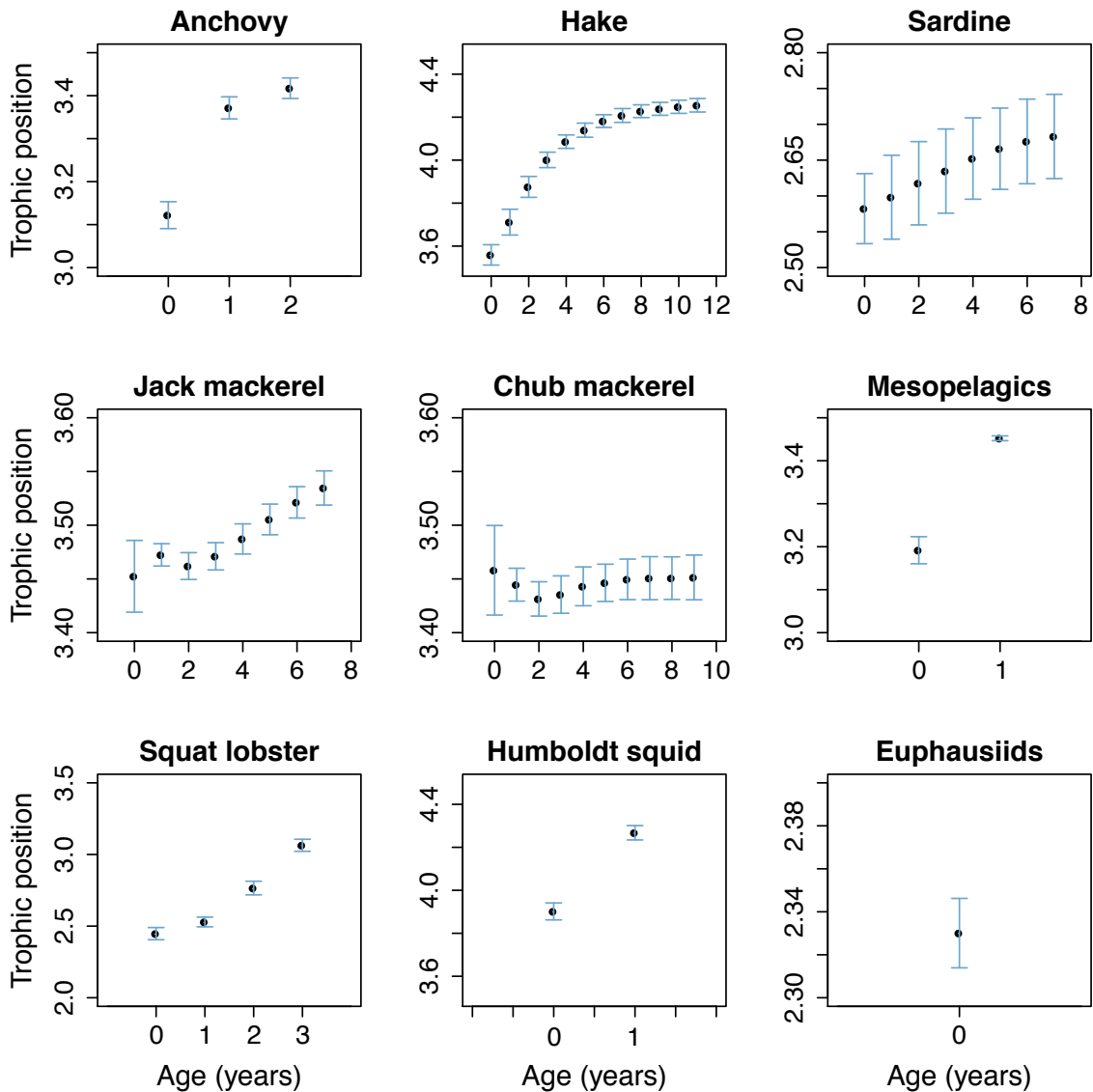hausiids (Figure 3.7 right) where both simulations converge after exhibiting different trajectories during the spin-up. This may suggest that the initial conditions are also not so important in OSMOSE once it reaches equilibrium. When comparing these two experiments with the climatological simulation, the effect of introducing interannual variability in food is evidenced by a shift of the mean biomass of euphausiids. In the hybrid configuration, anchovy and euphausiids exhibit a maximum relative interannual variability of 8.8 and 14.6 % of the mean value, respectively. However, in the climatological run, they also exhibit an interannual variability of about 4.1 and 1.1 %, respectively. Therefore, about half of the interannual variability in anchovies comes from the internal dynamics of OSMOSE rather than from the change in plankton forcing. In the case of euphausiids, most of the variability can be directly related to the change in plankton forcing. This is also evident when comparing the hybrid and interannual configuration. Both experiments exhibit almost the same results for the euphausiids, but they differ in the case of anchovies. (Figure 3.7). Such difference does not come from the plankton input but rather from the stochasticity and trophic interactions through the foodchain in OSMOSE.

Figure 3.5. Trophic levels per age class (yearly) of every group simulated by OSMOSE, starting from age–class 0. The mean of 25 years of simulation after spin-up is provided and the error bars indicate the standard deviation.

While the hybrid and interannual runs do show a different pattern than the climatological run, their interannual fluctuations tend to be small compared to the high temporal variability in the observations. Other groups show almost no difference between the climatological and the interannual and hybrid configurations. Two important changes in the ecosystem were observed after the El Niño of 1998: an increase in pelagic squat lobster and a complete collapse of sardines. These are not replicated by the model, which keeps all groups relatively constant before and after the El Niño (Figure 3.6) and highlights the importance of including other sources of temporal variability in end-to-end models, such as species spatial distribution, in addition to food (see Appendix 3.7.3).

We also investigated the importance of total food concentration on fish biomass by reducing the accessibility coefficient (AC) by 10 %. The reduction leads to a small decrease in fish biomass (Figure 3.6). In contrast, a 10 % increase in the larval mortality (LM) of anchovies has a much larger impact on this species than decreasing the AC (Figure 3.6). Therefore, in this configuration, the LM plays a greater role in controlling the biomass of fish. Finally, we also observe a clear bottom-up effect of reducing anchovy biomass on some of the other species. The effect is especially strong on squat lobster which increases when anchovy decreases, evidencing the same niche utilisation of the two species (Figure 3.6).
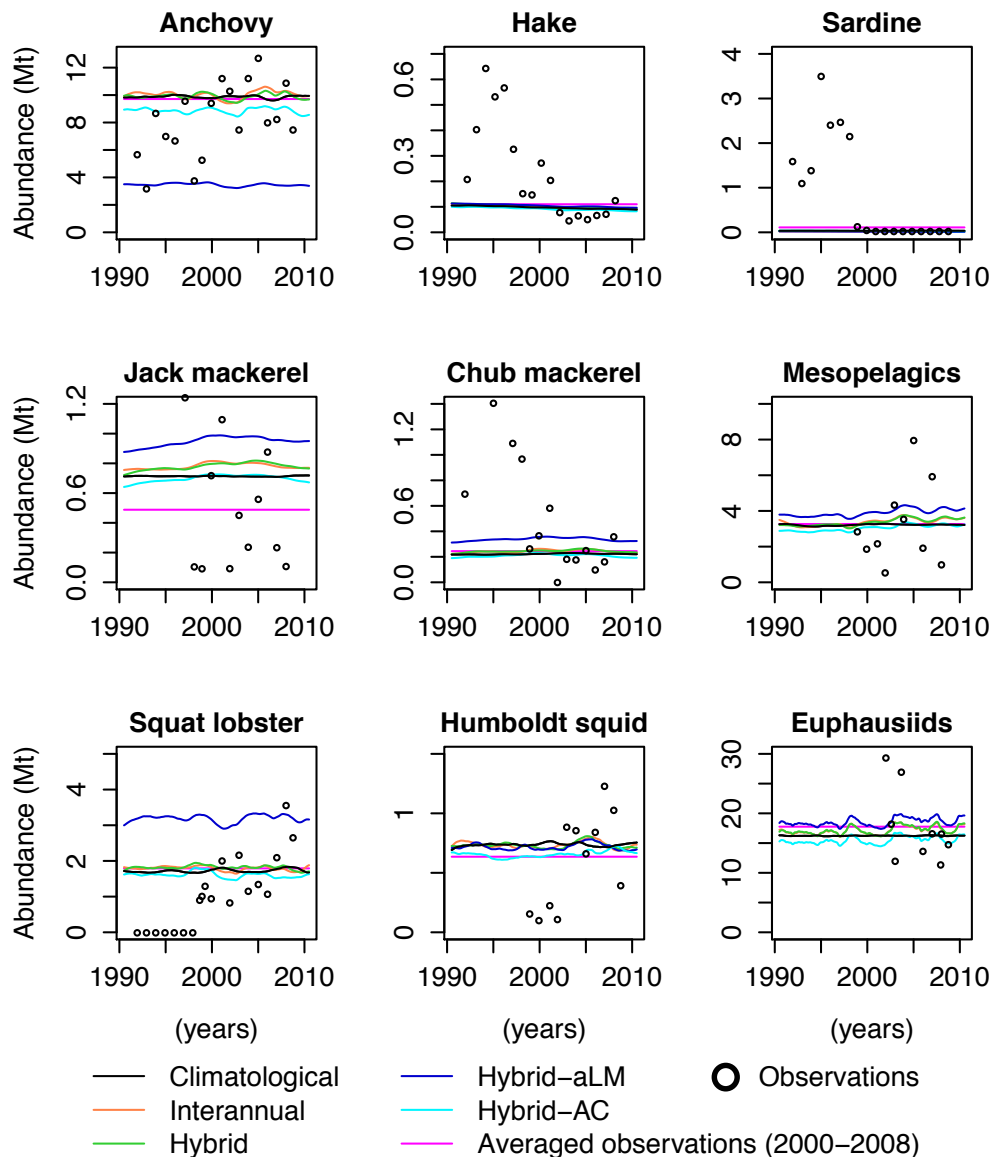
Figure 3.6. Biomass 12-months running mean after spin-up (see Sect. 3.3.3), as well as observations (dots) and 2000 to 2008 averaged observations used to calibrate the model. Observations source: Dimitri Gutierrez, Instituto del Mar del Peru (IMARPE), personal communication. Also available in Oliveros-Ramos et al. (2017), their Fig. 13

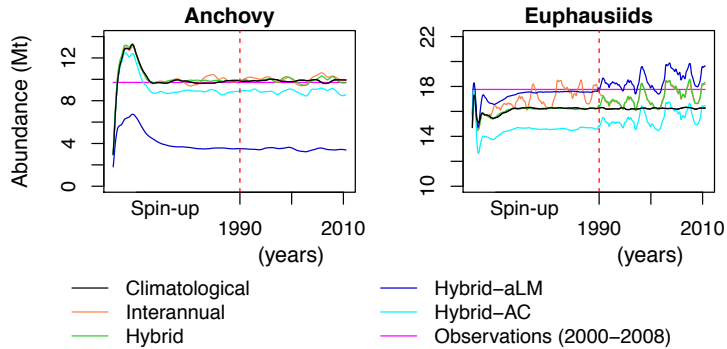### 3.4.4 Plankton accessibility coefficient effect on model temporal variability

Figure 3.7. Same as Figure 3.6 including spin-up of anchovies and euphausiids.

The plankton accessibility coefficient (AC) is a parameter that scales the plankton available for fish to eat. Because the AC was calibrated for each plankton group individually, its differences across plankton groups (low for large zooplankton and higher for the other groups) might mask the impact of seasonal or temporal variability of plankton on fish. To further investigate this issue, in Fig. 3.8, we examined the total amount of plankton (i.e., without multiplication by AC), and the variation of plankton as food (after multiplication by AC). For this specific analysis, we focused on the anchovy habitat. Therefore, we isolated the region inhabited by about 90 % of the anchovies (Figure 3.8 right). To isolate this region, we first omitted cells in the averaged climatological distribution map without anchovies and, out of the remaining cells, we selected those where the probability of finding anchovies was larger than the mean over the domain. The maximum interannual variability of total plankton in this region is 21 and 18 % with and without the calibrated plankton accessibility coefficient, respectively, and the maximum seasonal variability is 18 and 19 % (Figure 3.8 left and middle). Thus, the interannual variability of total plankton in this region as food is increased by the AC as much as 3 %. Furthermore, applying a plankton AC shifts the seasonal peak of highest food availability from October to May (Figure 3.8 middle).
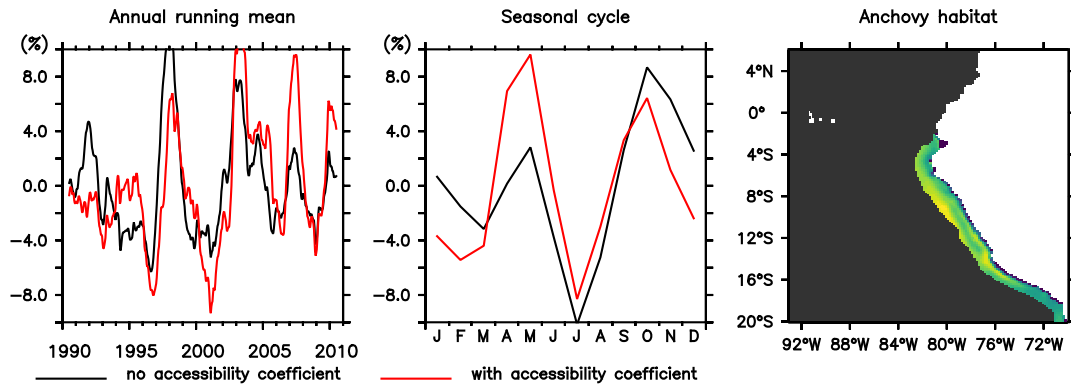
Figure 3.8. Interannual (left) and seasonal (middle) variability of total plankton in the region occupied by about 90 % of anchovies (anchovy habitat in the right panel), calculated taking into account the plankton accessibility coefficient (red) and without plankton accessibility coefficient (black).

Finally, we assessed the effect of applying the same AC to all plankton groups. In OSMOSE, in addition to the AC, the food availability to each fish group is also affected by the predator-prey size ratio, and not all plankton groups are

Table 3.2. Euphausiids diet proportions

experiment	P_S	P_L	Z_S	Z_L	others
Hybrid	34.3	37.4	24.4	2.9	1.0
Hybrid-eqAC	29.7	19.9	31.0	18.6	0.8

preyed by all planktivorous fish. For example, sardines prey on small particles such as plankton while anchovies prefer euphausiids. The temporal variability of plankton comes directly from the bigoeochemical model; while euphausiids are explicitly represented in OSMOSE and affected by the variability of their main plankton prey but also the trophic interactions with their predators. Therefore, interspecies competition and predation between species of OSMOSE may also play a role, possibly causing non-linear effects. To further investigate this, in a final experiment (Hybrid-eqAC), we set the AC parameter to a constant value of 10 % for every plankton group, thereby omitting any effects caused by the different AC values. For analysis, we focused on the impact of this change on the diet of euphausiids which are the main planktivorous group in OSMOSE and constitue about 85 % of the anchovies diet. The large, homogenous AC of 10 % increases the contribution of large zooplankton to the diet of euphausiids six times, from only 3% to 18.6 % (Table 3.2). Furthermore, setting up an equal AC for all groups also decreases the direct consumption of large phytoplankton by euphausiids by almost half (Table 3.2). This group is replaced by small zooplankton as the main prey of euphausiids. This implies that the temporal variability of zooplankton has a greater impact on euphausiids as well as their subsequent predators.

72

3.5 Discussion

Our study shows a weak effect of temporal variability in the biogeochemical model on higher trophic levels (HTL), which may be attributed to several reasons. First, it is possible that the plankton temporal variability in the CROCO-BioEBUS model is, in fact, too weak. Compared to satellite data (see 3.4.1), the surface chlorophyll in the model displays a similar variability. However, as shown in Sect. 3.4.4, the interannual variability in integrated plankton of CROCO-BioEBUS that was provided as forcing to OSMOSE is close to 20 % of the mean. This is small compared to the variability observed for anchovies. A second reason may be that the link between the biogeochemical model CROCO-BioEBUS and the HTL model OSMOSE is too weak. This link is done only through plankton food forcing for juvenile and adult fish. Other possible links may include the effect of oxygen, temperature and food availability on larval survival and through interannually-varying distribution maps. In Appendix 3.7.3, we provide an alternative configuration where additional interannual variability is introduced by applying interannual distribution maps instead of climatological. To our knowledge, the study by Oliveros-Ramos et al. (2017) is the only modelling project that has successfully replicated the regime shift after the El Niño event of 1998. They achieved this, in addition to including interannual distribution maps, by calibrating time-varying parameters. While such an approach successfully replicates the interannual variability in the system, it masks the interactions between the biogeochemical and HTL because the temporally varying model parameters account for all temporal variability, which is not necessarily justified, not allowing to pinpoint processes. For instance, in Oliveros-Ramos et al. (2017, their Figure 10), anchovy larval mortalities (LM) fluctuated more than 2-fold around the central value. In our study, we found that OSMOSE is very sensitive to the value of LM, with a 10% change decreasing the biomass of anchovy by more than half. The impact is much stronger than the effect caused by a 10 % decrease in available food. This suggests that the key to reproduce the interannual variability of the fisheries in the NHCS may not be in the food provided to adults but rather on the survival of larvae. Finally, it may be that also in the real ocean, there is not a straightforward bottom-up control of HTL as supported by Ayón, Purca, and Guevara-Carrasco (2004). They found no significant correlation between zooplankton and anchovy observations off Peru between the period of 1984 to 2001, pointing to other potential drivers than food production. Therefore, the main driver of the interannual variability in the NHCS might not be as simple as adult fish following the trends in plankton concentrations. This may be a peculiarity of the NHCS

73

that makes the modelling of this ecosystem so challenging. Simulating environmental variability in OSMOSE only through changes in plankton food for juvenile and adult fish has, in fact, produced stronger impacts in other ecosystems. Fu et al. (2012) evaluated the effects of interannual variability in plankton input on their OSMOSE model configuration for the Strait of Georgia in British Columbia, Canada. In their study, interannual variability in phytoplankton produced strong effects of more than ±50 % on their small forage fish, herring (Fu et al., 2012, their Figure 5a). This is much larger than the response observed in our study.

The maximum sustainable yield is the maximum amount of fish that can be taken from the system while keeping the population growth at sustainable levels. Past studies emphasize the importance of recruitment and mortality on the growth rate of fish populations (Tsikliras and Froese, 2019). Therefore, understanding the drivers of recruitment is essential to assess the growth of a population and, in turn, its maximum sustainable yield. In OSMOSE, recruitment is controlled by the LM parameter which represents the additional natural mortality during the first 15 days of life of eggs and larvae. It intends to account for processes that happen during the earliest life stages of fish when mortality is very high but hard to estimate from empirical studies. For instance, spatio-temporal match between larvae and plankton allows fish recruitment (Cushing, 1990). In upwelling regions, this occurs at an optimal wind stress (Cury and Roy, 1989; Cushing, 1990). In this way, the LM parameter in OSMOSE also accounts for the impact of environmental processes on larvae such as wind-dependence mixing. Our OSMOSE configuration proved to be highly sensitive to the LM parameter. Following the setting-up of other OSMOSE configurations (e.g., Vergnon, Shin, and Cury, 2008; Marzloff et al., 2009; Travers et al., 2009; Fu et al., 2012; Grüss et al., 2015; Halouani et al., 2016), we estimated this parameter during the calibration process of the model. Therefore, it was used, in combination with the plankton accessibility coefficient (AC), to adjust the fish biomass to observed levels. Alternatives to calibrating this parameter may include to find a mechanistic representation of the fine scale larvae dynamics in relation to the physical environment and food availability.

In Tab. 3.3, we compared some larval mortalities used in our configuration against literature values of egg and larval survival compiled by Dahlberg (1979). We compared survival rates of Pacific sardine and jack mackerel (Dahlberg, 1979, their Table 1). Because Dahlberg (1979) did not provide estimations for Peruvian anchovy, we compared our anchovies LM against Japanese anchovy (Dahlberg, 1979, their Table 2). The relationship between the daily larval mortality (LM/15 days = μ) and survival (S) in OSMOSE is given by $S = \frac{N(t+\Delta t)}{N(t)} = e^{-\mu \Delta t}$ (using the exponential approach provided

in OSMOSE source code: https://github.com/osmose-model/osmose/tree/master/java). The daily survival rates in OSMOSE are smaller than in Dahlberg (1979) (Table 3.3). However, this comparison has to be taken with caution since the egg and first-feeding larvae period in OSMOSE (15 days) is shorter than the periods reported by Dahlberg (1979) (Table 3.3). Therefore, the high mortality of the initial days of life of fish is concentrated over a shorter timeframe and it is not surprising that the survival rates are lower.

Table 3.3. Comparison of survival rates (dimensionless) during egg and larval stages (period of estimation provided in days) provided by Dahlberg (1979) and in our configuration. Species provided by Dahlberg (1979): Anchovy, *Engraulis japonica* (Nakai et al., 1955); Jack mackerel, *Trachurus symmetricus* (Farris, 1961); sardine, Pacific sardine (Murphy, 1961, scientific name not provided)

	Species	Anchovy	Sardine	Jack mackerel
Dahlberg (1979)	Period of estimation (days)	31	50	57
	Survival per day	0.799	0.883	0.83
OSMOSE	Period of estimation (days)	15	15	15
	Survival per day	0.555	0.461	0.524

Finding a mechanistic link between the LM and the environmental drivers will be a crucial step in the development of end-to-end models. Roy (1993) found a relationship between wind speed and recruitment of anchovy and sardine populations in several eastern boundary upwelling systems. This is based on the hypothesis that low wind and upwelling is linked to low primary productivity and recruitment; high wind-speeds, on the other hand, generates strong mixing that disperses larvae away from the food. Therefore, there is an "Optimal Environmental Window" (Cury and Roy, 1989) where the wind is neither too strong, nor too weak and maximum recruitment is achieved (Roy, 1993). From a modelling perspective, Lett et al. (2008) proposed an explicit simulation of the larval stages of fish as a Lagrangian individual-based model with salinity, temperature and velocity inputs. A simple experiment to increase the effect of food availability on fish in OSMOSE is to link the LM to the food availability through a linear relationship. Other potential improvements for the larval parameterisation in OSMOSE may include to either link the LM parameter to environmental conditions, for instance, through the relationship found by Roy (1993); or to include a whole new larval sub-model in OSMOSE, similar to the one proposed by Lett et al. (2008). The time-series of estimated larval mortalities by Oliveros-Ramos et al. (2017) provides a good fitting hindcast. A statistical relationship with the physical parametes and traces of the biogeochemical model could then be derived to produce estimates for

future projections. This may not only reduce the uncertainty in the LM but, because LM and AC act in opposite directions, it would potentially also provide insights into better estimations of the AC during the calibration process by reducing the number of parameters to be optimised.

There is no model that fits all purposes but models are useful tools to investigate certain questions. Every question, however, poses specific requirements for the model. OS-MOSE was originally developed to investigate trophic interactions among HTL such as fish (Shin and Cury, 2001; Shin and Cury, 2004). At this time, fish schools were divided into piscivorous and non-piscivorous fish and their maximum populations were regulated by a carrying capacity (Shin and Cury, 2001; Shin and Cury, 2004). Later on, it was modified to also include explicit food forcing from plankton groups (Travers, 2009) which could be derived from satellite and surveys data (Marzloff et al., 2009) or biogeochemical models (Travers et al., 2009). At this point, a carrying capacity parameter was not necessary anymore since limited resources were explicitly modelled. However, the AC was implemented to scale the biomass of plankton that is available to the fish. The reasoning behind is that not all plankton in the water-column is available for the fish to feed (Travers et al., 2009). This parameter is, however, poorly understood and it is usually calibrated. A blind calibration of the AC may, however, obscures the interactions between higher and lower trophic levels in the end-to-end model. The study by Travers-Trolet et al. (2014) and Travers-Trolet, Shin, and Field (2014) looked at the combined effects of top-down and bottom-up pressures on a two-way coupled $N_2P_2Z_2D_2$-OSMOSE model system. The fish-to-plankton feedback was achieved by calculating a mortality map of plankton based on the consumption by fish. The maximum consumption of every plankton group was given by the AC which came from a calibration. Since, in a two-way coupling system, fish consumption has a direct impact on zooplankton mortality, the AC might also affect the biogeochemistry of the model. Therefore, special attention has to be taken for the choice of this parameter.

3.6 Conclusion

We set up a climatological configuration for the northern Humboldt Current System coupling the higher trophic levels model OSMOSE with the physical-biogeochemical model CROCO-BioEBUS. Changing the climatological plankton forcing to an interannual time-series did not replicate the strong fluctuations in fish, especially sardine and anchovy, seen before and after the El Niño event of 1998. Temporal changes in

the habitat of fish may be an additional source of interannual variability. These were included by Oliveros-Ramos et al. (2017) as interannually-varying distribution maps based on statistical methods. In climate projections, these could be directly linked to the variables in the biogeochemical model. Alternative coupling methods linking other environmental drivers, for instance temperature and oxygen, with life stages of higher trophic levels, for instance larvae, may shed light into the main causes of the strong fluctuations of small pelagic fish in the northern Humboldt Current System. This, in turn, may reduce the uncertainty in the plankton accessibility coefficient which is the most poorly constrained parameter in OSMOSE. When the main goal of using OS-MOSE is to explore the interactions between higher trophic levels and biogeochemistry, including plankton, we recommend a thoughtful consideration of what the plankton accessibility coefficient represents in the model. For example, some of the large zoo-plankton may perform vertical migrations and hide in the oxygen minimum zone. In this case, it would not be available for the fish during part of the day and it would require a different accessibility coefficient. However, if this information is missing while parameters need to be calibrated, for evaluating the link between the biogeochemical processes and OSMOSE, we recommend to calibrate the same accessibility coefficient for all plankton groups.

3.7 Appendix

3.7.1 Higher trophic levels model parameters

Tab. 3.4 provides the parameters used to run OSMOSE. The original name of each parameter as it is read by the model is provided. Fig. 3.9 provides the seasonality of the anchovy landings. Additional parameters and the distribution maps are provided in the Supplement.
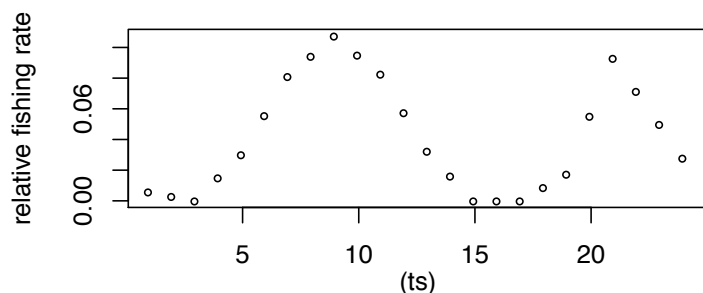

Figure 3.9. Seasonal variability in the fishing rate of anchovy. The sum of all points for 24 time-steps in one year is 1. These were calculated from monthly landings data provided by Gutierrez-Aguilar and Instituto del Mar del Peru (IMARPE) (personal communication).

Table 3.4. Parameters. Species and groups are: a for anchovy, h for hake, s for sardine, jm for jack mackerel, chm for chub mackerel, m for mesopelagics, sl for squat lobster, hs for Humboldt squid, e for euphausiids. For a detailed explanation on each parameter please refer to Shin and Cury (2004), as well as the official OSMOSE documentation: http://documentation.osmose-model.org/index.html. Source: Oliveros-Ramos and Lujan-Paredes, personal communication, based on the configuration by Oliveros-Ramos et al. (2017). *Marzloff et al. (2009) **Tam et al. (2008) ***Adjusted ****Calibrated.

Parameter	Unit	a	h	s	jm	chm	m	sl	hs	e
simulation.ncschool	n	24	12	12	24	12	148	4	48	148
species.lInf	cm	19.5	68	38.71	81.6	40.6	8	4.2	95	2.6
species.K	1/yr	0.76	0.,025	0.22	0.,167	0.41	1.15	0.,375	1.1	1.8
species.t0	years	-0.14	-0.,269	-1.34	-0.28	-0.05	-0.06	-328	-0.09	-198
species.vonbertalanffy.threshold.age	years	0.35	0.5	0.5	0.5	0.5	0.35	0.5	1	0.1
species.length2weight.condition.factor	g/cm	0.0065	0.,007	0.0089	0.0135	0.0086	0.00832	0.,174	0.,005	0.00925
species.length2weight.allometric.power	—	3	3.05	2.99	2.9248	3.26	3.15	3.03	3.4	3
species.relativefecundity	—					1				
species.egg.size	cm					0.1				
species.egg.weight	g					0.0005386				
species.sexratio	—	0.5	0.5	0.5	0.5	0.5	0.5	0.5	0.5	0.5
species.maturity.size	cm	12	35	21	29	29	2.5	1.9	66	0.8
species.lifespan	years	3	12	8	8	10	2	4	1.5	1
mortality.starvation.rate.max	1/ts	1	0.05	0.1	0.15	0.05	0.5	0.1	0.1	0.5
predation.efficiency.critical	—	0.57	0.57	0.57	0.57	0.57	0.57	0.57	0.57	0.57
predation.ingestion.rate.max	g food/ g fish/ year	3.5	3.5	3.5	3.5	3.5	3.5	3.5	3.5	3.5
predation.predPrey.sizeRation.max	—	8,6	3, 2.5	25, 150	20, 15	20, 15	3.5	2	2.5, 2, 1	15, 10
predation.predPrey.sizeRation.min	—	800, 200	50, 50	1000, 10000	300, 200	300, 200	100	150	35, 55, 70	3000, 2000
predation.predPrey.stage.threshold	cm	10	18	13	20	20	—	—	30, 60	0.6
movement.distribution.method	—					maps				
movement.randomwalk.range	cells/ts					1				
mortality.algorithm	—					stochastic				
mortality.fishing.recruitment.size	cm	12	35	21	26	26	2.5	1.9	30	0.8
mortality.natural.rate*	1/yr	0.34	0.3	0.3***	0.24	0.25	1.19	0.3	6.27	0.954**
mortality.fishing.rate*	1/yr	1.1	0.3	0.4	0.3	0.5	0	0	0.11***	0
mortality.natural.larva.rate****	1/ts	8.83	9.63	11.6***	9.7	9.16	4.63	0.61	4.47	2.6
mortality.subdt***	n					10				
osmose.version	—				Osmose 3 Update 3 Release 3 (2018/11/28)					
ltl.java.classname	—				fr.ird.osmose.ltl.LTLFastForcing					
grid.java.classname	—				fr.ird.osmose.grid.OriginalGrid					
predation.predPrey.stage.structure	—					size				
predation.accessibility.structure	—					size				
q-factor (see main text)	—	0.87	0.41	0.74	0.54	0.76	0.16	0.88	0.31	0.5
population.seeding.biomass	(tons)	8×10^6	2.1×10^5	1×10^{4}***	4.36×10^6	9×10^5	1.5×10^7	1×10^7	3×10^6	4×10^7

3.7.2 Calibration evolution

The calibration ran for 400 generations using 75 individuals. The global fitness function evolved from an original global fitness of 521.59 on the first generation, to 0.29 on generation 200. From here, it only decreased to 0.26 at generation 400. Figs. 3.10 and 3.11 show the evolution of the parameter sets over the first half of the calibration.
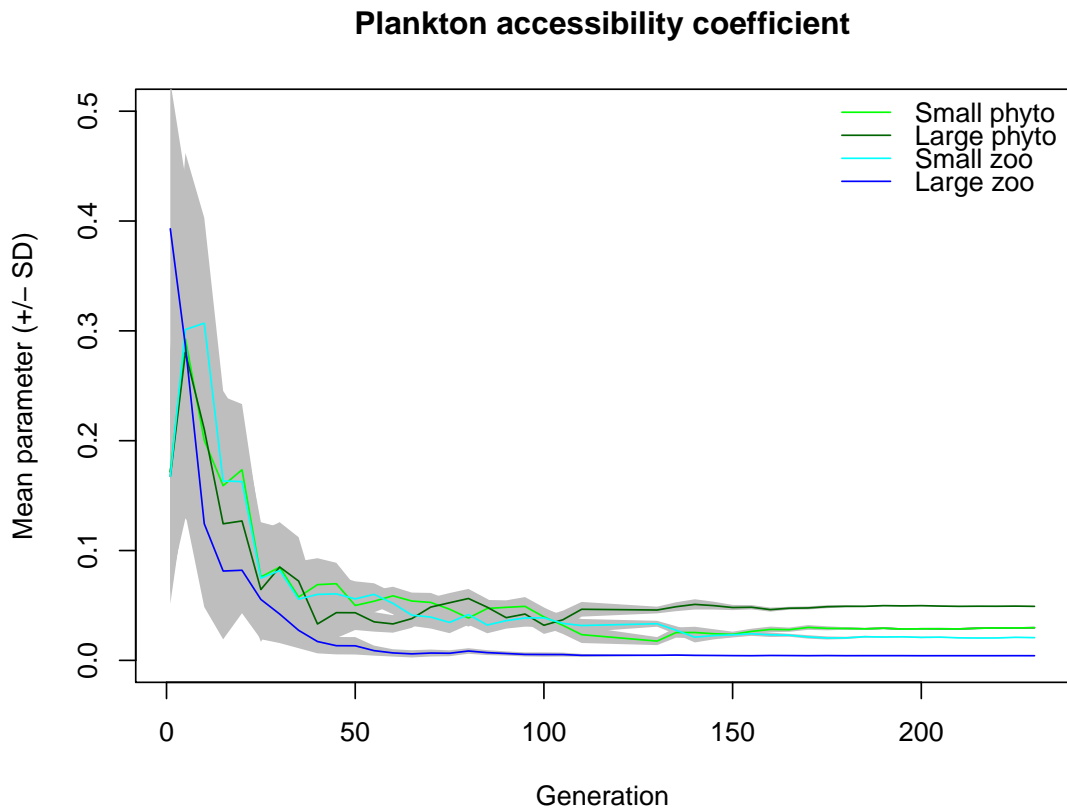
Plankton accessibility coefficient

Figure 3.10. Mean plankton accessibility coefficient (dimensionless) and standard deviation (shaded area) of the parameters in the 75 individuals of the calibration.
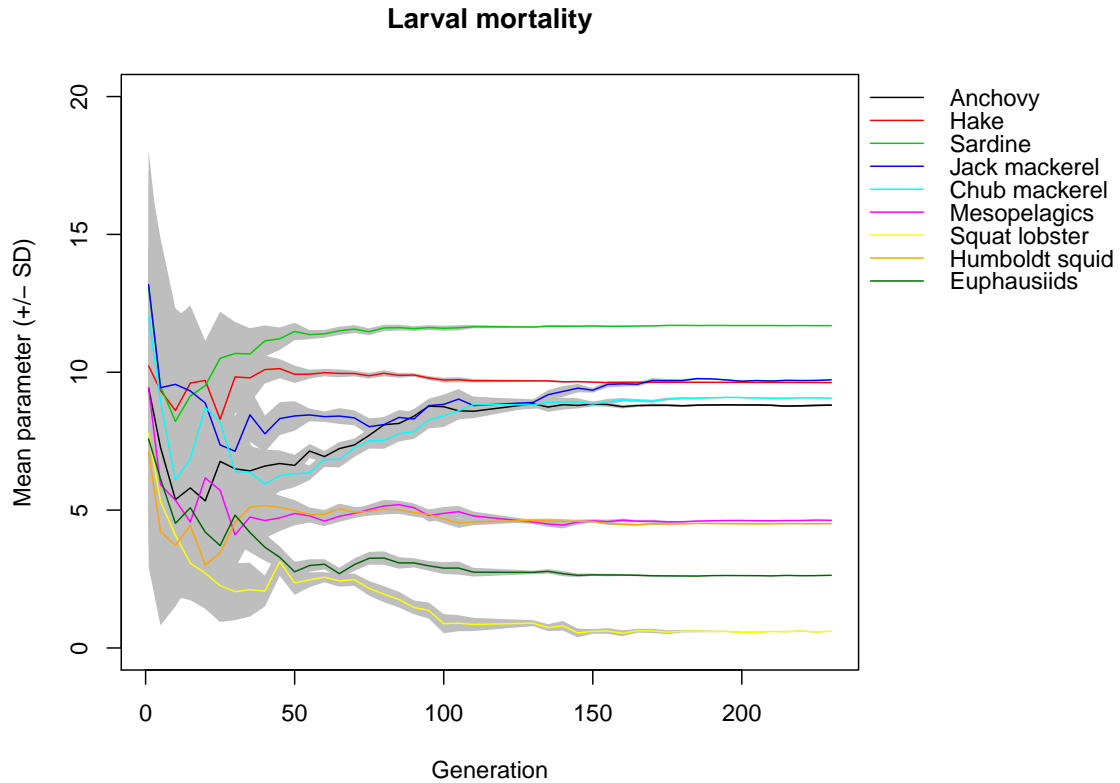
Larval mortality

Figure 3.11. Same as Fig. 3.10 for the larval mortality (1/ts)

3.7.3 Configuration with interannual distribution maps

In this section we examine the hybrid configuration (see Section 3.3.3) running with interannually-varying distribution maps from 1992 to 2008 instead of climatological distribution maps. The initalisation, food forcing and parameters are the same as in the hybrid configuration. The interannual distribution maps are the same as used by Oliveros-Ramos et al. (2017).

Applying interannual variability to the distribution maps has a visible impact on the fish when compared to using climatological maps (Figure 3.12). Compared to the hybrid configuration, in the configuration with interannual maps, some of the groups, for instance Humboldt squid, exhibit a stronger interannual variability (Figure 3.12).
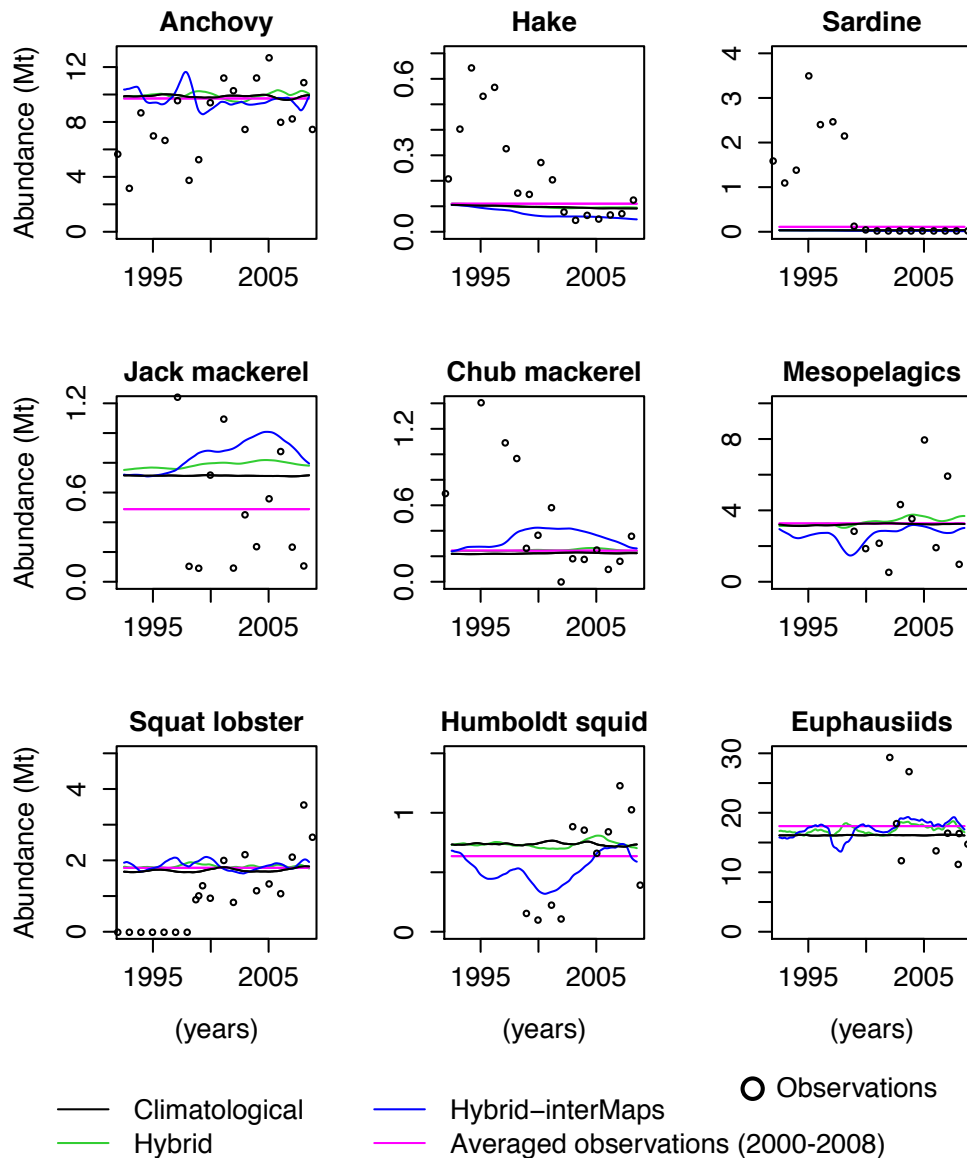
Figure 3.12. Biomass 12-month running mean after spin-up of the climatological and hybrid configurations (see Sect. 3.3.3), and the hybrid configuration with interannual distribution maps from 1992 to 2008 (HybridinterMaps), as well as observations (dots) and 2000 to 2008 averaged observations used to calibrate the model. Observations source: Dimitri Gutierrez, Instituto del Mar del Peru (IMARPE), personal communication. Also available in Oliveros-Ramos et al. (2017), their Fig. 13

3.7.4   Plankton interannual and seasonal variability

Plankton has interannual and seasonal variability. These are highly affected by the accessibility coefficient (intV = 13 % and 9.1 % and seasV = 19 % and 27 %, Figure 3.13) in the full domain. On the other hand, the accessibility coefficient has a smaller effect when considering only the anchovy habitat (see Sect. 3.4 for a description of the anchovy habitat; intV and seasV differences are only 3 and 1 %, respectively, Figure

3.13).
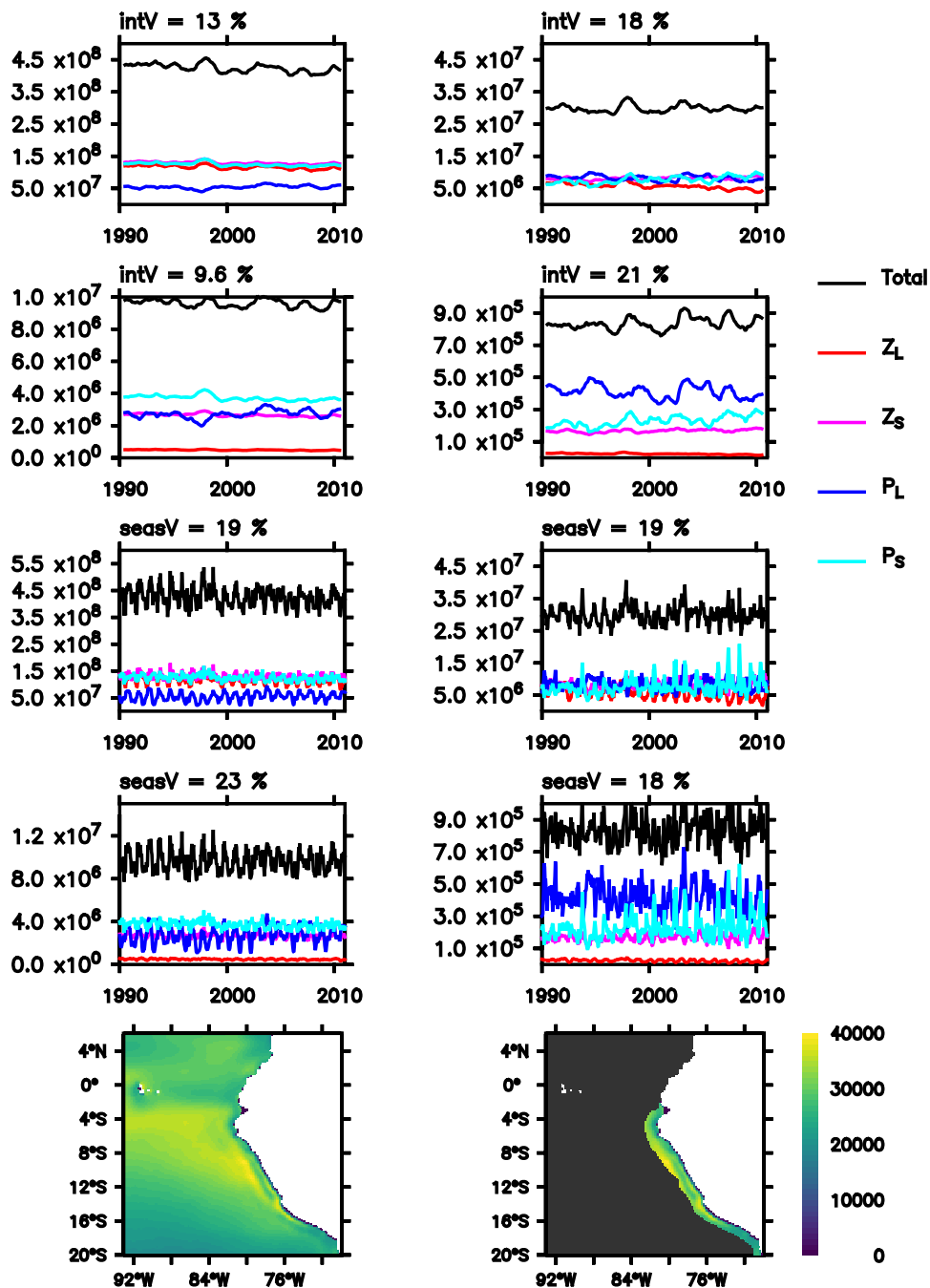
Figure 3.13. Rows top to bottom: annual running mean of plankton, annual running mean of plankton multiplied by their respective accessibility coefficients, plankton time-series multiplied by their respective accessibility coefficients (tonnes) and time-averaged total plankton (tonnes per grid cell). intV and seasV refer to the relative difference between the maximum and minimum of the annual running mean and the seasonal cycle, respectively. Columns: plankton in the whole domain (left) and plankton in the region where 90 % of the anchovies live.

Acknowledgements

Author contributions

MHC, IK and JG designed the experiments. MHC calibrated the OSMOSE climatological configuration, ran and analysed the experiments, and led the writing of the paper. TX tuned and ran the interannual hindcast of the CROCO-BioEBUS model. IK, JG, IF and YS provided guidance and scientific expertise. All authors contributed to the discussion of results and writing of the paper.

3.8 Supplement

3.8.1 Abstract

The supplement provides details on the calibration set-up of OSMOSE. It also provides parameters that, for the sake of simplicity, were not included in the main body of the paper and also the distribution maps of all higher trophic levels. An alternative configuration with other sets of parameters is also provided. Finally, we included a more detailed description of the differences in euphausiids diets between the Hybrid and Hybrid-eqAC configuration.

3.8.2 Calibrated parameters

Tab. 3.5 provides the calibrated parameters, including the initial guess and boundaries used in the model. Initial guess and boundaries were set based on previous work as well as the results of calibration tests and adjustments by hand in order to avoid species collapses since the beginning of the calibration at least in one of the individual sets of parameters. In addition, the anchovy landings and biomass were already within the order of magnitude of the observations. This was done to avoid local minima. ts unit refers to model time-step (24 per year).

Table 3.5. Calibrated parameters. Low and high are the minimum and maximum values that the parameter could take during the calibration process. AC stands for plankton accessibility coefficient and LM for larval mortality. Species and groups are: a for anchovy, h for hake, s for sardine, jm for jack mackerel, chm for chub mackerel, m for mesopelagics, sl for squat lobster, hs for humboldt squid, e for euphausiids, sp for small phytoplankton, lp for large phytoplankton, sz for small zooplankton and lz for large zooplankton.

Parameter	Unit	Initial guess	Low	High
AC-sp	—	0.1	0	1
AC-lp	—	0.1	0	1
AC-sz	—	0.1	0	1
AC-lz	—	0.4	0	1
LM-a	1/ts	9	0	30
LM-h	1/ts	10.42	0	30
LM-s	1/ts	13.1	0	30
LM-jm	1/ts	13.31	0	30
LM-cm	1/ts	12.6233	0	30
LM-m	1/ts	9.2	0	30
LM-sl	1/ts	7	0	30
LM-hs	1/ts	6	0	30
LM-e	1/ts	6.7	0	30

3.8.3 Additional parameters

Fig. 3.14 and Tab. 3.6 contain parameters that also were used to run the model but were not included in the main text.
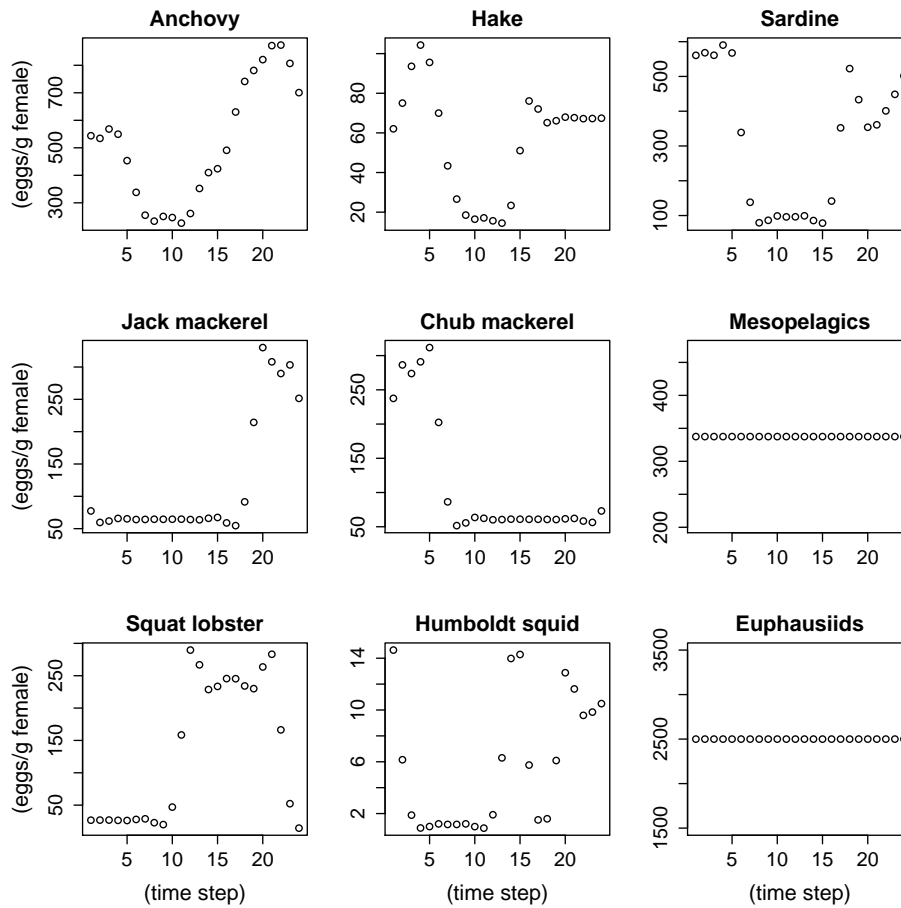
Figure 3.14. Seasonal egg production. Source: Oliveros-Ramos and Lujan-Paredes, personal communication, based on the configuration by Oliveros-Ramos et al. (2017). Note that this model configuration has 24 time-steps per year.

Table 3.6. Predation accessibility matrix. Source: Oliveros-Ramos and Lujan-Paredes, personal communication, based on the configuration by Oliveros-Ramos et al. (2017).

	anchovy	hake	sardine	jurel	caballa	meso	munida	pota	euphausidos
anchovy	1	0.2	0.9	0.9	0.9	0.55	0.9	0.6	0.6
hake	0.1	1	0.15	0.15	0.15	0.45	25	0.65	0.5
sardine	0.9	0.2	1	0.9	0.9	0.6	0.9	0.6	0.6
jurel	0.9	0.15	0.9	1	0.9	0.6	0.9	0.7	0.6
caballa	0.9	0.15	0.9	0.9	1	0.9	0.9	0.6	0.6
meso	0.55	0.45	0.6	0.6	0.9	1	0.5	0.95	0.9
munida	0.05	0.02	0.05	0.9	0.9	0.5	1	0.5	0.55
pota	0.6	0.65	0.6	0.6	0.6	0.95	0.5	1	0.95
euphausidos	0.6	0.5	0.6	0.5	0.6	0.9	0.55	0.95	0.6
small phyto	1	0.06	1	0.5	0.8	1	1	1	1
large phyto	1	0.06	1	0.5	0.8	1	1	1	1
small zoo	1	0.06	1	0.5	0.8	1	1	1	1
large zoo	1	0.06	1	0.5	0.8	1	1	1	1

3.8.4 Distribution maps

The distribution maps used in this study were derived from the distribution maps produced by Oliveros-Ramos (2014) using niche-based Generalised Additive Models (GAM). These maps provide the potential distribution of species over the time period of 1992 to 2008. For our study, we averaged the maps from 2000 to 2008, after the El Niño event of 1998 and the corresponding regime shift, to produce climatological distribution maps. There are four maps per species or functional group describing its seasonal distribution (Figures 3.15 to 3.17). At the beginning of the season, the model distributes randomly all schools over the map and the probability of a species being placed on each cell is given by the value of the cell.
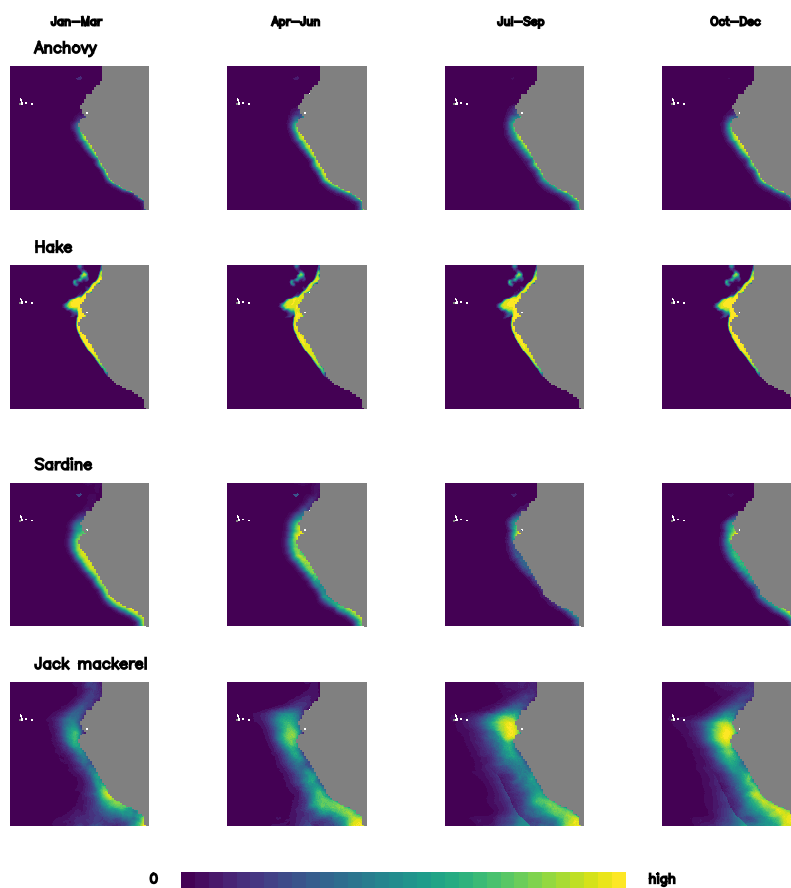
Figure 3.15. Seasonal distribution maps of anchovy, hake, sardine and jack mackerel. Probability of a school appearing in each grid-cell. The sum of all probabilities in a map is 1.
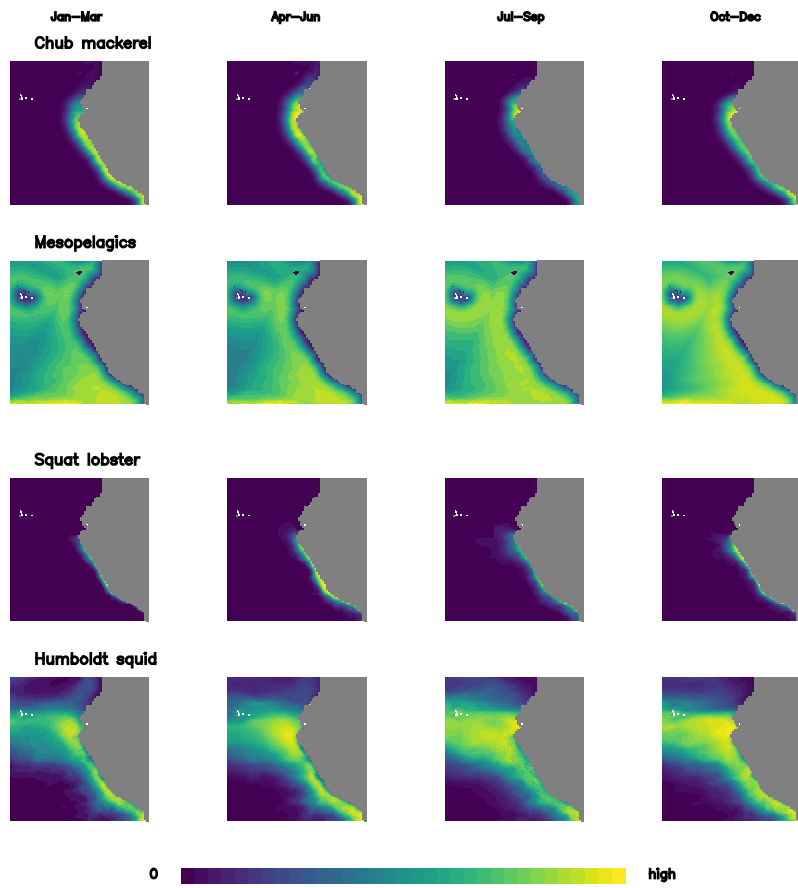
Figure 3.16. Same as Fig. 3.15 for chub mackerel, mesopelagic fish, squat lobster and Humboldt squid.
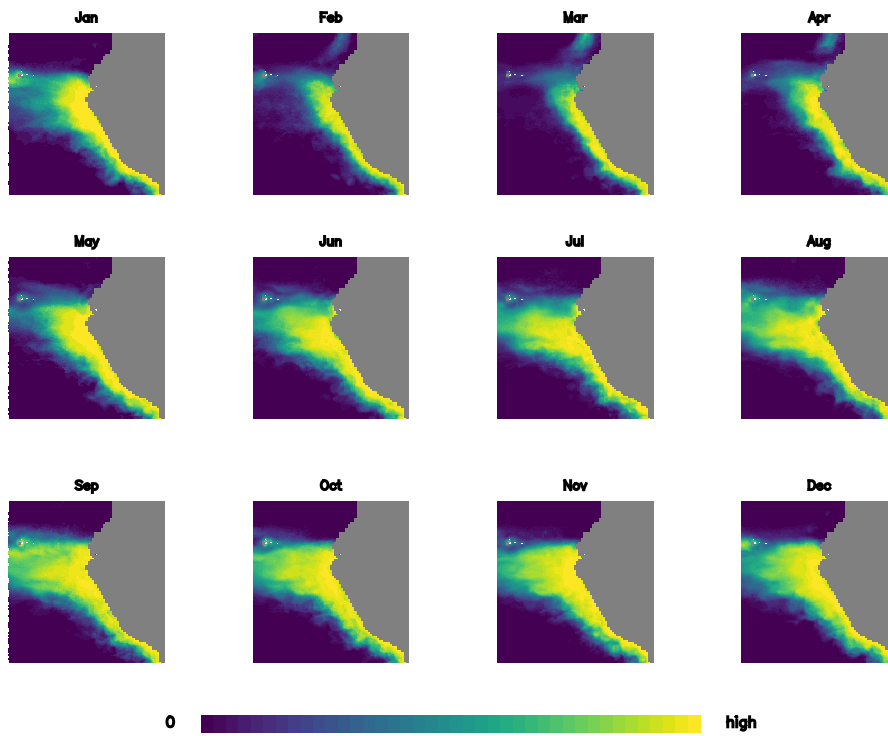
Figure 3.17. Euphausiids monthly distribution maps. (see Figure 3.15)

3.8.5 Alternative configuration

The evolutionary algorithm used to calibrate the model produced a relatively good configuration with the exception that the sardine collapsed after the initial 50 years used to run the calibration (Figure 3.18). Therefore, we manually adjusted the larval mortality of sardines after calibrating.
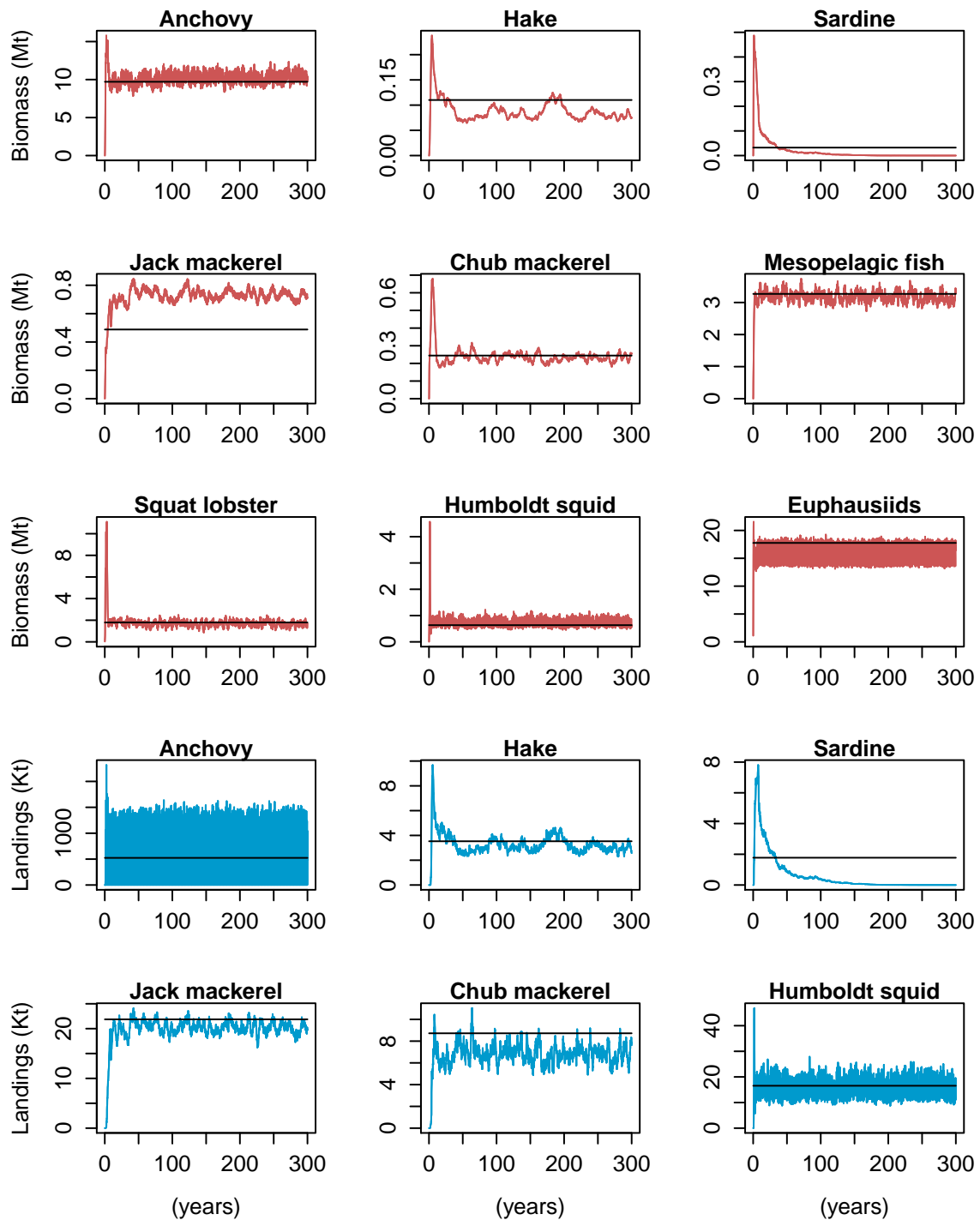
Figure 3.18. Model biomass (red) and monthly landings (blue) over 300 years simulation and averaged observations (black) before the larval mortality of sardines was adjusted.

3.8.6 Euphausiids diet

Euphausiids diet preferences is affected when changing the plankton accessibility co-
efficient (Figure 3.19). In the Hybrid configuration, their main prey is large phyto-
plankton and their consumption of large zooplankton is negligible. On the other hand,
when setting up equal accessibility coefficients to all plankton groups, euphausiids
prefer to prey on small phyto- and zooplankton. Furthermore, their consumption of
large phyto- and zooplankton is almost equal (Figure 3.19). There is also a difference
in the interannual variability of the total food consumption by euphausiids between
experiments Hybrid and Hybrid-eqAC. In the former, the highest consumption occurs
around 2003 and in the latter around 1998 (Figure 3.19).
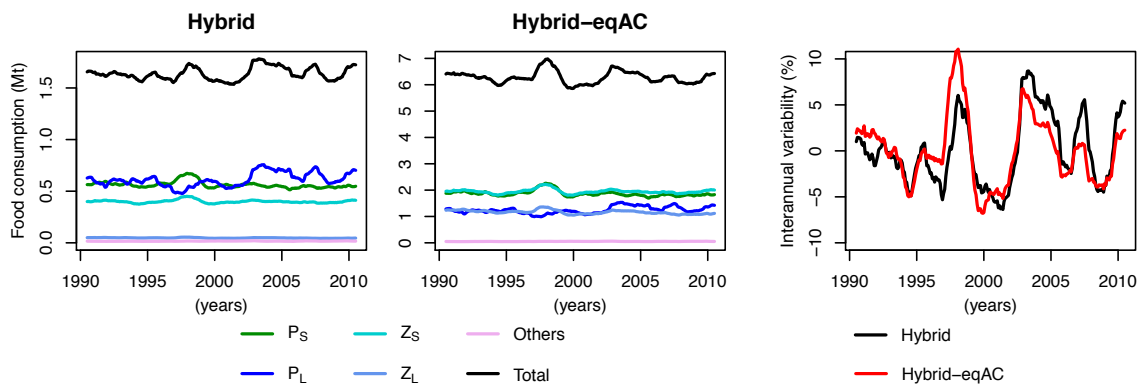
Figure 3.19. Food consumption by euphausiids (left and middle) and interannual anomaly in the total
diet (right)

Fishing pressure impacts on anchovy and hake off Peru

Mariana Hill Cruz

This chapter explores the impact of changes in fishing pressure on two fishes in OSMOSE.

4.1   Abstract

The Peruvian anchovy (*Engraulis ringens*) is a small pelagic fish. It is the largest single-species fishery in the world and it is used mainly for the production of fishmeal and fish oil. The Peruvian hake (*Merluccius gayi*) is a predatory demersal fish that is valued for direct human consumption, mainly as frozen products. In this study, I compared the response of both species to certain fishing mortality scenarios using a climatological set-up of the multispecies model OSMOSE for the northern Humboldt Current System. I observed that hake landings benefit from a decreased fishing pressure. In addition, the resilience of the anchovy fishery may increase if a higher threshold for their minimum catch size was implemented. The results of this study provide insights into better management strategies that could be beneficial for the two species based on their life–strategies.

4.2   Introduction

The waters off Peru, in the northern Humboldt Current System, are the most productive part of the ocean in terms of fish (Bakun and Weeks, 2008). They host the Peruvian anchovy (*Engraulis ringens*) which is the largest single-species fishery of the

planet (Ñiquen Carranza et al., 2000; Chavez et al., 2003). Its production peaked in 1971 at 12.3Mt (Aranda, 2009). It is mainly used to produce fishmeal and fish oil. As the largest producer of these products, Peru generated in average 1.7 and 0.27 Mt of fishmeal and fish oil, respectively, between 2001 and 2006 (Péron, François Mittaine, and Le Gallic, 2010). Fishmeal is used mainly in aquaculture as food and also to feed land stock animals which are eventually consumed by humans (Shepherd and Jackson, 2013). Fish oil is used in aquaculture and for direct human consumption as nutritional supplements (St. John et al., 2016).

Anchovy is a small pelagic fish living in large congregations in the nutrient-rich waters off Peru between 0 and 60 m depth (Ñiquen Carranza et al., 2000). Its main source of food are euphausiids followed by copeopods (Espinoza and Bertrand, 2008). It spawns all year round with the biggest peak between September and November and a smaller peak between February and April. This second peak leads to the greatest recruitment of the year (studies included in Pauly and Tsukayama, 1987b). Fishing is prohibited during austral spring and autumn to protect the populations during these spawning peaks. In addition, the minimum catch size of anchovy is 12 cm (Salvatteci and Mendo, 2005; Arias Schreiber, 2012). Anchovy is prone to fluctuations and collapses due to the interannual variability in the oceanographic conditions of the NHCS. It collapsed during the El-Niño events of 1972, 1983 and 1998. It is believed that at least the collapse of 1972 was also influenced by overfishing (Alheit and Niquen, 2004; Arias Schreiber, 2012). Since 1995, the fishery has benefited from regulatory efforts to ensure its sustainability, as well as suitable environmental conditions (Arias Schreiber, 2012).

The Peruvian hake (*Merluccius gayi*) is a large demersal fish that lives in the coastal waters off South America between 1° N and 14° S, extending up to 18° S during El-Niño events (Guevara-Carrasco and Lleonart, 2008). The wider dispersion during this period is thought to have contributed to decreased cannibalism (Guevara-Carrasco and Lleonart, 2008). Hake is valued for human consumption due to its white meat (Del Solar, Sánchez R., and Piazza L., 1965) and it has been industrially exploited since the 1960s to be exported as frozen food (Guevara-Carrasco and Lleonart, 2008). The hake fishery collapsed in 2002 and a moratorium of 20 months was implemented (Guevara-Carrasco and Lleonart, 2008). However, the fishery biomass remained low throughout the 2000s (Guevara-Carrasco and Lleonart, 2008).

Hake and anchovy are two fisheries of the Peruvian upwelling system of high economic importance. They have very different life strategies and both have been subjected to overfishing in the past. In this study, I used the climatological configuration,

presented in Chapter 3, which was calibrated to replicate the average biomasses of anchovy and hake from 2000 to 2008, to analyse and compare the responses of anchovy and hake to different fishing scenarios. This study is relevant as a starting point for exploring management strategies that may be successful for each of the two species based on their specific life strategies.

4.3 Methods

For this study, I used the one-way coupled CROCO–BioEBUS–OSMOSE climatological set-up described in Chapter 3. CROCO–BioEBUS (Shchepetkin and McWilliams, 2005; Gutknecht et al., 2013a) is a regional physical–biogeochemical model specifically designed for studying eastern boundary upwelling systems. OSMOSE (Shin and Cury, 2001; Shin and Cury, 2004) is an individual-based model that simulates the life-cycle of fish and other higher trophic levels. The climatological set-up for the Humboldt system simulates the mean ecosystem state from years 2000 to 2008. It consists of four plankton groups and nine species of higher trophic levels including the Peruvian anchovy (*Engraulis ringens*) and Peruvian hake (*Merluccius gayi*). Using this configuration as a starting point, I performed 17 simulations changing the fishing rate of anchovy (F_a) and hake (F_h), as well as the minimum fishing size of anchovy (A_{min}). When changing the fishing rate of anchovy and hake, I applied two basic scenarios: a) F_i- means that the first year of the simulation equals the fishing rate in the control simulation (F_{a_0} = 1.1, F_{h_0} = 0.3 yr^{-1}) and then it is decreased by 5 % of F_{i_0} every 10 years until $F_i = \frac{F_{i_0}}{2}$; for the remaining years $F_i = \frac{F_{i_0}}{2}$. b) F_i+ means that the fishing rate of the first year also equals F_{i_0} and afterwards 5 % of F_{i_0} is added to the fishing rate in 10-years intervals. I simulated two sets of experiments. The first set looked at the effects of modifying the minimum fishing size of anchovy, as well as its fishing rate (A_{min} and F_a, respectively). The fishing rate of hake was not modified in these experiments (Table 4.1). For the second set of experiments, I modified the fishing rates of hake and anchovy (F_a and F_h), as described above, without changing the minimum fishing size of anchovy (Table 4.2). I ran all simulations for 100 years of spin-up and then for an additional 200 years period. The annual mortality rates were kept constant at F_{a_0} = 1.1 and F_{h_0} = 0.3 yr^{-1} during the spin-up. All results were plotted without showing the spin-up. Because OSMOSE is a stochastic model, results vary slightly among replicates of the same set-up. Therefore, I ran each simulation 20 times and averaged the outputs. I also reported the running mean of 12 months to filter the seasonal variability.

Table 4.1. List of experiments changing anchovy minimum fishing size (A_{min}; cm) as well as anchovy fishing rate (F_a). The fishing rate of hake is kept at the control value ($F_h = 0.3$ yr^{-1}).

	$F_a = F_{a_0}$	$F_a = F_a+$
A_{min} = 9	C9	+A9
A_{min} = 10	C10	+A10
A_{min} = 11	C11	+A11
A_{min} = 12	C12 (control)	+A12
A_{min} = 13	C13	+A13
A_{min} = 14	C14	+A14
A_{min} = 15	C15	+A15

Table 4.2. List of experiments changing anchovy and hake fishing rates (F_i). The minimum fishing size of anchovy remains constant (A_{min} = 12 cm).

Experiment	F_a	F_h
C12 (control)	F_{a_0}	F_{h_0}
+A12	F_a+	F_{h_0}
–A	F_a-	F_{h_0}
+H	F_{a_0}	F_h+
–H	F_{a_0}	F_h-

4.4 Results

First, I examine the effects of increasing and decreasing the minimum catch size of anchovy in addition to increasing its fishing rate. The minimum catch size of 12 cm allows for landings almost as high as 600 Kt at the control fishing rate of 1.1 yr^{-1} (Figure 4.1, bottom left, black line). There is a tipping point at a fishing rate of about 1.8 yr^{-1}, around year 125, where the fishing pressure is so high that the landings start to decrease as the fishing rate increases (Figure 4.1, bottom right, black line). Decreasing the minimum catch size of anchovy switches the tipping point to a fishing pressure almost as low as the 1.1 yr^{-1} rate at the beginning of the simulation (Figure 4.1, bottom right, yellow line). Interestingly, decreasing the minimum catch size of anchovy any further than 11 cm does not increase the landings (Figure 4.1, bottom left). Furthermore, it generates a stronger decrease in landings when fishing pressure decreases. Increasing the minimum catch size of anchovy results in lower landings at the control fishing rate (Figure 4.1, bottom left, blue lines). Nonetheless, it increases the resilience of the species to fishing pressure (Figure 4.1, top right, blue lines) enough to allow for a steady increment in catches up to fishing rates as high as 2.2 yr^{-1} by year 200 (Figure 4.1, bottom right, blue lines).

Hake exhibits a higher sensitivity than anchovy to changes in the fishing rate (Figure 4.2) and it is driven to a collapse when the fishing rate doubles (Figure 4.2, +H). Its biomass increases more than twice when the fishing rate is halved (Figure 4.2, –H). This increase is high enough to generate an increase of about two thirds in the landings, despite the lower fishing rate (Figure 4.2, –H).

In summary, anchovy landings usually increase as fishing rate increase, despite a decrease in its biomass, up to certain threshold. In the case of hake, landings benefit more from a decrease in the fishing rate and are prone to collapse when the fishing rate increases.
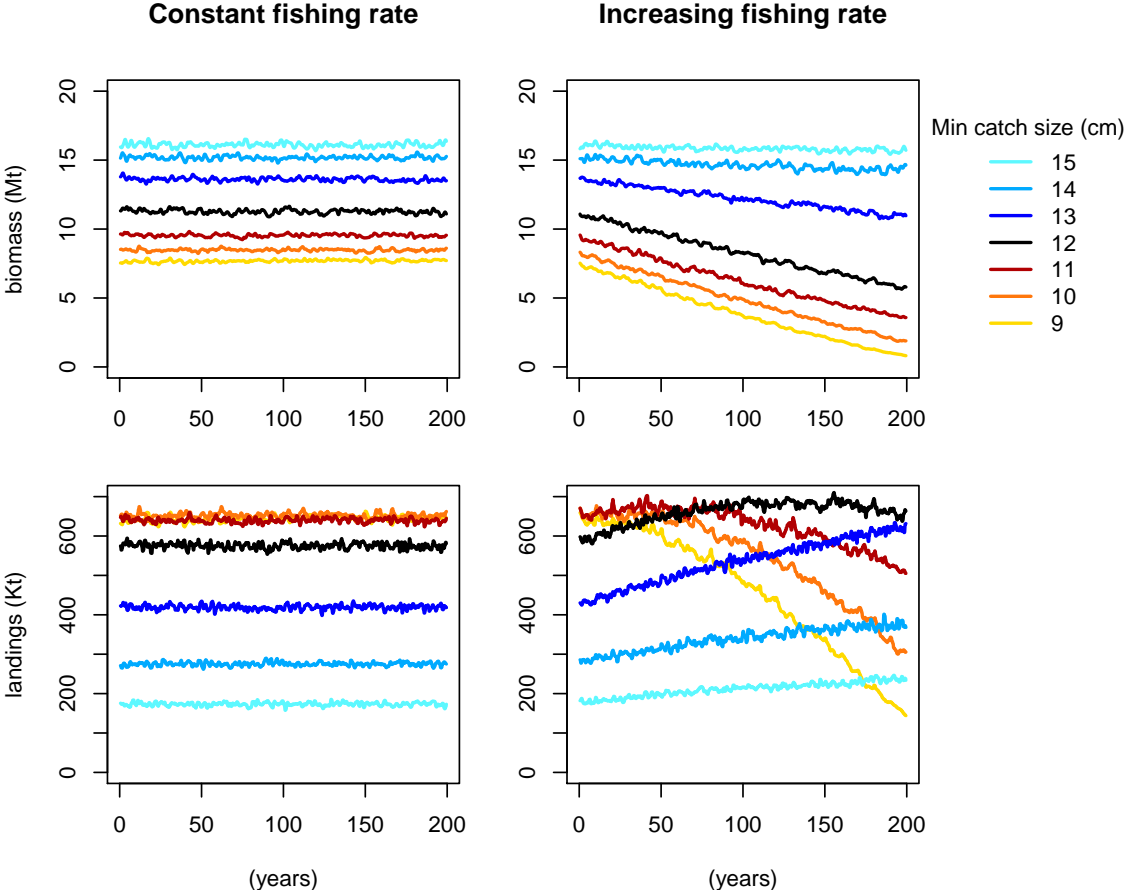

Figure 4.1. Annual running mean of the anchovy biomass (top) and monthly landings (bottom) for scenarios C9 to C15 (left) and +A9 to +A15 (right). Fishing rate is 1.1 yr^{-1} in the first year of the simulation and it remains constant in scenarios C9 to C15 (left) and increases by 5 % every ten years in scenarios +A9 to +A15 (right)
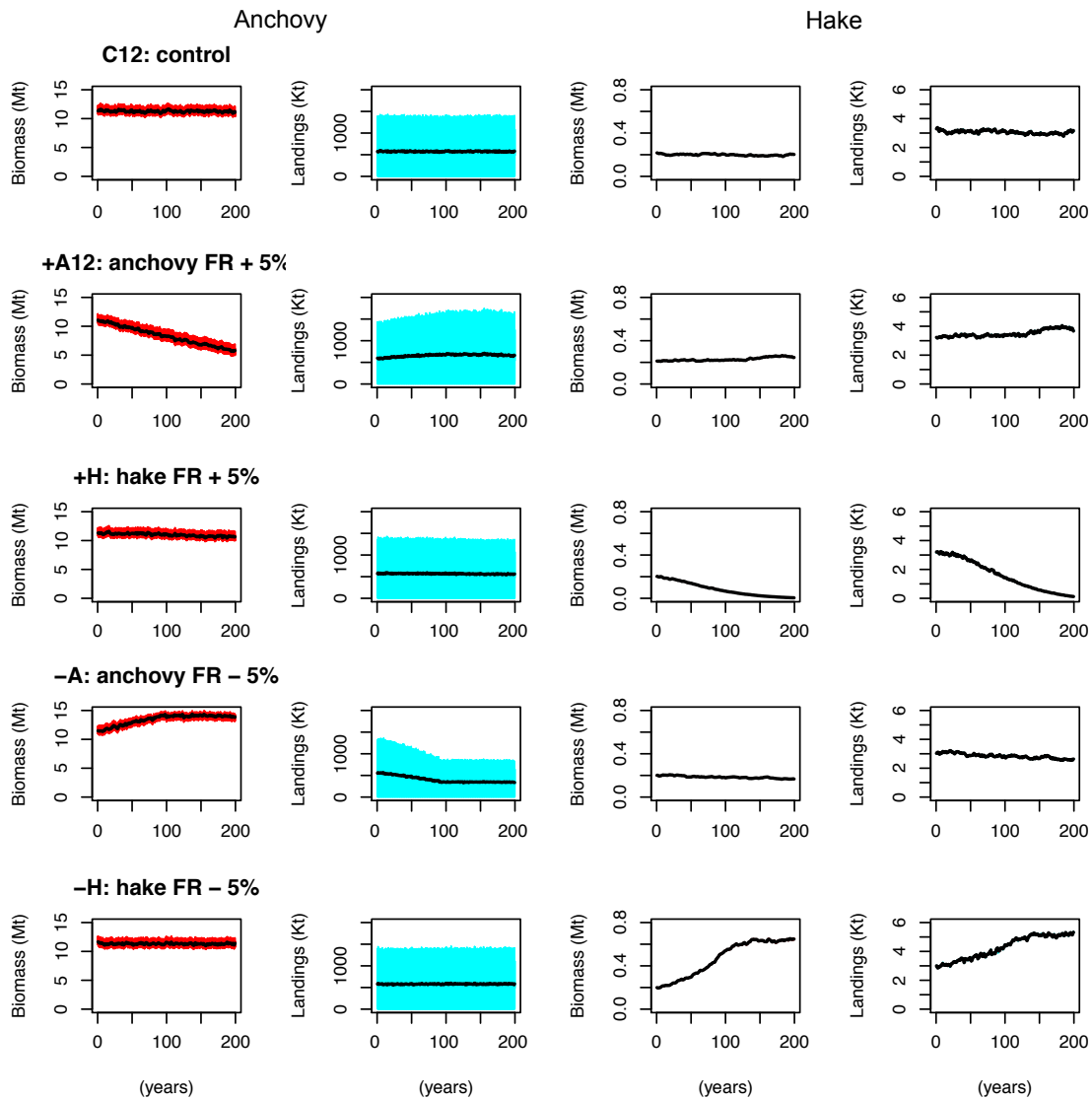
Figure 4.2. Anchovy (columns 1 and 2) and hake (columns 3 and 4 from left to right) biomass (red) and monthly landings (cyan). Black lines provide the running mean of 12 months. Anchovy fishing is subjected to seasonal fishing closures. Therefore, monthly landings fluctuation between zero and their maximum during the fishing season. Fishing rate is 1.1 yr^{-1} and 0.3 yr^{-1} in the first year of simulation for anchovy and hake, respectively. Afterwards, fishing rates are decreased or increased by 5 % every ten years depending on the experiment. See Sect. 4.3 for details on the specific experiments.

4.5 Discussion

This study explored the response of two commercially exploited species, the Peruvian anchovy and the Peruvian hake, in the northern Humboldt Current System (NHCS), to fishing scenarios. Anchovy is a small pelagic fish that lives up to 4 years (Marzloff et al., 2009) and it is considered to reach maturity at 12 cm (Marzloff et al., 2009). In this study, an increase of fishing pressure in anchovy generates a tipping point at a

fishing pressure about two thirds higher than the control. Here I call "tipping point" the point at which any further increase in the fishing pressure does not increase the landings but rather reduces them. Decreasing the minimum catch size does not show a considerable improvement in the landings and makes them rather more vulnerable to a tipping point when the fishing pressure increases. On the other hand, increasing the minimum catch size improves the resilience of the population to a higher fishing pressure. Larger individuals produce more eggs and have longer spawning seasons (Pauly and Soriano, 1987). Hence, this might be an alternative measure to protect the fishery from overfishing, especially after years of recruitment failure. In addition, Salvatteci and Mendo (2005) pointed out that, while the minimum catch size is 12 cm, with a tolerance for individuals smaller than this size of 10 % of the catch, smaller individuals have been harvested. In my study, the minimum catch size was set to 12 cm with no tolerance range and assuming no bycatch. Therefore, the control scenario in this study is rather conservative. Furthermore, Pauly and Soriano (1987) reported a 50 % maturity of individuals at 14 cm. This is further supported by Ñiquen Carranza et al. (1999). Thus, in reality, the 12 cm minimum catch size may be removing a considerable amount of individuals that have not reproduced yet.

Hake has longer generation times than anchovy and it is less resilient to overfishing. Fernández Ramírez (1987) reported female individuals as old as 9 years off the coast of Peru. In OSMOSE, the maximum, age of 12 years was employed following Marzloff et al. (2009). Before the 1990s, individuals matured at around 2.5 years of age (Guevara-Carrasco and Lleonart, 2008) and 27 to 29 cm in length (Canal Loayza, 1989), with most spawning individuals more than 3 years old (Guevara-Carrasco and Lleonart, 2008). The age and size at maturity, however, has decreased throughout the years (Guevara-Carrasco and Lleonart, 2008). Large, long–lived species with lower population growth are considered to be less resilient to fishing pressure (Jennings, Greenstreet, and Reynolds, 1999). In this study, I observed that hake is negatively affected by an increased fishing rate to the point of collapsing, (this was not observed for anchovy). On the other hand, decreasing the fishing pressure by half benefits hake by yielding almost 70% higher landings and 200% higher biomass relative to the control means. In contrast, Marzloff et al. (2009) reported an increase in biomass of twice their reference state after a complete removal of the fishing pressure (Marzloff et al., 2009). Both my study and the study by Marzloff et al. (2009) agree that lower fishing pressure would be beneficial for the hake fishery. From this, I conclude, that hake in the model is in an overfished state. The model was calibrated based on the hake state in the 2000s (see Chapter 3). This period of time corresponds to a known collapse of the hake fishery due to overfishing (Ballón et al., 2008; Guevara-Carrasco and Lleonart, 2008), in

agreement with the model. In 2002, a moratorium on fishing hake was implemented for 20 months (Guevara-Carrasco and Lleonart, 2008). Hake population did not show and immediate recovery and hake biomass remained low at least for the following six years (Guevara-Carrasco and Lleonart, 2008).

This study analysed the impacts of increasing fishing pressure on hake and anchovy in an idealised climatological simulation. In reality, the NHCS is affected by interannual variability, specifically El Niño–Southern Oscillation (Barber and Chavez, 1983; Fiedler, 2002; Alheit and Niquen, 2004), as well as regimes of cold and warm water (Chavez et al., 2003; Alheit and Niquen, 2004). During El Niño conditions, anchovies migrate to deeper waters, closer to the coast and further south (Ñiquen Carranza et al., 2000). Major anchovy collapses in the past (e.i., 1972–1973, 1982–1983 as well as the decline in 1997–1998) have been associated with recruitment failure during El Niño events (Boerema and Gulland, 1973; Clark, 1976; Alheit and Niquen, 2004). Therefore, I would expect that an interannual simulation that replicates the environmental effect on anchovy would result in a lower resilience to fishing pressure than the climatological set-up. On the other hand, larger longed–lived fish have been considered to have a higher resilience to environmental variability than smaller fish (MacCall, 2002; Hsieh et al., 2010; Maselko, Andrews, and Hohenlohe, 2020). In the case of hake, it is not yet clear whether the El Niño event has a positive or negative impact. While it stresses the fish due to reduced food availability (Ballón et al., 2008) it also expands its area of occurrence southwards, decreasing cannibalism and catchability (Guevara-Carrasco, Rodríguez, and Rodríguez, 2004). Future studies should consider the impact of fishing pressure in a setting with interannual variability. To do so, it is first necessary to capture the underlying links to the environment that are responsible of the interannual variability in anchovy and hake populations.

In this study, I focused only on anchovy and hake. However, in recent years, the fisheries management paradigm has been switching from the traditional single–species management to an ecosystem based fisheries management (see Marasco et al., 2007). In this context, the multispecies maximum sustainable yield refers to the maximum yield that can be provided by a system rather than a single fishery (Worm et al., 2009). In the case of the NHCS, the exploitation of small pelagic fish shifted from being monospecific, mainly anchovy, in the 1960s, to multispecific after the anchovy collapse of 1972 and increase in the populations of sardine (*Sardinops sagax*) and jack and chub mackerel (*Trachurus murphyi* and *Scomber japonicus*, respectively) (Ñiquen Carranza et al., 2000). Therefore, it is worth to consider the effect of fishing pressure on these species as well in further studies. Smith et al. (2011) pointed out that reducing the fishing pressure on

small fish by half would only decrease the maximum sustainable yield to 80 % while providing large benefits to the surrounding ecosystem. In addition, the potential value, not only yield, of the ecosystem should also be considered (Bieg and McCann, 2020). Only 1 % of the anchovy landings are used for direct human consumption as canned food (Ñiquen Carranza et al., 2000). Hake, on the contrary, is valued for direct human consumption and it is industrially commercialised as frozen food (Guevara-Carrasco and Lleonart, 2008). A management strategy that aims not necessarily to the optimal exploitation of anchovy, but also to rebuilding other species in the region with higher value, might be an alternative to increase the profits while ensuring the health of the ecosystem (see Bieg and McCann, 2020). Finally, rethinking the value of small pelagic fish for direct human consumption might be an alternative to increase the ecosystem profits (Christensen et al., 2014) and also to ensure global food security (Tacon and Metian, 2009).

4.6   Conclusion

In this study, I showed potential outcomes of alternative management scenarios for anchovy and hake. For the simulated years, hake shows to be more sensitive to fishing pressure and a reduced fishing pressure may be beneficial for hake landings. On the other hand, anchovy exhibits a higher resilience to increased fishing rate in this climatological set-up, especially when increasing the minimum catch size. Fishing only adult anchovies is important to ensure the resilience of the population, especially under increased fishing pressure. This study focused merely on the top-down aspect and on two species. Further work should look at the effects of changing fishing management scenarios for all targeted species of the ecosystem in combination to environmental –interannual–, variability.

Acknowledgements

Diving deeper: Mesopelagic fish biomass estimates comparison using two different models

Mariana Hill Cruz, Iris Kriest and Julia Getzlaff

This chapter contains the draft of a paper comparing mesopelagic fish simulated by two end-to-end models: OSMOSE, which was used in Chapters 3 and 4 as well, and the Anderson model.

5.1   Abstract

Small pelagic fish in the northern Humboldt Current System (NHCS) are the world's main source of fishmeal and fish oil for feeding aquaculture and land stocks. However, a growing population on a planet with limited resources demands finding new sources of protein. Hence, fisheries are turning their perspectives towards mesopelagic fish, which have, so far, remained relatively unexploited and poorly studied. Estimating the biomass of mesopelagic fish is the first step for gaining basic knowledge on these fishes and reducing uncertainties. In this study we employed two food-web models – OSMOSE and the Anderson model – coupled to a regional physical–biogeochemical model to simulate mesopelagic fish in the eastern tropical South Pacific ocean. The Anderson model provides a larger biomass of mesopelagic fish and follows the same temporal trend as the physical–biogeochemical model. On the other hand, temporal variability in OSMOSE is affected by its more complex life cycle and food-web. The Anderson model is more convenient to understand the feedbacks between mesopelagic fish and biogeochemistry and to do uncertainty analysis. OSMOSE is convenient to understand the interactions of the ecosystem and how including different life stages

affect the model response. The strengths of both models complement each other and should be considered when studying mesopelagic fish from a holistic perspective.

5.2 Introduction

A growing population on a planet with limited resources faces the challenge of food security through the sufficient supply of mankind with carbohydrates, fats and proteins (Prosekov and Ivanova, 2018). Especially with regard to proteins, fish is of key importance: for example, small epipelagic fish are used for the production of fishmeal and fish oil which are used to feed aquaculture animals, land stocks and to produce nutritional capsules for human consumption (Shepherd and Jackson, 2013). The averaged global fishmeal and fish oil production between 2001 and 2006 was 6.3 and 0.95 Mt per year, respectively (Péron, François Mittaine, and Le Gallic, 2010). From these, 1.7 and 0.27 Mt came from small pelagic fish landed in Peru (Péron, François Mittaine, and Le Gallic, 2010). Small epipelagic fish in the northern Humboldt Current System (NHCS) represent around 10% of the global fish landings (Chavez et al., 2008). However, the exploitation potential of these coastal stocks is limited (Tarazona and Arntz, 2001) and they have collapsed in the past due to overfishing and recruitment failure, impacting the ecosystem (Duffy, 1983; Tarazona and Arntz, 2001; Alheit and Niquen, 2004; Herling, Culik, and Hennicke, 2005). Their susceptibility to high temporal variability (Chavez et al., 2003) in combination with the possible impacts of climate change on the NHCS, bring uncertainty for their exploitation in the upcoming decades (see Salvatteci et al., 2022). Alternative fish stocks may be necessary in the coming years to satisfy the demand for fishmeal and release the pressure on currently over-exploited epipelagic fish. Hence, fisheries are turning their perspectives towards mesopelagic fish, which have, so far, remained relatively unexploited (St. John et al., 2016). These may be used to support the supply of fishmeal and also as for source nutraceutical products (St. John et al., 2016). However, exploiting these resources without prior knowledge on their fundamental ecological and biogeochemical role, poses threats for the mesopelagic community and, potentially, also for the ocean health and global climate (St. John et al., 2016; Martin et al., 2020).

Estimating the biomass of mesopelagic fish is the first step for gaining basic knowledge on these fishes and reducing uncertainties. There is high uncertainty in the global biomass of mesopelagic fish with estimates as low as 1 Gt (Gjøsæter and Kawaguchi, 1980) and as high as 11 to 15 Gt of wet weight (Irigoien et al., 2014). In the NHCS, *Vin-*

ciguerria lucetia, also known as Panama lightfish, and myctophids, commonly known as lanternfish, have been reported as the main constituents of the mesopelagic fish community (Cornejo Urbina and Koppelmann, 2006; Marzloff et al., 2009). These are vertical migrants whose distribution has been reported on the upper 50 m depth during the night and between 200 and 400 m during the day (Cornejo Urbina and Koppelmann, 2006). The biomass of *Vinciguerria* sp. off the coast of Peru has been estimated between 2.9 (Castillo Valderrama et al., 1999) and 11.1 Mt (Castillo Valderrama et al., 1998). Furthermore, while small commercially exploited epipelagic fish concentrate in the nutrient-rich coastal upwelling waters off Peru, the distribution of *V.* sp. extends to oceanic waters (Castillo Valderrama et al., 1999; Cornejo Urbina and Koppelmann, 2006).

Ecosystem and fisheries models are valuable tools to understand the dynamics of the ecosystems and their potential response under certain scenarios. Numerous models exist to simulate either single fisheries or whole ecosystems (see Fulton, 2010; Tittensor et al., 2018). However, most models including higher trophic levels, or fish, are zero to two dimensional and no vertical movement is represented (e.g., Bianchi et al., 2021). Exceptions include Rose et al. (2015) and Aumont et al. (2018). Aumont et al. (2018) made an estimation of carbon exported my vertical migrations between the epipelagic zone and deep water. In their study, the higher trophic levels were divided into 20 size classes. However, no individual species, neither life cycles were explicitly included. A sustainable exploitation of mesopelagic fish requires not only to estimate its biomass but also to understand the population vital rates such as recruitment and growth (St. John et al., 2016). Therefore, further alternatives for modelling mesopelagic fish are needed.

Modelling the biomass of mesopelagic fish in the eastern tropical South Pacific (ETSP), and the uncertainties associated with it, is a first step towards understanding the role of these fishes in the ecosystem. In this study, we employed two food-web models coupled to a regional physical–biogeochemical model to simulate mesopelagic fish in the ETSP. We compared how the different complexities of the two models affect the estimations of biomass of the mesopelagic fish and their temporal variability. This is a first step towards understanding the trophic-web of the deep ocean and how it can be modelled.

5.3   Methods

In this study, we calculated the abundance of mesopelagic fish in the eastern tropical South-Pacific (ETSP) by using one physical-biogeochemical model: CROCO-BioEBUS (Shchepetkin and McWilliams, 2005; Gutknecht et al., 2013a) coupled to two different models of higher trophic levels (from now on called fish models): the simple food-web model by Anderson et al. (2019) and the multispecies individual-based model OSMOSE (Shin and Cury, 2001; Shin and Cury, 2004). Primary production, phytoplankton and zooplankton were estimated using the physical-biogeochemical model and these in turn were used to force the two fish models.

5.3.1   The physical-biogeochemical model: CROCO-BioEBUS

We employed the Coastal and Regional Ocean COmmunity model (CROCO Shchepetkin and McWilliams, 2005, https://www.croco-ocean.org/,) coupled online with the Biogeochemical model for Eastern Boundary Upwelling Systems (BioEBUS Gutknecht et al., 2013a). The simulation description, parameters and coupling with OSMOSE are available in José et al. (2019) and Xue et al. (2021) and in Chapter 3. For this study, we used the same simulation as in Chapter 3. The model has a spatial resolution of $\frac{1}{12}°$ and spans from to $33°$ S to $10°$ N and 69 to $118°$ W and has 32 sigma layers. For this study, we utilised only the model output from $20°$ S to $6°$ N and 93 to $70°$ W. It is spun-up for 30 years using the forcing of 1990 and then a hindcast from 1990 to 2010 is simulated. The model is forced at the boundaries with temperature, salinity and current velocities from Simple Ocean Data Assimilation (SODA, Carton, Chepurin, and Chen, 2018), oxygen and nitrate from monthly climatology CSIRO - Commonwealth scientific and industrial research organisation Atlas of Regional Seas (CARS, Ridgway, Dunn, and Wilkin, 2002) and at the surface with heat fluxes, humidity, precipitation and temperature from Climate Forecast System Reanalysis (CFSR, Saha et al., 2010) and winds from Cross-Calibrated Multi-Platform product (CCMP, Atlas et al., 1996). See José et al. (2019) for more details on the model set-up and forcing.

5.3.2   The multispecies model: OSMOSE

The Object-oriented Simulator of Marine Ecosystems (OSMOSE Shin and Cury, 2001; Shin and Cury, 2004, http://www.osmose-model.org/) is a multispecies individual-

based model that simulates the whole life cycle of fish. It includes processes of predation, growth, reproduction, harvesting and mortality. The model groups individuals of the same species and age class in schools. Every school has several state variables including age, size, location and number of individuals. Schools are located in a 2-dimensional grid of $\frac{1}{6}°$. In every time-step, organisms move randomly within a given area and prey on other schools that share the same spatial location. Every species can prey on organisms from other schools or plankton that fall within certain predator-prey size ratio. Therefore, the food-web in the model emerges from the size structure of all organisms. The model includes nine groups: anchovy, hake, sardine, jack mackerel, chub mackerel, mesopelagic fish, squat lobster, Humboldt squid and euphausiids, which interact with each other through predation and resources utilisation. A detailed description of the model configuration used in this study as well as its calibration is available in Chapter 3.

CROCO-BioEBUS is coupled to OSMOSE through plankton. Small and large phyto- and zooplankton produced by CROCO-BioEBUS are integrated above the oxygen minimum zone (90 μmol O_2 kg^{-1}, Karstensen, Stramma, and Visbeck, 2008) and transformed to wet weight multiplying by the factors: 720, 720, 675 and 1000 mg WW mmol N^{-1}, respectively (Travers-Trolet, Shin, and Field, 2014, their Tab. 4). The plankton fields are then regridded from $\frac{1}{12}°$ to $\frac{1}{6}°$ and used as forcing to run OSMOSE. OSMOSE is spun-up with climatological plankton input for 25 years and then run for another 21 years using the BioEBUS plankton hindcast from 1990 to 2010.

OSMOSE provides the possibility to output several diagnostics, including all mortality sources such as starvation, predation, fishing and additional mortality. After running the simulation, we computed the averaged total mortality rate of juvenile and adult fish and used it as an input parameter for the Anderson model, as described in Sect. 5.3.3.

Finally, we compared how the trophic-web in OSMOSE affects the mesopelagic fish against a simulation where mesoepalgic fish is the only fish in the ecosystem. For this, we performed another OSMOSE simulation where all groups except the mesopelagic fish were forced to collapse by increasing their larval mortality by two to three orders of magnitude. This simulation is denominated as "OSMOSE without trophic-web" (see Figure 5.2).

5.3.3   The mesopelagic fish model: Anderson Model

Anderson et al. (2019) proposed a simple food-web model to estimate biomass of mesopelagic fish based on primary production. The model is a set of linear equations that transfer carbon from primary production to mesopelagic fish through three paths: detritivorous, vertically migrant and epipelagic zooplankton. These three groups are consumed by carnivorous zooplankton. Mesopelagic fish, in turn, consume all four zooplankton groups. As sink, a mortality rate is applied to the mesopelagic fish which represents all sources of mortality including predation. The description of the model and parameters is available in Anderson et al. (2019). From here onward, we call this model "Anderson model".

We coupled the Anderson model to BioEBUS by extracting total primary production from the BioEBUS hindcast diagnostics from 1990 to 2010 (see Section 5.3.1). We masked all data of regions shallower than 200 m and used it as 2-dimensional forcing for the Anderson model. In addition to the primary production, we also changed the mortality parameter. The original parameter by Anderson et al. (2019) is 0.67 yr^{-1}. We made two runs with the averaged diagnostics moralities of juvenile and adult mesopelagic fish in OSMOSE that we computed from the simulation described in Sect. 5.3.2: 3.0 and 1.65 yr^{-1} (Table 5.1).

5.4   Results

The spatial distribution of mesopelagic fish simulated with OSMOSE (Figures 5.1) and with the Anderson model using BioEBUS primary production (Figures 5.1) is similar. Mesopelagic fish are absent in the coastal shallow water and

Table 5.1. Mortality diagnostics (yr^{-1}) in OSMOSE averaged after spin-up.

	predation	starvation	additional	total
juveniles	1.75	0.1	1.17	3.02
adults	0.16	0.3	1.19	1.65

their largest concentration is present off Peru. The Anderson model produces higher biomass than OSMOSE (Figure 5.1 top left). The biomass with high mortality (Figure 5.1 top middle) is only around one fifth higher than the biomass in OSMOSE. On the other hand, the biomass simulated by the set-up with low mortality (Figure 5.1 top right) is more than twice as high as in OSMOSE. The seasonal patter in the two fish models has the same trend. However, it is much stronger in the Anderson model

than in OSMOSE (Figure 5.1, bottom). On the other hand, the relative interannual variability in OSMOSE is higher than in the Anderson model and it does not follow the same trend as the plankton input (Figure 5.2 bottom. Maximum absolute cross correlation of 0.197, see Section 5.7).

While, in the Anderson model, the temporal variability is driven by the primary production forcing, in OSMOSE, it is the result of the interplay of many factors. These include, the explicit life cycle of the fish, the trophic interactions with predators and different sources of prey, the spatial distribution and the variability in different sources of mortality. The main predator of mesopelagic fish in OSMOSE is the Humboldt squid. Their main prey are euphausiids and then large zooplankton (see Section 5.7). Removing all fish groups from the OSMOSE configuration, except for the mesopelagics (Figure 5.2, pink line), results in a decrease in the amplitude of the interannual anomaly of mesopelagic fish biomass. In this simulation, there is a cross correlation of 0.65 between the 12-month running means of plankton forcing and mesopelagic biomass with a lag of 8 months (see Section 5.7). This points to an impact of simulating a complex life cycle in OSMOSE, including egg production, by delaying the biomass response to plankton abundance. In summary, both models show a similar seasonal cycle following the trend of the plankton and primary production. On the other hand, the interannual variability in OSMOSE is stronger and follows a different pattern even when mesopelagic fish are the only higher trophic level present in this model.
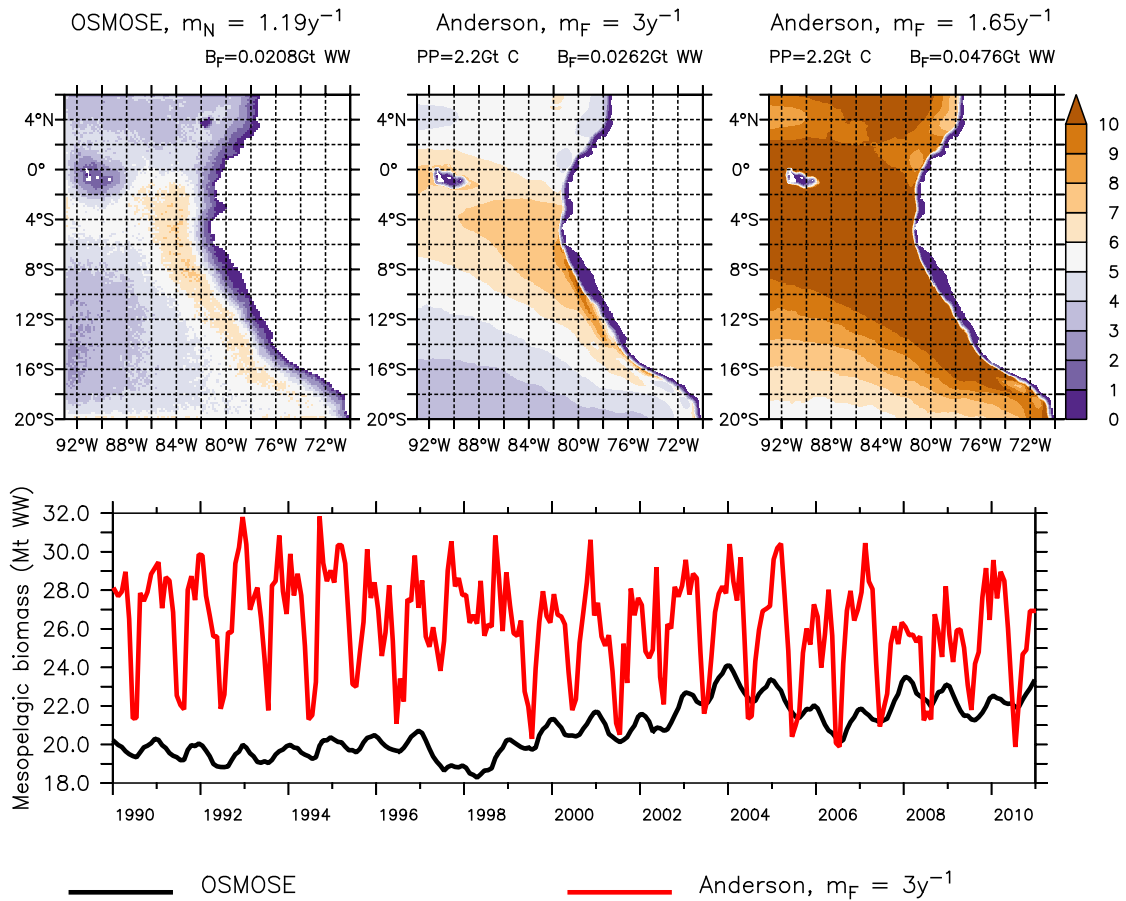
Figure 5.1. Mesopelagic fish simulated by OSMOSE (top-left and bottom-black) and the Anderson model (top right and bottom red), using plankton and primary production forcing from CROCO-BioEBUS, respectively. Top row shows the averaged output in grams of wet weight per square meter (g WW m^{-2}) from 1990 to 2010 and the bottom shows the total biomass over the domain for the same time period. PP is the total primary production forcing for the Anderson model, m_F is the mortality input for the Anderson model, m_N is the additional natural mortality parameter for OSMOSE, the total mortality in OSMOSE consists of this value plus predation and starvation mortality (see Table 5.1) and B_F is the total fish biomass.
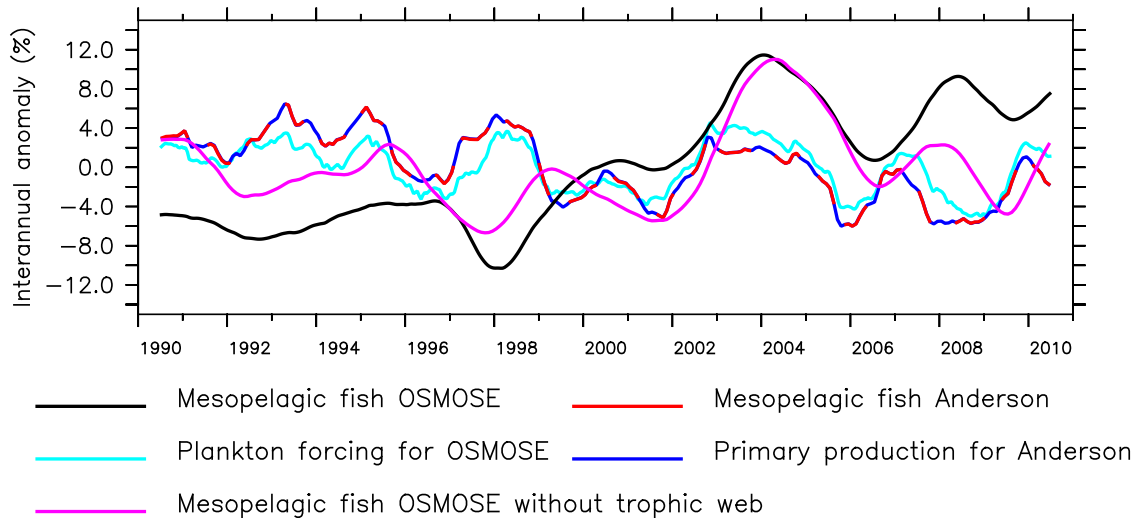
Figure 5.2. Anomaly of the 12-month running mean of total mesopelagic fish biomass calculated by OSMOSE (black) and the Anderson model (red), primary production used as input for the Anderson model (blue), total plankton biomass used to force OSMOSE (cyan) and OSMOSE mesopelagic fish when all other fish groups collapsed (pink; see Section 5.3.2).

5.5 Discussion

Our study consisted of comparing the biomass estimates of mesopelagic fish in the eastern tropical South Pacific ocean (ETSP) using a physical-biogeochemical model coupled one-way to two different fish models. The OSMOSE model was calibrated to match observed biomasses of mesopelagic fish off Peru between 2000 and 2008 provided by the Instituto del Mar del Peru (Chapter 3). Nonetheless, acoustic estimates of mesopelagic fish are prone to high uncertainty (Marzloff et al., 2009; Davison, Koslow, and Kloser, 2015; Davison, Lara-Lopez, and Anthony Koslow, 2015) so these values should be taken with care. We ran the Anderson model using two different mortalities which had been previously calculated with the OSMOSE simulation. The scenario with the higher mortality (juvenile mortality in OSMOSE) provides the closest estimate to OSMOSE. However, both mortality values are higher than the mortality rate of 0.67 yr^{-1} used by Anderson et al. (2019) for estimating mesopelagic fish biomass. Therefore, a model run with the original parameter would provide a much higher biomass estimate than OSMOSE. Anderson et al. (2019) performed a comprehensive uncertainty analysis providing low and high boundaries for the globally integrated biomass estimate. This allows to understand the potential mesopelagic biomass given current levels of primary production in the system. As far as the high uncertainty remains, both low and high boundaries should be taken into account for a precau-

tionary perspective. Their uncertainty analysis also evidenced the high sensitivity of the model to the mortality parameter which is highly uncertain (Anderson et al., 2019, their Figure 3). A comprehensive parameter uncertainty analysis as done in Anderson becomes more complicated with OSMOSE since running this individual-based model requires higher computational resources and also the model species may collapse under certain conditions (see Sect. 3.8.5). On the other hand, the several parameters, including mortality terms such as specific mortalites for adults and also for eggs and larvae (see Chapter 3), in OSMOSE allow for modelling a more complex trophic-web and life cycle.

OSMOSE represents the whole life cycle of the fish, from egg production to growth and recruitment of fish. In our simulation, we observed that the seasonal cycle is muted and that the interannual variability exhibits a different pattern than the plankton input. Even when removing the interactions with other species of the ecosystem, the interannual variability preserved its distinctive pattern. This evidences the impact of simulating different life stages. The impact of changes in the plankton is delayed in OSMOSE since adult fish require time to produce eggs and these in turn must hatch and grow to increase biomass. The Anderson model does not distinguish life stages of mesopelagic fish; hence it does not consider an egg and larval mortality. On the contrary, the abundance is calculated merely based on the amount of available biomass (primary production). Hence, this model may not be adequate to evaluate recruitment, or reproductive success. This is evidenced by the identical temporal trend of the model and the primary production forcing. In a given scenario, for example with increased mortality due to fishing pressure, the Anderson model can provide the potential yield of the system and how much fish biomass would remain. However, since it is not able to provide a population growth rate based on life traits, it may not be used to estimate how fast the population can replace fish that have been harvested.

OSMOSE represents fish based on their life traits and trophic interactions with the rest of the ecosystem. As a multispecies model, it is also useful for exploring fishing strategies in an ecosystem-based fisheries management context (Briton et al., 2019; Guo et al., 2019; Fu et al., 2019; Fu et al., 2020). There is growing evidence of the importance of mesopelagic fish in deep water food chains (Mann, 1984; Davison, Lara-Lopez, and Anthony Koslow, 2015; Saunders et al., 2019). In our study, the main predator of mesopelagic fish is the Humboldt squid (see Section 5.7). This is a species of economic importance (Gilly et al., 2013) that feeds mainly on mesopelagic fish (Markaida and Sosa-Nishizaki, 2003). Therefore, any prospect on the exploitation of mesopelagic fish in the ETSP should consider the potential impacts on this species. In OSMOSE, it is pos-

sible to evaluate changes in the ecosystem structure under different conditions because trophic chains emerge from the size ratios of predators and preys in the ecosystem. As an individual-based model, OSMOSE represents the consumption of prey based on the spatial overlap of predator and prey. This is possible due to the horizontal movement of fish between grid cells. The movement is random but it is restricted by distribution maps.

The spatial distribution of mesopelagic fish shows a similar patter in OSMOSE and Anderson regardless of the different distribution maps used in each model. The distribution maps in OSMOSE were derived using habitat niche models by Oliveros-Ramos (2014). In the Anderson model, mesopelagic fish are constrained to areas deeper than 200 m and the concentration of fish depends on the amount of primary production. In contrast to Anderson, the distribution maps in OSMOSE vary with time and can be used to simulate migrations (see Grüss, Drexler, and Ainsworth, 2014; Oliveros-Ramos, 2014). Although, in this study, we only included climatological distribution maps, in Section 3.7.3 we observed that interannual variability in the habitat produced a larger effect on fish abundance than interannual variability in plankton. In the Anderson model, there is no horizontal movement of fish. OSMOSE does include horizontal movement of fish. On the other hand, due to the computational constrains of the individual-based model, as well as the link between spatial and temporal resolution, it has only been used at regional scales (see Fulton, 2010, their Figure 3).

Both OSMOSE and the Anderson model lack a vertical dimension of fish distribution, but parameterise its effect on the trophic-web. In the case of OSMOSE, this is done through a predatory accessibility matrix which constrain which fish groups can feed on others based on their theoretical position in the water column. The Anderson model went a step further by also parameterising vertical migrations of mesopelagic fish. It assumes in its trophic chain that migrant fish feed on epipelagic zooplankton for half of the days and on migrating zooplankton all day (Anderson et al., 2019). Vertical migrations are especially important in the context of mesopelagic fish due to their role in the active transport of organic matter to the deep ocean (Davison et al., 2013; Belcher, Saunders, and Tarling, 2019; Hernández-León et al., 2019) and its implications for carbon capture and oxygen loss and nutrient cycles (Martin et al., 2020).

As it is a mass conserving model, the Anderson model is useful for representing the mass transfer between nutrients, plankton and mesopelagic fish, especially when coupled to a biogeochemical model. On the other hand, the link between lower and higher trophic levels is still poorly represented in OSMOSE. OSMOSE was developed in the

early 2000s as modelling tool for studying multispecies marine communities under fishing pressure (see Shin and Cury, 2004). In the earliest versions of OSMOSE, the link between biogeochemistry and fish was not explicitly modelled. Instead, fishes were divided into piscivorous and non-piscivours groups and a carrying capacity was utilised to regulate the maximum amount of biomass of non-piscivorous fish (Shin and Cury, 2001). Travers (2009) introduced explicit plankton as a source of food for the fish. Since then, OSMOSE gained attention, among other things, as a tool for evaluating the effect of plankton on fish (e.g., Travers and Shin, 2010; Fu et al., 2012; Travers-Trolet et al., 2014; Fu et al., 2019). However, in Chapter 3, we pointed out that the relationship between plankton and higher trophic levels in OSMOSE should be interpreted with care. While the Anderson model might have a simplified representation of the trophic chain, its beauty lays on the direct link between biogeochemistry and mesopelagic fish. Its simplicity makes it ideal for making diverse experiments to address the potential effects of changing the biogeochemistry in the system on the fish, especially in global models. Some examples of bottom-up experiment set-ups may include changes in the primary production due to variability in the wind, in the temperature –e.i., due to climate change– or in the light and nutrient supply due to geoengineering interventions (e.g., Landry et al., 2000; Krumhardt et al., 2017; Malik et al., 2020). In a two-way coupled fashion, the Anderson model can also be used to investigate the impact of fisheries on biogeochemistry. The direct impact of consumption by fish on plankton can be studied by applying a mortality pressure derived from the food consumption (e.g., Travers-Trolet et al., 2014; Getzlaff and Oschlies, 2017; Maar et al., 2018; Hill Cruz et al., 2021). The organic matter transport to the deep ocean can be parameterised by considering the time that vertical migrants spend in the deep water. Finally, the impact of fishing on deep ocean carbon sequestration and oxygen consumption can be evaluated by analysing the remineralisation of death organic matter coming from fish (Bianchi et al., 2021).

5.6 Conclusion

We simulated the mesopelagic fish in the eastern tropical South Pacific employing two end-to-end models. Both OSMOSE and Anderson provide a realistic biomass estimation considering the high uncertainty in observed mesopelagic fish biomass. OSMOSE has a weaker seasonal cycle but a stronger interannual variability. On the contrary, the Anderson model follows the same temporal pattern as the primary production forcing. Looking ahead, both models have strengths and disadvantages. OSMOSE provides a

richer representation of the life cycle and trophic interactions of the fish community. This is crucial for studies steered towards implementations of fisheries management. Anderson's strength lies in the direct link between the biogeochemistry and the fish representation, which is useful for understanding potential boundaries for the available biomass of mesopelagic fish given certain biogeochemical conditions. In the end, the best representation should consider the advantages of both models and manages to integrate them. This may not necessary involve the development of a new model but making comparative studies as the one presented here.

Author contributions

IK and MHC suggested the experiments. MHC carried out the simulations. All authors discussed the results and wrote the manuscript.

5.7   Appendix

OSMOSE is a multispecies model that simulates the life cycle of fish. Euphausiids are the main prey of mesopelagic fish followed by plankton. The main predator of mesopelagics is the Humboldt squid (Figure 5.4). Removing all species except the mesopelagic fish increases the cross correlation between mesopelagics biomass and plankton forcing (Figure 5.3).
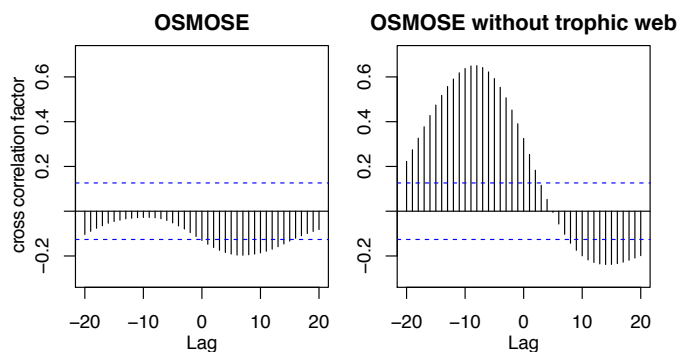
Figure 5.3. Cross correlation between the yearly running means of plankton forcing and meopelagic fish biomass in OSMOSE simulations with monthly time-steps.
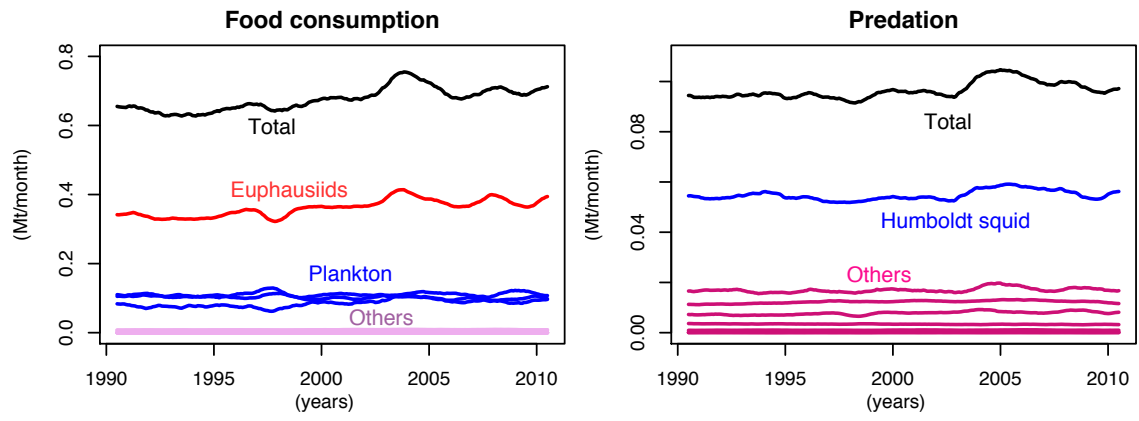
Figure 5.4. Monthly food consumption by (left) and predation on (right) mesopelagic fish.

Overall conclusion and outlook

6.1 Bottom–up and top–down effects in the northern Humboldt Current System

This project was driven by the aim of understanding the interactions between marine organisms and the environment where they live. Two types of interactions are typically recognised in ecology: top-down and bottom–up (see Lynam et al., 2017) and these occur at all trophic levels of an ecosystem. The typical example are the predator–prey interactions through food consumption and mortality (e.g., Frederiksen et al., 2006; Baum and Worm, 2009). At the biogeochemical level, nutrient availability allows for primary production (see Howarth, 1988) that sustains the whole ecosystem. On the upper end of the chain, fish removal by humans affects the food-web in a top–down fashion (Baum and Worm, 2009). The studies that have been presented in the different chapters of this thesis showed important effects both in the top–down and bottom–up directions. In the following sections, I provide an overview of the main findings of this project.

6.1.1 Bottom–up effects: How does variability in the biogeochemistry affect fish?

To explore the bottom–up effects in the northern Humboldt Current System (NHCS), I looked at the effects of variability in a physical–biogeochemical (bgc) model (CROCO–BioEBUS, see Section 1.4.1) on two one-way coupled higher trophic levels (HTL) models (OSMOSE and Anderson, see Sections 1.4.2 and 1.4.3). First, I looked at the sole impact of BioEBUS interannual variability on the multispecies model OSMOSE (Chapter 3) and then compared this with Anderson (Chapter 5), which focuses only on a group of fish (e.i., mesopelagics). For the multispecies case, the co-authors of the pa-

per and I found that the impacts of variability in plankton on HTL are more evident the lower in the trophic chain. For instance, euphausiids consume only plankton and their abundance shows a clear distinction when forcing OSMOSE with climatological or interannual plankton. For groups higher in the trophic chain, such as anchovies or, the extreme case, the predatory Humboldt squid, there is a strong variability caused by the internal dynamics of the model on top of the variability of the plankton forcing (Chapter 3).

The interannual variability on fish introduced by plankton dynamics in OSMOSE is weaker than the variability that has been historically observed (Chapter 3). However, in Chapter 5, we observed that the relative interannual variability in OSMOSE is, in fact, of the same magnitude, and even larger, than the interannual variability in plankton. This suggests that OSMOSE does not fail to transfer the temporal variablity of plankton to the fish, but rather that the driving mechanisms of the high fish variability are more complex. This is supported by the empirical study by Ayón, Purca, and Guevara-Carrasco (2004) which reported that the variability in anchovy off Peru does not directly correlate with plankton variability.

6.1.2 Top–down effects: How does fishing pressure affect fish and how does variability in fish affect the biogeochemistry?

For the top–down interactions, Chapter 4 evidences the different responses to fishing pressure of species with contrasting life–strategies: a short–living small pelagic fish (anchovy) and a larger predatory demersal fish (hake). I observed that anchovy has a higher resilience than hake. While anchovy generally can handle high fishing pressures in a climatological simulation, increased fishing pressure generates a collapse of hake. However, historical collapses of anchovy have been associated with interannual variability such as El Niño events and warm water regimes (Boerema and Gulland, 1973; Clark, 1976; Chavez et al., 2003; Alheit and Niquen, 2004; Arias Schreiber, 2012). Therefore, the high resilience of anchovy in a climatological setting is non-surprising. I also concluded that the hake fishery may benefit from lower fishing pressures since this would result in an increase of the biomass big enough to offset the reduction in the fishing rate and produce a net increase in landings.

In order to understand the potential impacts of fish variability on plankton, we explored the effect of changing zooplankton mortality on the biogeochemistry of the NHCS (Chapter 2). We observed that, although the mortality of both small and large

zooplankton was modified, large zooplankton was the main driver of the response of the plankton ecosystem. This is due to its role as the top explicit predator in the bgc model. Chapter 2 also shows the importance of considering the diversity of plankton in sensitivity studies. Already with only two size classes of phytoplankton and zooplankton, the trophic interactions play a key role by buffering the response of the community. In reality, the plankton community is far more complex.

6.2 Lessons learnt from using end-to-end models

Different models were designed for answering specific questions and picking the most adequate model requires an understanding of its strengths and limitations, as well as the peculiarities of the system to be studied. Modelling the NHCS entails two main challenges. The first challenge is the representation of the processes associated with the shallow and intense oxygen minimum zone (OMZ). These include, from the nitrogen loss reactions at the biogeochemical level, to the concentration of epipelagic fish populations near the surface and the vertically migrants hiding in the OMZ at the ecological level. Secondly, the environmental interannual variability has an impact on the ecosystem that is not yet fully understood, hence the challenge of replicating this variability in the models.

In an end-to-end modelling system, plankton is the link between the bgc and HTL components; therefore, it is important to be tuned. Zooplankton has traditionally been used as a closure term in bgc models to balance the other compartments of the model. It does not resemble a specific set of species but rather the whole community. This, in addition to the sparsity in field observations and sampling errors, make it especially difficult to tune (see Section 2.5.1 and references there). In this project, we made a tuning effort of the CROCO(ROMS)-BioEBUS model. This resulted in an improved representation of the large zooplankton compartment of BioEBUS in Chapter 3 compared to Chapter 2.

When coupling the bgc and HTL models, it is important to consider in which ways the biogeochemistry and HTL may interact. In the case of this project, we focused on the plankton food for fish as the main driver of interannual variability. We did observe an impact on the fish that is comparable to the variability in plankton. However, we concluded that other drivers may be more important to simulate the extreme fluctuations in fish such as anchovy and sardines. The possibilities for including other drivers are discussed in Sect. 6.3.1.

When comparing two different HTL models (OSMOSE and Anderson, Chapter 5), we observed a linear–like response of Anderson in contrast to a complex response in OSMOSE. We concluded that the non-linear response of OSMOSE is driven by the explicit life-cycle of this model as well as the trophic interactions in the ecosystem. Therefore, this model is useful for studying complex, non-linear interactions in the ecosystem. On the other hand, Anderson allows us to evaluate the direct impact of changes in primary production on mesopelagic fish biomass. In addition, its simplicity makes it a good candidate for exploring the impact of HTL on biogeochemistry (two-way coupling) more easily than with OSMOSE. Bridging the gap between these two very different model, as well as areas of opportunity for the further development of models including mesopelagic fish, is approached in Sect. 6.3.2.

This project builds on previous work to provide mechanistic understanding of the ecological interactions and sensitivity in the NHCS. I detected some pressing challenges and opportunities for modelling the NHCS that should be addressed in further studies. Regarding top–down and bottom–up drivers, this doctoral project aimed at understanding them separately. Therefore, a purely one-way coupling approach was implemented. This is necessary to substract underlying responses out of the complexity of the ecosystem. However, feedbacks may occur when top–down and bottom–up processes interact (e.g., Travers et al., 2009; Travers-Trolet et al., 2014). Therefore, a two-way coupling system may be required as follow up work. Considerations for implementing a fully–coupled system are provided in Sect. 6.3.3.

6.3   Outlook

6.3.1   Modelling temporal variability in the NHCS

Challenges remain for modelling the strong interannual variability of the nothern-Humboldt Current System (NHCS) and especially the regime shifts in fish. Environmental variability in OSMOSE is represented through the plankton consumption by juvenile and adult fish, the distribution maps, which represent the habitat of the fish, and egg production. In Chapter 4, I mention some of the variables that are associated with the response of hake to El Niño, including changes in its distribution and associated responses in cannibailsm and catchability (see Chapter 4 and references there). Furthermore, Boerema and Gulland (1973) pointed out that the mortality of adult anchovies does not seem to severely increase during El Niño years. Instead, the anchovy collapse

of 1972 was associated with a recruitment failure (Boerema and Gulland, 1973). In this section, I explore how temporal variability could be further represented in OSMOSE.

In addition to plankton forcing and distribution maps, the impact of environmental processes on fish is parameterised through the plankton accessibility coefficient (AC) and the larval mortality (LM) in OSMOSE. These two parameters are among the most uncertain in OSMOSE (Travers-Trolet et al., 2014). Therefore, efforts should focus on, either searching for an alternative way to represent environmental drivers, especially regarding early life stages, or to reduce the uncertainty on these parameters. The approach by Oliveros-Ramos et al. (2017) consisted of estimating a time-series of AC and LM using landings and biomass data. A next step would be to use an inverse approach to find a relationship between the estimated parameters and the variables in the physical-biogeochemical model. Another approach would be to find a mechanistic link between the observations and OSMOSE through a sub-model (e.g., larval model by Hermann et al., 2001; Lett et al., 2008). This requires a bigger effort but I think that it could be more reliable in the long term since the mechanistic relationships would allow to simulate non-linear effects as well (see Griffen et al., 2016).

In addition to environmental variability, fishing pressure has also changed over time due to factors such as fishing seasons, regulatory policies, new technology and increase in the fishing fleet (see Aranda, 2009). For instance, the Peruvian anchovy fishery fleet had only 25 registered vessels in 1951 (Aranda, 2009). Lack of regulations allowed the fleet to grow to 1744 boats by 1964 (Aranda, 2009). After the fisheries collapse of 1972, the fleet decreased an remained relatively low through the 1980s (see Aranda, 2009, their Figure 2). In 1990, the fleet consisted of 386 vessels which increased again to 727 by 1996 and to 1200 by 2009 (Aranda, 2009). In the case of hake, its fishing pressure increased throughout the 1990's from about 40 vessels in 1990 to 74 in 2001 (Guevara-Carrasco and Lleonart, 2008).

Adding all these sources of variability to OSMOSE step by step would allow us to study separately the individual effect of each driver and to understand their combined effect. For instance, the first two steps –introducing interannual variability through plankton food for the fish and interannually varying habitat maps– have already been done over the work of this thesis. The next step would be to include the variability in larval mortality, either with a sub-model or with a statistical method. Once the temporal dynamics of the fish biomass are replicated, then the impact of a changing fishing rate should help to explain the differences between temporal trends in biomass and landings. The top–down human pressure on the system can be also highly dy-

namic, hence the importance of exploring it separately. A trend in the fishing rate of anchovy could be derived, for instance, from the time-series of the fleet size provided by Aranda (2009, their Figure 2). This process resembles the step-wise calibration proposed by Oliveros-Ramos et al. (2017), with the difference that I would advocate for seeking mechanistic relationships. For this, I stress the importance of understanding the variability that is introduced by each component of the model also separately.

Finally, when we talk about regime shifts, it is also important to step back for a moment and consider our definition of regime shift. There was an El Niño event in 1998 that had a noticeable impact on the ecosystem. However, the sardine–anchovy shift was a longer process than the 17 years simulated by the model. The sardine collapse after El Niño of 1998 was in fact the tail of a greater decline (see Chavez et al., 2003). In this sense, the period between 1992 and 2008 that we simulated in Chapter 3 is not a steady–shift–steady period but rather a section of a longer, gradual change. In this case, I would consider to simulate a larger period of time that encompasses the interdecadal fluctuations of anchovy and sardine, rather than a small section of one of those fluctuations. Biological studies focusing on short periods of time are not rare due to several constrains such as the difficulty to assemblage different time-series or to communicate between different laboratories (Pauly and Tsukayama, 1987a). Producing longer hindcast model simulation is limited by the availability of data –in the case of this project, I only had access to a 17 years time-series–. This data many times exists but it is not publicly available, or not in English. In this regard, I consider that open science and data sharing are a crucial step for advancing science at its full potential.

6.3.2 Modelling mesopelagic fish

Mesopelagic fish are a potential marine resource in the sight of the fishing industry. These represent a huge amount of biomass in the order of magnitude of gigatonnes (Gjøsæter and Kawaguchi, 1980; Irigoien et al., 2014). In face of the current climate change problem and the rush to understand and find ways to capture carbon, there is concern about the role of mesopelagic fish in carbon sequestration in the deep ocean (Martin et al., 2020). In particular, mesopelagic fish transport organic matter to the ocean interior through diel vertical migrations (Davison et al., 2013; Belcher, Saunders, and Tarling, 2019; Hernández-León et al., 2019). The daily up and down movement performed by mesopelagic organisms is the largest migration on Earth. Additionally, while the role of mesopelagic fish in the marine ecosystem is still largely unknown, there is increasing evidence of their importance for the deep water trophic web (Mann,

1984; Davison, Lara-Lopez, and Anthony Koslow, 2015; Saunders et al., 2019).

In Chapter 5, we compared mesopelagic fish in OSMOSE and the Anderson model and identified the strengths of approaching the same problem with different modelling systems, as well as the high uncertainty associated to mesopelagic fish. The same mortality of adult and juvenile fish in OSMOSE and the single compartment of mesopelagic fish in Anderson generated a higher biomass in Anderson. However, the biomass in OSMOSE was calibrated by adjusting the AC and LM which are highly unconstrained parameters. Anderson is mass conserving and uncertainty analysis can be more easily performed; therefore, biomass estimations of this model could be used as input to calibrate OSMOSE in further studies. The multispecies approach of the latter could then be used for more detailed studies resolving inter- and intraspecific interactions.

From a top–down perspective, data on top–predators could be helpful to constrain the models and also to study further trophic interactions in the deep ocean and its connection to the epipelagic ecosystem. In the waters off Peru, sperm whales (*Physeter macrocephalus*) prey on squids and especially on Humboldt squids (Majluf and Reyes, 1989), which in turn consume mesopelagic fish (Markaida and Sosa-Nishizaki, 2003). The biomass of these whales off Peru is estimated to be in the order of tens of thousands (Majluf and Reyes, 1989). Therefore, a bio-energetic balance of deep divers such as sperm whales could provide a lower boundary for constraining the abundance of mesopelagic fish. In addition, this would bring information on the potential impacts of harvesting mesopelagic fish on the ecosystem. Worldwide, there is a wide range of other deep–diving large predators that feed in the mesopelagic ecosystem, including pinnipeds, cetaceans, sharks and bony fish such as swordfish (see Braun et al., 2022). These species have important ecological roles also in the epipelagic zone and some of them are commercially exploited (Braun et al., 2022). Understanding the use and importance of the mesopelagic zone for these organisms is, therefore, crucial before exploiting the deep ocean (Braun et al., 2022). Furthermore, deep divers have been suggested to play themselves also a role in the carbon capture and nutrient cycles (Lavery et al., 2010). Hence, including them in dynamic models may also close nutrient budgets between epi- and mesopelagic environments.

In my view, the exploitation of mesopelagic fish should follow an ecosystem-based management approach. This approach has already been proposed for currently exploited ecosystems (e.g., Shannon et al., 2004; Fletcher et al., 2010; Link et al., 2011). Therefore, it is important to implement models that not only balance the nutrient and carbon fluxes in a mass conserving fashion, but also consider the ecosystem interac-

tions (see Section 1.3.2). For this, after initial exploratory studies like the one proposed in Chapter 5, I would focus on developing a multispecies end-to-end model for the deep ocean. An explicit vertical component, in addition to the horizontal dimensions, would be important in order to include the interactions of the mesopelagic fauna with epi- and, potentially, also bathypelagic organisms.

6.3.3 Towards a fully coupled end-to-end model for the NHCS

A fully two-way coupled modelling system is the next step to evaluate the interactions and potential feedbacks between top–down and bottom–up drivers once these have been understood separately. For instance, Travers-Trolet et al. (2014) observed that the interaction of fishing pressure (top–down) and climate change (bottom–up) have a dampening effect. In this section, I discuss some lessons learnt during my project that may be relevant when attempting to set-up a two-way coupled end-to-end model of the NHCS.

A fully coupled system for the NHCS could follow the basic set-up proposed by Travers-Trolet, Shin, and Field (2014) with slight changes and also including environmental impacts on the habitat for the fish and on the LM. The two-way coupling approach suggested by Travers-Trolet, Shin, and Field (2014) links fish and biogeochmistry through plankton consumption and mortality. In a coupled system, fish feed on plankton, as in Chapters 3 to 5, and the effect of fish predation on plankton is represented by modifying the mortality of phyto- and zooplankton. The maximum mortality that can be experienced by the plankton depends on the AC (see Travers-Trolet, Shin, and Field, 2014). Therefore, the first change that I would consider is to use one AC for all groups in order to avoid introducing biases to the impact on every plankton group.

The sensitivity of the model to LM, as well as the potential role of LM in simulating the interannual variability of fish, has been already discussed in previous sections, as well as the potential role of recruitment failure in the interannual variability of small pelagic fish off Peru (Chapter 3). Therefore, I consider it important to include variability in the LM in order to study environmental effects on fish, especially in the context of the high environmental variability of the NHCS (see Alheit and Niquen, 2004). Some suggestions to include a dynamic LM have been proposed in Sect. 6.3.1. However, these have methodological constrains. In idealised scenarios, the potential environmental impact through LM could also be studied simply by modifying the parameter similarly to the

experiment by Guo et al. (2019).

Finally, a set-up that aims at exploring potential climate scenarios should take into account the effect of environmental changes on the habitat of the fish. In the OSMOSE configuration used during my thesis, the habitat of the fish is constrained by distribution maps. These were derived from interannual maps developed by Oliveros-Ramos (2014) using habitat niche models that relate the occurrence of fish with measured variables such as oxygen, depth, temperature and chlorophyll (Oliveros-Ramos, 2014). I averaged these interannual maps to produce a climatology as explained in Chapter 3. However, in Sect. 3.7.3, we observed that applying interannually varying distribution maps produces an impact comparable, and for some species bigger, to the interannual variability in the plankton food. Therefore, it is important to also extend the hindcast of the distribution maps to any climate scenarios that we intend to explore with OSMOSE. This can be done by coupling the habitat niche models to the environmental variables of the physical-biogeochemical model for every time-step, rather than using prescribed maps. This set-up would be useful for exploring how changes in the habitat could affect the ecosystem, including fish distribution, biomass and species interactions, in a changing ocean.

Bibliography

Alarcón-Muñoz, R, LA Cubillos, and C Gatica (2008). "Jumbo squid (*Dosidicus gigas*) biomass off central Chile: effects on Chilean hake (*Merluccius Gayi*)". In: *CalCOFI Reports* 49, pp. 157–166.

Alheit, J and M Niquen (2004). "Regime shifts in the Humboldt Current ecosystem". In: *Progress in Oceanography* 60 (2), pp. 201–222. ISSN: 0079-6611. DOI: 10.1016/j.pocean. 2004.02.006.

Allgeier, JE, DE Burkepile, and CA Layman (2017). "Animal pee in the sea: consumer-mediated nutrient dynamics in the world's changing oceans". In: *Global Change Biology* 23 (6), pp. 2166–2178. DOI: 10.1111/gcb.13625.

Anderson, TR, WC Gentleman, and B Sinha (2010). "Influence of grazing formulations on the emergent properties of a complex ecosystem model in a global ocean general circulation model". In: *Progress in Oceanography* 87 (1). 3rd GLOBEC OSM: From ecosystem function to ecosystem prediction, pp. 201 –213. ISSN: 0079-6611. DOI: 10.1016/j.pocean.2010.06.003.

Anderson, TR, AP Martin, RS Lampitt, CN Trueman, SA Henson, and DJ Mayor (2019). "Quantifying carbon fluxes from primary production to mesopelagic fish using a simple food web model". In: *ICES Journal of Marine Science* 76 (3), pp. 690–701. ISSN: 1054-3139. DOI: 10.1093/icesjms/fsx234.

Antezana, T (2010). "*Euphausia mucronata*: A keystone herbivore and prey of the Humboldt Current System". In: *Deep Sea Research Part II: Topical Studies in Oceanography* 57 (7), pp. 652–662. ISSN: 0967-0645. DOI: 10.1016/j.dsr2.2009.10.014.

Aranda, M (2009). "Evolution and state of the art of fishing capacity management in Peru: The case of the anchoveta fishery". In: *Pan-American Journal of Aquatic Sciences* 4 (2), pp. 146–153.

Archibald, KM, DA Siegel, and SC Doney (2019). "Modeling the Impact of Zooplankton Diel Vertical Migration on the Carbon Export Flux of the Biological Pump". In: *Global Biogeochemical Cycles* 33 (2), pp. 181–199. DOI: 10.1029/2018GB005983.

Arhonditsis, G and M Brett (2004). "Evaluation of the current state of mechanistic aquatic biogeochemical modeling". In: *Marine Ecology Progress Series* 271, pp. 13–26. DOI: 10.3354/meps271013.

Arias-Schreiber, M (1996). *Informe sobre el estado de conocimiento y conservación de los mamíferos marinos en el Perú*. Instituto del Mar del Perú. Informe Progresivo vol. 38. URL: https://repositorio.imarpe.gob.pe/handle/20.500.12958/1193 (visited on May 19, 2022).

Arias Schreiber, M (2012). "The evolution of legal instruments and the sustainability of the Peruvian anchovy fishery". In: *Marine Policy* 36 (1), pp. 78–89. ISSN: 0308-597X. DOI: 10.1016/j.marpol.2011.03.010.

Atlas, R, RN Hoffman, SC Bloom, JC Jusem, and J Ardizzone (1996). "A Multiyear Global Surface Wind Velocity Dataset Using SSM/I Wind Observations". In: *Bulletin of the American Meteorological Society* 77 (5), pp. 869–882. DOI: 10.1175/1520-0477(1996)077⟨0869:AMGSWV⟩2.0.CO;2.

Aumont, O, C Ethé, A Tagliabue, L Bopp, and M Gehlen (2015). "PISCES-v2: an ocean biogeochemical model for carbon and ecosystem studies". In: *Geoscientific Model Development* 8, pp. 2465–2513. DOI: 10.5194/gmd-8-2465-2015.

Aumont, O, O Maury, S Lefort, and L Bopp (2018). "Evaluating the Potential Impacts of the Diurnal Vertical Migration by Marine Organisms on Marine Biogeochemistry". In: *Global Biogeochemical Cycles* 32 (11), pp. 1622–1643. DOI: 10.1029/2018GB005886. eprint: https://agupubs.onlinelibrary.wiley.com/doi/pdf/10.1029/2018GB005886.

Ayón, P, MI Criales-Hernandez, R Schwamborn, and HJ Hirche (2008a). "Zooplankton research off Peru: A review". In: *Progress in Oceanography* 79 (2-4), pp. 238–255. DOI: 10.1016/j.pocean.2008.10.020.

Ayón, P, S Purca, and R Guevara-Carrasco (2004). "Zooplankton volume trends off Peru between 1964 and 2001". In: *ICES Journal of Marine Science* 61 (4), pp. 478–484. ISSN: 1054-3139. DOI: 10.1016/j.icesjms.2004.03.027.

Ayón, P, G Swartzman, A Bertrand, M Gutiérrez, and S Bertrand (2008b). "Zooplankton and forage fish species off Peru: large-scale bottom-up forcing and local-scale depletion". In: *Progress in Oceanography* 79 (2-4), pp. 208–214. DOI: 10.1016/j.pocean.2008.10.023.

Baklouti, M, V Faure, L Pawlowski, and A Sciandra (2006). "Investigation and sensitivity analysis of a mechanistic phytoplankton model implemented in a new modular numerical tool (Eco3M) dedicated to biogeochemical modelling". In: *Progress in Oceanography* 71, pp. 34–58. DOI: 10.1016/j.pocean.2006.05.003.

Bakun, A and K Broad (2003). "Environmental 'loopholes' and fish population dynamics: comparative pattern recognition with focus on El Niño effects in the Pacific". In: *Fisheries Oceanography* 12 (4-5), pp. 458–473. DOI: 10.1046/j.1365-2419.2003.00258.x.

Bakun, A and CS Nelson (1991). "The Seasonal Cycle of Wind-Stress Curl in Subtropical Eastern Boundary Current Regions". In: *Journal of Physical Oceanography* 21 (12), pp. 1815–1834. DOI: 10.1175/1520-0485(1991)021⟨1815:TSCOWS⟩2.0.CO;2.

Bakun, A and SJ Weeks (2008). "The marine ecosystem off Peru: What are the secrets of its fishery productivity and what might its future hold?" In: *Progress in Oceanography* 79 (2). The Northern Humboldt Current System: Ocean Dynamics, Ecosystem Processes, and Fisheries, pp. 290–299. ISSN: 0079-6611. DOI: 10.1016/j.pocean.2008.10.027.

Ballón, M, C Wosnitza-Mendo, R Guevara-Carrasco, and A Bertrand (2008). "The impact of overfishing and El Niño on the condition factor and reproductive success of Peruvian hake, Merluccius gayi peruanus". In: *Progress in Oceanography* 79 (2). The Northern Humboldt Current System: Ocean Dynamics, Ecosystem Processes, and Fisheries, pp. 300–307. ISSN: 0079-6611. DOI: 10.1016/j.pocean.2008.10.016.

Bănaru, D, F Diaz, P Verley, R Campbell, J Navarro, C Yohia, R Oliveros-Ramos, C Mellon-Duval, and YJ Shin (2019). "Implementation of an end-to-end model of the Gulf of Lions ecosystem (NW Mediterranean Sea). I. Parameterization, calibration and evaluation". In: *Ecological Modelling* 401, pp. 1–19. ISSN: 0304-3800. DOI: 10.1016/j.ecolmodel.2019.03.005.

Barber, RT and FP Chavez (1983). "Biological consequences of El Niño". In: *Science* 222 (4629), pp. 1203–1210. DOI: 10.1126/science.222.4629.1203.

Barrett, RC, JP Caulkins, AJ Yates, and D Elliott (1985). "Population dynamics of the Peruvian anchovy". In: *Mathematical Modelling* 6 (6), pp. 525–548. ISSN: 0270-0255. DOI: 10.1016/0270-0255(85)90052-1.

Barton, AD, S Dutkiewicz, G Flierl, J Bragg, and MJ Follows (2010). "Patterns of Diversity in Marine Phytoplankton". In: *Science* 327 (5972), pp. 1509–1511. ISSN: 0036-8075. DOI: 10.1126/science.1184961.

Baum, JK and B Worm (2009). "Cascading top-down effects of changing oceanic predator abundances". In: *Journal of Animal Ecology* 78 (4), pp. 699–714. DOI: 10.1111/j.1365-2656.2009.01531.x.

Beddington, JR and RM May (1977). "Harvesting Natural Populations in a Randomly Fluctuating Environment". In: *Science* 197 (4302), pp. 463–465. ISSN: 0036-8075. DOI: 10.1126/science.197.4302.463. eprint: https://science.sciencemag.org/content/197/4302/463.full.pdf.

Behrenfeld, MJ, RT O'Malley, DA Siegel, CR McClain, JL Sarmiento, GC Feldman, AJ Milligan, PG Falkowski, RM Letelier, and ES Boss (2006). "Climate-driven trends in contemporary ocean productivity". In: *Nature* 444 (7120), pp. 752–755. DOI: 10.1038/nature05317.

Belcher, A, R Saunders, and G Tarling (2019). "Respiration rates and active carbon flux of mesopelagic fishes (Family Myctophidae) in the Scotia Sea, Southern Ocean". In: *Marine Ecology Progress Series* 610, pp. 149–162. DOI: 10.3354/meps12861.

Bianchi, D, DA Carozza, ED Galbraith, J Guiet, and T DeVries (2021). "Estimating global biomass and biogeochemical cycling of marine fish with and without fishing". In: *Science Advances* 7 (41), eabd7554. ISSN: 23752548. DOI: 10.1126/sciadv.abd7554.

Biard, T, L Stemmann, M Picheral, N Mayot, P Vandromme, H Hauss, G Gorsky, L Guidi, R Kiko, and F Not (2016). "In situ imaging reveals the biomass of giant protists in the global ocean". In: *Nature* 532 (7600), pp. 504–507. DOI: 10.1038/nature17652.

Bieg, C and KS McCann (2020). "Fisheries restoration potential: Optimizing fisheries profits while maintaining food web structure, economy". In: *Food Webs* 25, e00168. ISSN: 2352-2496. DOI: 10.1016/j.fooweb.2020.e00168.

Boerema, LK and JA Gulland (1973). "Stock Assessment of the Peruvian Anchovy (Engraulis ringens) and Management of the Fishery". In: *Journal of the Fisheries Research Board of Canada* 30 (12), pp. 2226–2235. DOI: 10.1139/f73-351.

Braun, CD, MC Arostegui, SR Thorrold, YP Papastamatiou, P Gaube, J Fontes, and P Afonso (2022). "The Functional and Ecological Significance of Deep Diving by Large Marine Predators". In: *Annual Review of Marine Science* 14 (1), pp. 129–159. DOI: 10.1146/annurev-marine-032521-103517. eprint: https://doi.org/10.1146/annurev-marine-032521-103517.

Briton, F, L Shannon, N Barrier, P Verley, and YJ Shin (2019). "Reference levels of ecosystem indicators at multispecies maximum sustainable yield". In: *ICES Journal of Marine Science* 76 (7), pp. 2070–2081. ISSN: 1054-3139. DOI: 10.1093/icesjms/fsz104. eprint: https://academic.oup.com/icesjms/article-pdf/76/7/2070/31679591/fsz104.pdf.

Cai, WJ, X Hu, WJ Huang, MC Murrell, JC Lehrter, SE Lohrenz, WC Chou, W Zhai, JT Hollibaugh, Y Wang, P Zhao, X Guo, K Gundersen, M Dai, and GC Gong (2011). "Acidification of subsurface coastal waters enhanced by eutrophication". In: *Nature Geoscience* 4 (11), pp. 766–770. DOI: 10.1038/ngeo1297.

Canal Loayza, R (1989). *Evaluación de la capacidad y condición reproductiva de la Merluza (Merluccius gayi peruanus)*. Instituto del Mar del Perú. Boletín IMARPE vol. 13.2, pp. 39–70. URL: https://repositorio.imarpe.gob.pe/handle/20.500.12958/1135 (visited on May 19, 2022).

Carozza, DA, D Bianchi, and ED Galbraith (2016). "The ecological module of BOATS-1.0: a bioenergetically constrained model of marine upper trophic levels suitable for studies of fisheries and ocean biogeochemistry". In: *Geoscientific Model Development* 9 (4), pp. 1545–1565. DOI: 10.5194/gmd-9-1545-2016.

Carr, ME (2002). "Estimation of potential productivity in Eastern Boundary Currents using remote sensing." In: *Deep Sea Research Part II* 49 (1), pp. 59–80. DOI: 10.1016/S0967-0645(01)00094-7.

Carton, JA, GA Chepurin, and L Chen (2018). "SODA3: A New Ocean Climate Reanalysis". In: *Journal of Climate* 31 (17), pp. 6967–6983. DOI: 10.1175/JCLI-D-18-0149.1.

Carton, JA and BS Giese (2008). "A reanalysis of ocean climate using Simple Ocean Data Assimilation (SODA)". In: *Monthly Weather Review* 136 (8), pp. 2999–3017. DOI: 10.1175/2007MWR1978.1.

Castillo Valderrama, R, M Gutiérrez Torero, S Peraltilla Neyra, and N Herrera Almirón (1998). *Biomasa de recursos pesqueros a finales del invierno 1998. Crucero BIC Humboldt y BIC Jose Olaya Balandra 9808-09, de Paita a Tacna*. Instituto del Mar del Perú. Informe IMARPE 141. URL: https://repositorio.imarpe.gob.pe/handle/20.500.12958/1562 (visited on May 19, 2022).

– (1999). *Biomasas de las principales especies recursos pesqueros durante el verano 1999. Crucero BIC Jose Olaya Balandra 9902-03, de Tumbes a Tacna*. Instituto del Mar del Perú. Informe IMARPE 147. URL: https://repositorio.imarpe.gob.pe/handle/20.500.12958/1593 (visited on May 19, 2022).

Chavez, FP, A Bertrand, R Guevara-Carrasco, P Soler, and J Csirke (2008). "The northern Humboldt Current System: Brief history, present status and a view towards the future". In: *Progress in Oceanography* 79, pp. 95–105. DOI: 10.1016/j.pocean.2008.10.012.

Chavez, FP and M Messié (2009). "A comparison of eastern boundary upwelling ecosystems". In: *Progress in Oceanography* 83 (1-4), pp. 80–96. DOI: 10.1016/j.pocean.2009.07.032.

Chavez, FP, J Ryan, SE Lluch-Cota, and M Ñiquen (2003). "From anchovies to sardines and back: multidecadal change in the Pacific Ocean". In: *Science* 299 (5604), pp. 217–221. DOI: 10.1126/science.1075880.

Checkley, D, P Ayon, T Baumgartner, M Bernal, J Coetzee, R Emmett, R Guevara-Carrasco, L Hutchings, L Ibaibarriaga, H Nakata, Y Oozeki, B Planque, J Schweigert, Y Stratoudakis, and C van der Lingen (2009). "Habitats". In: *Climate Change and Small Pelagic Fish*. Ed. by D Checkley, J Alheit, Y Oozeki, and C Roy. Cambridge: Cambridge University Press. Chap. 3, pp. 64–146. DOI: 10.1017/CBO9780511596681.

Christensen, V, M Coll, J Buszowski, WWL Cheung, T Frölicher, J Steenbeek, CA Stock, RA Watson, and CJ Walters (2015). "The global ocean is an ecosystem: simulating

marine life and fisheries". In: *Global Ecology and Biogeography* 24 (5), pp. 507–517. DOI: 10.1111/geb.12281.

Christensen, V, S de la Puente, JC Sueiro, J Steenbeek, and P Majluf (2014). "Valuing seafood: The Peruvian fisheries sector". In: *Marine Policy* 44, pp. 302–311. ISSN: 0308-597X. DOI: 10.1016/j.marpol.2013.09.022.

Clark, WG (1976). "The lessons of the Peruvian anchoveta fishery". In: *California Cooperative Oceanic Fisheries Investigations Reports* 19, pp. 57–63.

Cornejo Urbina, R and R Koppelmann (2006). "Distribution patterns of mesopelagic fishes with special reference to *Vinciguerria lucetia* Garman 1899 (Phosichthyidae: Pisces) in the Humboldt Current Region off Peru". In: *Marine Biology* 149, pp. 1519–1537. DOI: 10.1007/s00227-006-0319-z.

Cropp, R and J Norbury (2020). "The emergence of new trophic levels in eco-evolutionary models with naturally-bounded traits". In: *Journal of Theoretical Biology* 496, p. 110264. ISSN: 0022-5193. DOI: 10.1016/j.jtbi.2020.110264.

Cury, P, A Bakun, RJ Crawford, A Jarre, RA Quinones, LJ Shannon, and HM Verheye (2000). "Small pelagics in upwelling systems: patterns of interaction and structural changes in "wasp-waist" ecosystems". In: *ICES Journal of Marine Science* 57 (3), pp. 603–618. DOI: 10.1006/jmsc.2000.0712.

Cury, P and C Roy (1989). "Optimal Environmental Window and Pelagic Fish Recruitment Success in Upwelling Areas". In: *Canadian Journal of Fisheries and Aquatic Sciences* 46 (4), pp. 670–680. DOI: 10.1139/f89-086.

Cury, P, L Shannon, and YJ Shin (2003). "The Functioning of Marine Ecosystems: a Fisheries Perspective". In: *Responsible Fisheries in the Marine Ecosystem*. Food and Agricultural Organization of the United Nations (FAO). Chap. 7, pp. 103–123.

Cushing, D (1990). "Plankton Production and Year-class Strength in Fish Populations: an Update of the Match/Mismatch Hypothesis". In: *Advances in Marine Biology* 26, pp. 249–293. ISSN: 0065-2881. DOI: 10.1016/S0065-2881(08)60202-3.

Daewel, U, SS Hjøllo, M Huret, R Ji, M Maar, S Niiranen, M Travers-Trolet, MA Peck, and KE van de Wolfshaar (2014). "Predation control of zooplankton dynamics: a

review of observations and models". In: *ICES Journal of Marine Science* 71 (2), pp. 254–271.

Dahlberg, MD (1979). "A review of survival rates of fish eggs and larvae in relation to impact assessments". In: *Marine Fisheries Review* 41 (3). URL: https://spo.nmfs.noaa.gov/content/review-survival-rates-fish-eggs-and-larvae-relation-impact-assessments (visited on May 19, 2022).

Davison, P, D Checkley, J Koslow, and J Barlow (2013). "Carbon export mediated by mesopelagic fishes in the northeast Pacific Ocean". In: *Progress in Oceanography* 116, pp. 14–30. ISSN: 0079-6611. DOI: 10.1016/j.pocean.2013.05.013.

Davison, P, A Lara-Lopez, and J Anthony Koslow (2015). "Mesopelagic fish biomass in the southern California current ecosystem". In: *Deep Sea Research Part II: Topical Studies in Oceanography* 112. CCE-LTER: Responses of the California Current Ecosystem to Climate Forcing, pp. 129–142. ISSN: 0967-0645. DOI: 10.1016/j.dsr2.2014.10.007.

Davison, PC, JA Koslow, and RJ Kloser (2015). "Acoustic biomass estimation of mesopelagic fish: backscattering from individuals, populations, and communities". In: *ICES Journal of Marine Science* 72 (5), pp. 1413–1424. ISSN: 1054-3139. DOI: 10.1093/icesjms/fsv023.

Del Solar, E, J Sánchez R., and A Piazza L. (1965). *Exploración de las áreas de abundancia de meluza (merluccius gayi peruanus) en la costa peruana a bordo del "Bettina"*. Instituto del Mar del Perú. Informe 8. URL: https://repositorio.imarpe.gob.pe/handle/20.500.12958/237 (visited on May 19, 2022).

Diaz, F, D Bănaru, P Verley, and YJ Shin (2019). "Implementation of an end-to-end model of the Gulf of Lions ecosystem (NW Mediterranean Sea). II. Investigating the effects of high trophic levels on nutrients and plankton dynamics and associated feedbacks". In: *Ecological Modelling* 405, pp. 51–68. ISSN: 0304-3800. DOI: 10.1016/j.ecolmodel.2019.05.004.

Doney, SC, VJ Fabry, RA Feely, and JA Kleypas (2009). "Ocean Acidification: The Other CO2 Problem". In: *Annual Review of Marine Science* 1 (1). PMID: 21141034, pp. 169–192. DOI: 10.1146/annurev.marine.010908.163834.

Duboz, R, D Versmisse, M Travers, E Ramat, and YJ Shin (2010). "Application of an evolutionary algorithm to the inverse parameter estimation of an individual-based

model". In: *Ecological Modelling* 221 (5), pp. 840–849. ISSN: 0304-3800. DOI: 10.1016/j.ecolmodel.2009.11.023.

Duffy, DC (1983). "Environmental uncertainty and commercial fishing: Effects on Peruvian guano birds". In: *Biological Conservation* 26 (3), pp. 227–238. ISSN: 0006-3207. DOI: [10.1016/0006-3207(83)90075-7](10.1016/0006-3207(83)90075-7).

– (1994). "The guano islands of Peru: the once and future management of a renewable resource". In: *Birdlife Conservation Series* 1, pp. 68–76.

Dutkiewicz, S, MJ Follows, and JG Bragg (2009). "Modeling the coupling of ocean ecology and biogeochemistry". In: *Global Biogeochemical Cycles* 23 (4), GB4017. DOI: [10.1029/2008GB003405](10.1029/2008GB003405).

Echevin, V, O Aumont, J Ledesma, and G Flores (2008). "The seasonal cycle of surface chlorophyll in the Peruvian upwelling system: A modelling study". In: *Progress in Oceanography* 79 (2), pp. 167–176. ISSN: 0079-6611. DOI: 10.1016/j.pocean.2008.10.026.

Edwards, AM and A Yool (2000). "The role of higher predation in plankton population models". In: *Journal of Plankton Research* 22 (6), pp. 1085–1112.

Espinoza, P and A Bertrand (2008). "Revisiting Peruvian anchovy (*Engraulis ringens*) trophodynamics provides a new vision of the Humboldt Current system". In: *Progress in Oceanography* 79 (2-4), pp. 215–227. DOI: 10.1016/j.pocean.2008.10.022.

Evans, GT and JS Parslow (1985). "A model of annual plankton cycles". In: *Biological oceanography* 3, pp. 327–347. URL: https://www.tandfonline.com/doi/abs/10.1080/01965581.1985.10749478 (visited on Apr. 23, 2021).

FAO (2020). *The State of World Fisheries and Aquaculture 2020. Sustainability in action*. FAO. Report. DOI: [10.4060/ca9231en](10.4060/ca9231en).

Farías, L, M Castro-González, M Cornejo, J Charpentier, J Faúndez, N Boontanon, and N Yoshida (2009). "Denitrification and nitrous oxide cycling within the upper oxycline of the eastern tropical South Pacific oxygen minimum zone". In: *Limnology and Oceanography* 54 (1), pp. 132–144. DOI: [10.4319/lo.2009.54.1.0132](10.4319/lo.2009.54.1.0132).

Farris, DA (1961). "Abundance and distribution of eggs and larvae of jack mackerel (*Trachurus symmetricus*)". In: *Fishery Bulletin U.S.* 61, pp. 247–279.

Fasham, MJ, PW Boyd, and G Savidge (1999). "Modeling the relative contributions of autotrophs and heterotrophs to carbon flow at a Lagrangian JGOFS station in the Northeast Atlantic: the importance of DOC". In: *Limnology and Oceanography* 44 (1), pp. 80–94. DOI: 10.4319/lo.1999.44.1.0080.

Fasham, M, H Ducklow, and S McKelvie (1990). "A nitrogen-based model of plankton dynamics in the oceanic mixed layer". In: *Journal of Marine Research* 48 (3), pp. 591–639. DOI: 10.1357/002224090784984678.

Fennel, K, J Wilkin, J Levin, J Moisan, J O'Reilly, and D Haidvogel (2006). "Nitrogen cycling in the Middle Atlantic Bight: Results from a three-dimensional model and implications for the North Atlantic nitrogen budget". In: *Global Biogeochemical Cycles* 20 (3), GB3007. DOI: 10.1029/2005GB002456. eprint: https://agupubs.onlinelibrary.wiley.com/doi/pdf/10.1029/2005GB002456.

Fernández Ramírez, F (1987). *Edad y crecimiento de la Merluza peruana (Merluccius gayi peruanus)*. IMARPE. Vol. 11.6, pp. 194–220. URL: https://hdl.handle.net/20.500.12958/992 (visited on May 19, 2022).

Fiechter, J, L Huckstadt, K Rose, and D Costa (2016). "A fully coupled ecosystem model to predict the foraging ecology of apex predators in the California Current". In: *Marine Ecology Progress Series* 556, pp. 273–285. DOI: 10.3354/meps11849.

Fiedler, PC (2002). "Environmental change in the eastern tropical Pacific Ocean: review of ENSO and decadal variability". In: *Marine Ecology Progress Series* 244, pp. 265–283. DOI: 10.3354/meps244265.

Field, J, R Francis, and K Aydin (2006). "Top-down modeling and bottom-up dynamics: Linking a fisheries-based ecosystem model with climate hypotheses in the Northern California Current". In: *Progress in Oceanography* 68 (2). Marine Ecosystem Structure and Dynamics, pp. 238–270. ISSN: 0079-6611. DOI: 10.1016/j.pocean.2006.02.010.

Fletcher, W, J Shaw, S Metcalf, and D Gaughan (2010). "An Ecosystem Based Fisheries Management framework: the efficient, regional-level planning tool for management agencies". In: *Marine Policy* 34 (6), pp. 1226–1238. ISSN: 0308-597X. DOI: 10.1016/j.marpol.2010.04.007.

Follows, MJ, S Dutkiewicz, S Grant, and SW Chisholm (2007). "Emergent Biogeography of Microbial Communities in a Model Ocean". In: *Science* 315 (5820), pp. 1843–1846. ISSN: 0036-8075. DOI: 10.1126/science.1138544.

Franz, J, G Krahmann, G Lavik, P Grasse, T Dittmar, and U Riebesell (2012). "Dynamics and stoichiometry of nutrients and phytoplankton in waters influenced by the oxygen minimum zone in the eastern tropical Pacific". In: *Deep Sea Research Part I: Oceanographic Research Papers* 62, pp. 20 –31. ISSN: 0967-0637. DOI: 10.1016/j.dsr.2011.12.004.

Frederiksen, M, M Edwards, AJ Richardson, NC Halliday, and S Wanless (2006). "From plankton to top predators: bottom-up control of a marine food web across four trophic levels". In: *Journal of Animal Ecology* 75 (6), pp. 1259–1268. DOI: 10.1111/j.1365-2656.2006.01148.x.

Fu, C, Y Shin, R Perry, J King, and H Liu (2012). "Exploring Climate and Fishing Impacts in an Ecosystem Model of the Strait of Georgia, British Columbia". In: *Global Progress in Ecosystem-Based Fisheries Management*. Alaska Sea Grant, University of Alaska Fairbanks, pp. 65–86. ISBN: 9781566121668. URL: http://seagrant.uaf.edu/bookstore/pubs/item.php?id=11932 (visited on May 19, 2022).

Fu, C, Y Xu, A Grüss, A Bundy, L Shannon, JJ Heymans, G Halouani, E Akoglu, CP Lynam, M Coll, EA Fulton, L Velez, and YJ Shin (2019). "Responses of ecological indicators to fishing pressure under environmental change: exploring non-linearity and thresholds". In: *ICES Journal of Marine Science* 77 (4), pp. 1516–1531. ISSN: 1054-3139. DOI: 10.1093/icesjms/fsz182.

Fu, C, Y Xu, C Guo, N Olsen, A Grüss, H Liu, N Barrier, P Verley, and YJ Shin (2020). "The Cumulative Effects of Fishing, Plankton Productivity, and Marine Mammal Consumption in a Marine Ecosystem". In: *Frontiers in Marine Science* 7, p. 840. ISSN: 2296-7745. DOI: 10.3389/fmars.2020.565699.

Fulton, E, M Fuller, A Smith, and A Punt (2004). *Ecological Indicators of the Ecosystem Effects of Fishing: Final Report*. CSIRO. R99/1546. DOI: 10.4225/08/585c169120a95.

Fulton, EA (2010). "Approaches to end-to-end ecosystem models". In: *Journal of Marine Systems* 81 (1). Contributions from Advances in Marine Ecosystem Modelling Research II 23-26 June 2008, Plymouth, UK, pp. 171–183. ISSN: 0924-7963. DOI: 10.1016/j.jmarsys.2009.12.012.

Fulton, EA, JS Link, IC Kaplan, M Savina-Rolland, P Johnson, C Ainsworth, P Horne, R Gorton, RJ Gamble, ADM Smith, and DC Smith (2011). "Lessons in modelling and management of marine ecosystems: the Atlantis experience". In: *Fish and Fisheries* 12 (2), pp. 171–188. DOI: 10.1111/j.1467-2979.2011.00412.x.

Getzlaff, J and A Oschlies (2017). "Pilot Study on Potential Impacts of Fisheries-Induced Changes in Zooplankton Mortality on Marine Biogeochemistry". In: *Global Biogeochemical Cycles* 31 (11), pp. 1656–1673. DOI: 10.1002/2017GB005721.

Gilly, WF, JM Beman, SY Litvin, and BH Robison (2013). "Oceanographic and biological effects of shoaling of the oxygen minimum zone". In: *Annual review of marine science* 5, pp. 393–420. DOI: 10.1146/annurev-marine-120710-100849.

Gjøsæter, J and K Kawaguchi (1980). *A review of the world resources of mesopelagic fish.* Food Agriculture Organization. FAO Fisheries Technical Paper 193, p. 157.

Gorsky, G, MD Ohman, M Picheral, S Gasparini, L Stemmann, J Romagnan, A Cawood, S Pesant, C García-Comas, and F Prejger (2010). "Digital zooplankton image analysis using the ZooScan integrated system". In: *Plankton Research* 32, pp. 285–303. DOI: 10.1093/plankt/fbp124.

Griffen, B, B Belgrad, Z Cannizzo, E Knotts, and E Hancock (2016). "Rethinking our approach to multiple stressor studies in marine environments ". In: *Marine Ecology Progress Series* 543, pp. 273–281. DOI: 10.3354/meps11595.

Grüss, A, M Drexler, and CH Ainsworth (2014). "Using delta generalized additive models to produce distribution maps for spatially explicit ecosystem models". In: *Fisheries Research* 159, pp. 11–24. ISSN: 0165-7836. DOI: 10.1016/j.fishres.2014.05.005.

Grüss, A, MJ Schirripa, D Chagaris, M Drexler, J Simons, P Verley, YJ Shin, M Karnauskas, R Oliveros-Ramos, and CH Ainsworth (2015). "Evaluation of the trophic structure of the West Florida Shelf in the 2000s using the ecosystem model OSMOSE". In: *Journal of Marine Systems* 144, pp. 30–47. ISSN: 0924-7963. DOI: 10.1016/j.jmarsys.2014.11.004.

Guénette, S, V Christensen, and D Pauly (2008). "Trophic modelling of the Peruvian upwelling ecosystem: Towards reconciliation of multiple datasets". In: *Progress in Oceanography* 79 (2). The Northern Humboldt Current System: Ocean Dynamics,

Ecosystem Processes, and Fisheries, pp. 326–335. ISSN: 0079-6611. DOI: 10.1016/j.pocean.2008.10.005.

Guevara-Carrasco, R and J Lleonart (2008). "Dynamics and fishery of the Peruvian hake: Between nature and man". In: *Journal of Marine Systems* 71 (3). The Wrapping Up of the IDEA Project: pp. 249–259. ISSN: 0924-7963. DOI: 10.1016/j.jmarsys.2007.02.030.

Guevara-Carrasco, R, F Rodríguez, and A Rodríguez (2004). *Biological characteristics of Peruvian hake during the 2001 summer cruise*. Instituto del Mar del Perú. Informe IMARPE vol. 32.3, pp. 257–262. URL: https://repositorio.imarpe.gob.pe/handle/20.500.12958/1830 (visited on May 19, 2022).

Guidino, C, E Campbell, B Alcorta, V Gonzalez, J Mangel, A Pacheco, S Silva, and J Alfaro-Shigueto (2020). "Whale watching in northern Peru: An economic boom?" American English. In: *Tourism in Marine Environments*, pp. 1–10. ISSN: 1544-273X. DOI: 10.3727/154427320X15819596320544.

Guo, C, C Fu, N Olsen, Y Xu, A Grüss, H Liu, P Verley, and YJ Shin (2019). "Incorporating environmental forcing in developing ecosystem-based fisheries management strategies". In: *ICES Journal of Marine Science* 77, pp. 500–514. ISSN: 1054-3139. DOI: 10.1093/icesjms/fsz246.

Gutiérrez, M, A Ramirez, S Bertrand, O Móron, and A Bertrand (2008). "Ecological niches and areas of overlap of the squat lobster 'munida' (Pleuroncodes monodon) and anchoveta (Engraulis ringens) off Peru". In: *Progress in Oceanography* 79 (2). The Northern Humboldt Current System: Ocean Dynamics, Ecosystem Processes, and Fisheries, pp. 256–263. ISSN: 0079-6611. DOI: 10.1016/j.pocean.2008.10.019.

Gutknecht, E, I Dadou, B Le Vu, G Cambon, J Sudre, V Garçon, E Machu, T Rixen, A Kock, A Flohr, et al. (2013a). "Coupled physical/biogeochemical modeling including O2-dependent processes in the Eastern Boundary Upwelling Systems: application in the Benguela". In: *Biogeosciences* 10, pp. 3559–3591. DOI: 10.5194/bg-10-3559-2013.

Gutknecht, E, I Dadou, P Marchesiello, G Cambon, B Le Vu, J Sudre, V Garçon, E Machu, T Rixen, A Kock, et al. (2013b). "Nitrogen transfers off Walvis Bay: a 3-D coupled physical/biogeochemical modeling approach in the Namibian upwelling system". In: *Biogeosciences* 10, pp. 4117–4135. DOI: 10.5194/bg-10-4117-2013.

Halouani, G, F Lasram, YJ Shin, L Velez, P Verley, T Hattab, R Oliveros-Ramos, F Diaz, F Ménard, M Baklouti, A Guyennon, R Ms, and F Le Loc'h (2016). "Modelling food web structure using an end-to-end approach in the coastal ecosystem of the Gulf of Gabes (Tunisia)". In: *Ecological Modelling* 339, pp. 45–57. DOI: 10.1016/j.ecolmodel.2016.08.008.

Hamersley, MR, G Lavik, D Woebken, JE Rattray, P Lam, EC Hopmans, JSS Damsté, S Krüger, M Graco, D Gutiérrez, and MMM Kuypers (2007). "Anaerobic ammonium oxidation in the Peruvian oxygen minimum zone". In: *Limnology and Oceanography* 52 (3), pp. 923–933. DOI: 10.4319/lo.2007.52.3.0923.

Herling, C, BM Culik, and JC Hennicke (2005). "Diet of the Humboldt penguin (Spheniscus humboldti) in northern and southern Chile". In: *Marine Biology* 147 (1), pp. 13–25. DOI: 10.1007/s00227-004-1547-8.

Hermann, AJ, S Hinckley, BA Megrey, and JM Napp (2001). "Applied and theoretical considerations for constructing spatially explicit individual-based models of marine larval fish that include multiple trophic levels". In: *Journal of Materials Science* 58, pp. 1030–1041. DOI: 10.1006/jmsc.2001.1087.

Hernández-León, S, MP Olivar, ML Fernández de Puelles, A Bode, A Castellón, C López-Pérez, VM Tuset, and JI González-Gordillo (2019). "Zooplankton and Micronekton Active Flux Across the Tropical and Subtropical Atlantic Ocean". In: *Frontiers in Marine Science* 6. ISSN: 2296-7745. DOI: 10.3389/fmars.2019.00535.

Hill Cruz, M, I Kriest, J José, R Kiko, H Hauss, and A Oschlies (2021). "Zooplankton mortality effects on the plankton community of the northern Humboldt Current System: sensitivity of a regional biogeochemical model". In: *Biogeosciences* 18, pp. 2891–2916. DOI: 10.5194/bg-18-2891-2021.

Hirst, A and T Kiørboe (2002). "Mortality of marine planktonic copepods: global rates and patterns". In: *Marine Ecology Progress Series* 230, pp. 195–209. URL: https://www.int-res.com/abstracts/meps/v230/p195-209/ (visited on May 19, 2022).

Holbrook, NJ, J Brown, J Davidson, M Feng, A Hobday, J Lough, S McGregor, S Power, and J Risbey (2012). "El Niño–Southern Oscillation". In: *A Marine Climate Change Impacts and Adaptation Report Card for Australia 2012*. Ed. by E Poloczanska, A Hobday, and A Richardson. CSIRO Climate Adaptation Flagship. ISBN: 9780643109285. URL: http://hdl.handle.net/102.100.100/99770?index=1 (visited on Apr. 23, 2021).

Howarth, RW (1988). "Nutrient Limitation of Net Primary Production in Marine Ecosystems". In: *Annual Review of Ecology and Systematics* 19, pp. 89–110. ISSN: 00664162. URL: http://www.jstor.org/stable/2097149 (visited on May 19, 2022).

Hsieh, Ch, CS Reiss, JR Hunter, JR Beddington, RM May, and G Sugihara (2006). "Fishing elevates variability in the abundance of exploited species". In: *Nature* 443, pp. 859–862. DOI: 10.1038/nature05232.

Hsieh, Ch, A Yamauchi, T Nakazawa, and WF Wang (2010). "Fishing effects on age and spatial structures undermine population stability of fishes". In: *Aquatic Sciences* 72 (2), pp. 165–178. DOI: 10.1007/s00027-009-0122-2.

Hutchings, L (1992). "Fish harvesting in a variable, productive environment — searching for rules or searching for exceptions?" In: *South African Journal of Marine Science* 12 (1), pp. 297–318. DOI: 10.2989/02577619209504708.

IPCC (2013). *Climate Change 2013: The Physical Science Basis. Contribution of Working Group I to the Fifth Assessment Report of the Intergovernmental Panel on Climate Change*. Ed. by T Stocker, D Qin, GK Plattner, M Tignor, S Allen, J Boschung, A Nauels, Y Xia, V Bex, and P Midgley. Cambridge University Press. URL: https://www.ipcc.ch/report/ar5/wg1/ (visited on May 19, 2022).

Irigoien, X, K Flynn, and R Harris (2005). "Phytoplankton blooms: a 'loophole' in microzooplankton grazing impact?" In: *Journal of Plankton Research* 27 (4), pp. 313–321. DOI: 10.1093/plankt/fbi011.

Irigoien, X, TA Klevjer, A Røstad, U Martinez, G Boyra, JL Acuña, A Bode, F Echevarria, JI Gonzalez-Gordillo, S Hernandez-Leon, S Agusti, DL Aksnes, CM Duarte, and S Kaartvedt (2014). "Large mesopelagic fishes biomass and trophic efficiency in the open ocean". In: *Nature Communications* 5 (1), p. 3271. DOI: 10.1038/ncomms4271.

Jahncke, J, DM Checkley, and GL Hunt (2004). "Trends in carbon flux to seabirds in the Peruvian upwelling system: effects of wind and fisheries on population regulation". In: *Fisheries Oceanography* 13 (3), pp. 208–223. DOI: 10.1111/j.1365-2419.2004.00283.x.

Jennings, S, SPR Greenstreet, and JD Reynolds (1999). "Structural change in an exploited fish community: a consequence of differential fishing effects on species with contrasting life histories". In: *Journal of Animal Ecology* 68 (3), pp. 617–627. DOI: https://doi.org/10.1046/j.1365-2656.1999.00312.x.

José, YS, L Stramma, S Schmidtko, and A Oschlies (2019). "ENSO-driven fluctuations in oxygen supply and vertical extent of oxygen-poor waters in the oxygen minimum zone of the Eastern Tropical South Pacific". In: *Biogeosciences Discussions* 2019, pp. 1–20. DOI: 10.5194/bg-2019-155.

José, YS, H Dietze, and A Oschlies (2017). "Linking diverse nutrient patterns to different water masses within anticyclonic eddies in the upwelling system off Peru". In: *Biogeosciences* 14 (6), pp. 1349–1364. DOI: 10.5194/gmd-10-127-2017.

Kalvelage, T, G Lavik, P Lam, S Contreras, L Arteaga, CR Löscher, A Oschlies, A Paulmier, L Stramma, and MMM Kuypers (2013). "Nitrogen cycling driven by organic matter export in the South Pacific oxygen minimum zone". In: *Nature Geoscience* 6 (3), pp. 228–234. DOI: 10.1038/ngeo1739.

Karstensen, J, L Stramma, and M Visbeck (2008). "Oxygen minimum zones in the eastern tropical Atlantic and Pacific oceans". In: *Progress in Oceanography* 77 (4). A New View of Water Masses After WOCE. A Special Edition for Professor Matthias Tomczak, pp. 331–350. ISSN: 0079-6611. DOI: 10.1016/j.pocean.2007.05.009.

Karstensen, J and O Ulloa (2009). "Peru–Chile Current System". In: *Encyclopedia of Ocean Sciences*. Elsevier. Chap. Peru-Chile Current System, pp. 385–392. ISBN: 9780123744739. DOI: 10.1016/B978-012374473-9.00599-3.

Keller, DP, A Oschlies, and M Eby (2012). "A new marine ecosystem model for the University of Victoria Earth System Climate Model". In: *Geoscientific Model Development* 5 (5), pp. 1195–1220. DOI: 10.5194/gmd-5-1195-2012.

Kiko, R, P Brandt, S Christiansen, J Faustmann, I Kriest, E Rodrigues, F Schütte, and H Hauss (2020). "Zooplankton-Mediated Fluxes in the Eastern Tropical North Atlantic". In: *Frontiers in Marine Science* 7, p. 358. ISSN: 2296-7745. DOI: 10.3389/fmars.2020.00358.

Kiko, R and H Hauss (2019). "On the Estimation of Zooplankton-Mediated Active Fluxes in Oxygen Minimum Zone Regions". In: *Frontiers in Marine Science* 6, p. 741. ISSN: 2296-7745. DOI: 10.3389/fmars.2019.00741.

Kiko, R, H Hauss, M Dengler, S Sommer, and F Melzner (2015). "The squat lobster *Pleuroncodes monodon* tolerates anoxic "dead zone" conditions off Peru". In: *Marine Biology* 162 (9), pp. 1913–1921. DOI: 10.1007/s00227-015-2709-6.

Kiørboe, T (2013). "Zooplankton body composition". In: *Limnology and Oceanography* 58 (5), pp. 1843–1850. DOI: 10.4319/lo.2013.58.5.1843. eprint: https://aslopubs.onlinelibrary.wiley.com/doi/pdf/10.4319/lo.2013.58.5.1843.

Kirby, MX (2004). "Fishing down the coast: Historical expansion and collapse of oyster fisheries along continental margins". In: *Proceedings of the National Academy of Sciences* 101 (35), pp. 13096–13099. DOI: 10.1073/pnas.0405150101.

Kishi, MJ, M Kashiwai, DM Ware, BA Megrey, DL Eslinger, FE Werner, M Noguchi-Aita, T Azumaya, M Fujii, S Hashimoto, et al. (2007). "NEMURO—a lower trophic level model for the North Pacific marine ecosystem". In: *Ecological Modelling* 202 (1-2), pp. 12–25.

Koné, V, E Machu, P Penven, V Andersen, V Garçon, P Fréon, and H Demarcq (2005). "Modeling the primary and secondary productions of the southern Benguela upwelling system: A comparative study through two biogeochemical models". In: *Global Biogeochemical Cycles* 19 (4), GB4021. DOI: 10.1029/2004GB002427.

Kriest, I and A Oschlies (2015). "MOPS-1.0: towards a model for the regulation of the global oceanic nitrogen budget by marine biogeochemical processes". In: *Geoscientific Model Development* 8 (9), pp. 2929–2957. DOI: 10.5194/gmd-8-2929-2015.

Kriest, I, V Sauerland, S Khatiwala, A Srivastav, and A Oschlies (2017). "Calibrating a global three-dimensional biogeochemical ocean model (MOPS-1.0)". In: *Geoscientific Model Development* 10 (1), pp. 127–154. DOI: 10.5194/gmd-10-127-2017.

Krumhardt, KM, NS Lovenduski, MC Long, and K Lindsay (2017). "Avoidable impacts of ocean warming on marine primary production: Insights from the CESM ensembles". In: *Global Biogeochemical Cycles* 31 (1), pp. 114–133. DOI: 10.1002/2016GB005528.

Kwiatkowski, L, O Torres, L Bopp, O Aumont, M Chamberlain, JR Christian, JP Dunne, M Gehlen, T Ilyina, JG John, A Lenton, H Li, NS Lovenduski, JC Orr, J Palmieri, Y Santana-Falcón, J Schwinger, R Séférian, CA Stock, A Tagliabue, Y Takano, J Tjiputra, K Toyama, H Tsujino, M Watanabe, A Yamamoto, A Yool, and T Ziehn (2020). "Twenty-first century ocean warming, acidification, deoxygenation, and upper-ocean nutrient and primary production decline from CMIP6 model projections". In: *Biogeosciences* 17 (13), pp. 3439–3470. DOI: 10.5194/bg-17-3439-2020.

Lama, R López de la, S de la Puente, JC Sueiro, and KMA Chan (2021). "Reconnecting with the past and anticipating the future: A review of fisheries-derived cultural ecosystem services in pre-Hispanic Peru". In: *People and Nature* 3 (1), pp. 129–147. DOI: [10.1002/pan3.10153](10.1002/pan3.10153).

Landry, M Ondrusek, S Tanner, S Brown, J Constantinou, R Bidigare, K Coale, and S Fitzwater (2000). "Biological response to iron fertilization in the eastern equatorial Pacific (IronEx II). I. Microplankton community abundances and biomass". In: *Marine Ecology Progress Series* 201, pp. 27–42. DOI: 10.3354/meps201027.

Lavery, TJ, B Roudnew, P Gill, J Seymour, L Seuront, G Johnson, JG Mitchell, and V Smetacek (2010). "Iron defecation by sperm whales stimulates carbon export in the Southern Ocean". In: *Proceedings of the Royal Society B: Biological Sciences* 277 (1699), pp. 3527–3531. DOI: 10.1098/rspb.2010.0863.

Lehette, P and S Hernández-León (2009). "Zooplankton biomass estimation from digitized images: a comparison between subtropical and Antarctic organisms". In: *Limnology and Oceanography: Methods* 7 (4), pp. 304–308. DOI: [10.4319/lom.2009.7.304](10.4319/lom.2009.7.304). eprint: https://aslopubs.onlinelibrary.wiley.com/doi/pdf/10.4319/lom.2009.7.304.

Lehodey, P, F Chai, and J Hampton (2003). "Modelling climate-related variability of tuna populations from a coupled ocean–biogeochemical-populations dynamics model". In: *Fisheries Oceanography* 12 (4-5), pp. 483–494. DOI: [10.1046/j.1365-2419.2003.00244.x](10.1046/j.1365-2419.2003.00244.x).

Lett, C, P Verley, C Mullon, C Parada, T Brochier, P Penven, and B Blanke (2008). "A Lagrangian tool for modelling ichthyoplankton dynamics". In: *Environmental Modelling & Software* 23 (9), pp. 1210–1214. ISSN: 1364-8152. DOI: 10.1016/j.envsoft.2008.02.005.

Lima, ID and SC Doney (2004). "A three-dimensional, multinutrient, and size-structured ecosystem model for the North Atlantic". In: *Global Biogeochemical Cycles* 18 (3), GB3019. DOI: [10.1029/2003GB002146](10.1029/2003GB002146). eprint: https://agupubs.onlinelibrary.wiley.com/doi/pdf/10.1029/2003GB002146.

Lima, ID, DB Olson, and SC Doney (2002). "Intrinsic dynamics and stability properties of size-structured pelagic ecosystem models". In: *Plankton Research* 24, pp. 533–556. DOI: 10.1093/plankt/24.6.533.

Lingen, C van der, L Hutchings, and J Field (2006). "Comparative trophodynamics of anchovy Engraulis encrasicolus and sardine Sardinops sagax in the southern Benguela: are species alternations between small pelagic fish trophodynamically mediated?" In: *African Journal of Marine Science* 28 (3-4), pp. 465–477. DOI: 10.2989/18142320609504199.

Link, JS, A Bundy, WJ Overholtz, N Shackell, J Manderson, D Duplisea, J Hare, M Koen-Alonso, and KD Friedland (2011). "Ecosystem-based fisheries management in the Northwest Atlantic". In: *Fish and Fisheries* 12 (2), pp. 152–170. DOI: 10.1111/j.1467-2979.2011.00411.x. eprint: https://onlinelibrary.wiley.com/doi/pdf/10.1111/j.1467-2979.2011.00411.x.

Liu, WT, W Tang, and PS Polito (1998). "NASA scatterometer provides global ocean-surface wind fields with more structures than numerical weather prediction". In: *Geophysical Research Letters* 25 (6), pp. 761–764. DOI: 10.1029/98GL00544.

Lluch-Belda, D, RJM Crawford, T Kawasaki, AD MacCall, RH Parrish, RA Schwartzlose, and PE Smith (1989). "World-wide fluctuations of sardine and anchovy stocks: the regime problem". In: *South African Journal of Marine Science* 8 (1), pp. 195–205. DOI: 10.2989/02577618909504561.

Lynam, CP, M Llope, C Möllmann, P Helaouët, GA Bayliss-Brown, and NC Stenseth (2017). "Interaction between top-down and bottom-up control in marine food webs". In: *Proceedings of the National Academy of Sciences* 114 (8), pp. 1952–1957. DOI: 10.1073/pnas.1621037114.

Maar, M, M Butenschön, U Daewel, A Eggert, W Fan, SS Hjøllo, M Hufnagl, M Huret, R Ji, G Lacroix, MA Peck, H Radtke, S Sailley, M Sinerchia, MD Skogen, M Travers-Trolet, TA Troost, and K van de Wolfshaar (2018). "Responses of summer phytoplankton biomass to changes in top-down forcing: Insights from comparative modelling". In: *Ecological Modelling* 376, pp. 54–67. ISSN: 0304-3800. DOI: 10.1016/j.ecolmodel.2018.03.003.

MacCall, AD (2002). "Fishery-Management and Stock-Rebuilding Prospects Under Conditions of Low-frequency Environmental Variability and Species Interactions". In: *Bulletin of Marine Science* 70 (2), pp. 613–628. ISSN: 0007-4977. URL: https://www.ingentaconnect.com/content/umrsmas/bullmar/2002/00000070/00000002/art00015 (visited on May 19, 2022).

Maguire, JJ, M Sissenwine, J Csirke, R Grainger, and S Garcia (2006). *The state of world highly migratory, straddling and other high seas fishery resources and associated species*. Rome: Food and Agriculture Organization of the United Nations. FAO Fisheries Technical Paper 495.

Majluf, P and J Reyes (1989). "The Marine Mammals of Peru: A Review". In: *The Peruvian upwelling ecosystem: dynamics and interactions. ICLARM Conference Proceedings 18*. Ed. by D Pauly, P Muck, J Mendo, and I Tsukayama. Instituto del Mar del Peru (IMARPE) Callao, Peru; Deutsche Gesellschaft fuer Technische Zusammenarbeit (GIZ), GmbH, Eschbom, Federal Republic of Germany; and International Center for Living Aquatic Resources Management (ICLARM), Manila Philippines.

Malik, A, PJ Nowack, JD Haigh, L Cao, L Atique, and Y Plancherel (2020). "Tropical Pacific climate variability under solar geoengineering: impacts on ENSO extremes". In: *Atmospheric Chemistry and Physics* 20 (23), pp. 15461–15485. DOI: 10.5194/acp-20-15461-2020.

Mann, KH (1984). "Fish Production in Open Ocean Ecosystems". In: *Flows of Energy and Materials in Marine Ecosystems: Theory and Practice*. Ed. by MJR Fasham. Boston, MA: Springer US, pp. 435–458. ISBN: 978-1-4757-0387-0. DOI: 10.1007/978-1-4757-0387-0_17.

Marasco, RJ, D Goodman, CB Grimes, PW Lawson, AE Punt, and TJ Quinn (2007). "Ecosystem–based fisheries management: some practical suggestions". In: *Canadian Journal of Fisheries and Aquatic Sciences* 64 (6), pp. 928–939. DOI: 10.1139/f07-062.

Markaida, U and O Sosa-Nishizaki (2003). "Food and feeding habits of jumbo squid Dosidicus gigas (Cephalopoda: Ommastrephidae) from the Gulf of California, Mexico". In: *Journal of the Marine Biological Association of the United Kingdom* 83 (3), pp. 507–522. DOI: 10.1017/S0025315403007434h.

Martin, A, P Boyd, K Buesseler, I Cetinic, H Claustre, S Giering, S Henson, X Irigoien, I Kriest, L Memery, et al. (2020). "The oceans' twilight zone must be studied now, before it is too late". In: *Nature* 580. ISSN: 0028-0836. DOI: 10.1038/d41586-020-00915-7.

Marzloff, M, YJ Shin, J Tam, M Travers, and A Bertrand (2009). "Trophic structure of the Peruvian marine ecosystem in 2000-2006: Insights on the effects of management scenarios for the hake fishery using the IBM trophic model Osmose". In: *Journal of*

Marine Systems 75 (1-2), pp. 290–304. ISSN: 0924-7963. DOI: 10.1016/j.jmarsys.2008.10.009.

Maselko, J, KR Andrews, and PA Hohenlohe (2020). "Long-lived marine species may be resilient to environmental variability through a temporal portfolio effect". In: *Ecology and Evolution* 10 (13), pp. 6435–6448. DOI: [10.1002/ece3.6378](10.1002/ece3.6378). eprint: https://onlinelibrary.wiley.com/doi/pdf/10.1002/ece3.6378.

Maury, O (2010). "An overview of APECOSM, a spatialized mass balanced "Apex Predators ECOSystem Model" to study physiologically structured tuna population dynamics in their ecosystem". In: *Progress in Oceanography* 84 (1). Special Issue: Parameterisation of Trophic Interactions in Ecosystem Modelling, pp. 113–117. ISSN: 0079-6611. DOI: 10.1016/j.pocean.2009.09.013.

McInturf, AG, L Pollack, LH Yang, and O Spiegel (2019). "Vectors with autonomy: what distinguishes animal-mediated nutrient transport from abiotic vectors?" In: *Biological Reviews* 94 (5), pp. 1761–1773. DOI: [10.1111/brv.12525](10.1111/brv.12525).

Megrey, BA, KA Rose, RA Klumb, DE Hay, FE Werner, DL Eslinger, and SL Smith (2007). "A bioenergetics-based population dynamics model of Pacific herring (Clupea harengus pallasi) coupled to a lower trophic level nutrient–phytoplankton–zooplankton model: Description, calibration, and sensitivity analysis". In: *Ecological Modelling* 202 (1). Special Issue on NEMURO (North Pacific Ecosystem Model for Understanding Regional Oceanography) and NEMURO.FISH (NEMURO for Including Saury and Herring), pp. 144–164. ISSN: 0304-3800. DOI: 10.1016/j.ecolmodel.2006.08.020.

Messié, M and FP Chavez (2015). "Seasonal regulation of primary production in eastern boundary upwelling systems". In: *Progress in Oceanography* 134, pp. 1–18. ISSN: 0079-6611. DOI: 10.1016/j.pocean.2014.10.011.

Mitra, A, C Castellani, WC Gentleman, SH Jónasdóttir, KJ Flynn, A Bode, C Halsband, P Kuhn, P Licandro, MD Agersted, et al. (2014). "Bridging the gap between marine biogeochemical and fisheries sciences; configuring the zooplankton link". In: *Progress in Oceanography* 129, pp. 176–199. DOI: 10.1016/j.pocean.2014.04.025.

Möllmann, C, B Müller-Karulis, G Kornilovs, and MA St John (2008). "Effects of climate and overfishing on zooplankton dynamics and ecosystem structure: regime

shifts, trophic cascade, and feedback loops in a simple ecosystem". In: *ICES Journal of Marine Science* 65 (3), pp. 302–310. ISSN: 1054-3139. DOI: 10.1093/icesjms/fsm197.

Moriarty, R and TD O'Brien (2013). "Distribution of mesozooplankton biomass in the global ocean". In: *Earth System Science Data* 5 (1), pp. 45–55. DOI: 10.5194/essd-5-45-2013.

Moullec, F, N Barrier, S Drira, F Guilhaumon, P Marsaleix, S Somot, C Ulses, L Velez, and YJ Shin (2019a). "An End-to-End Model Reveals Losers and Winners in a Warming Mediterranean Sea". In: *Frontiers in Marine Science* 6, p. 345. ISSN: 2296-7745. DOI: 10.3389/fmars.2019.00345.

Moullec, F, L Velez, P Verley, N Barrier, C Ulses, P Carbonara, A Esteban, C Follesa, M Gristina, A Jadaud, A Ligas, EL Díaz, P Maiorano, P Peristeraki, MT Spedicato, I Thasitis, M Valls, F Guilhaumon, and YJ Shin (2019b). "Capturing the big picture of Mediterranean marine biodiversity with an end-to-end model of climate and fishing impacts". In: *Progress in Oceanography* 178, p. 102179. ISSN: 0079-6611. DOI: 10.1016/j.pocean.2019.102179.

Muck Peter, DP (1987). "Monthly Anchoveta Consumption of Guano Birds, 1953 to l982". In: *The Peruvian anchoveta and its upwelling ecosystem: three decades of change. ICLARM Studies and Reviews 15*. Ed. by D Pauly and I Tsukayama. Instituto del Mar del Peru (IMARPE) Callao, Peru; Deutsche Gesellschaft fuer Technische Zusammenarbeit (GIZ), GmbH, Eschbom, Federal Republic of Germany; and International Center for Living Aquatic Resources Management (ICLARM), Manila Philippines.: Instituto del Mar del Peru (IMARPE) Callao, Peru; Deutsche Gesellschaft fuer Technische Zusammenarbeit (GIZ), GmbH, Eschbom, Federal Republic of Germany; and International Center for Living Aquatic Resources Management (ICLARM), Manila Philippines., pp. 219–233.

Muck, P, B Rojas de Mendiola, and E Antonietti (1989). "Comparative studies on feeding in larval anchoveta (Engraulis ringens) and sardine (Sardinops sagax)". In: *The Peruvian Upwelling Ecosystem: Dynamics and Interactions*. Vol. 18. International Center for Living Resources Manila, Philippines, pp. 86–96.

Mullin, MM (1975). "An experimentalist's view of zooplankton models". In: *CalCOFI reports* 18, pp. 132–135.

Murphy, GI (1961). *Oceanography and variations in the Pacific sardine population*. Tech. rep., pp. 55–64.

Nakai, Z, S Usami, S Hattori, Y Honjo, and S Hayashi (1955). *Progress report of the cooperative Iwashi resources investigations*. Tokai Regional Fisheries Research Laboratory.

NASA Goddard Space Flight Center, Ocean Ecology Laboratory, Ocean Biology Processing Group (2018). *Moderate-resolution Imaging Spectroradiometer (MODIS) Aqua Chlorophyll Data; 2018 Reprocessing*. URL: https://oceancolor.gsfc.nasa.gov/data/10.5067/AQUA/MODIS/L3M/CHL/2018/ (visited on Oct. 28, 2021).

Neubert, MG, T Klanjscek, and H Caswell (2004). "Reactivity and transient dynamics of predator–prey and food web models". In: *Ecological Modelling* 179 (1), pp. 29–38. ISSN: 0304-3800. DOI: 10.1016/j.ecolmodel.2004.05.001.

Ñiquen Carranza, M, M Bouchon Corrales, S Cahuín Villanueva, and E Díaz Acuña (2000). *Pesquería de anchoveta en el mar peruano. 1950 - 1999*. Instituto del Mar del Perú. Vol. 19.1-2, pp. 117–123. URL: https://hdl.handle.net/20.500.12958/1003 (visited on May 19, 2022).

Ñiquen Carranza, M, A Echevarría Cazorla, S Cahuín Villanueva, M Bouchon Corrales, J Mori Ponce, and S Arrieta (1999). *Situación de la anchoveta y otros recursos pelágicos en el mar peruano a fines de 1998. Crucero BIC José Olaya Balandra 9811-12*. Instituto del Mar del Perú. Informe IMARPE 146, pp. 39–48. URL: https://repositorio.imarpe.gob.pe/handle/20.500.12958/1571 (visited on May 19, 2022).

O'Brien, T and R Moriarty (2012). *Global distributions of mesozooplankton abundance and biomass - Gridded data product (NetCDF) - Contribution to the MAREDAT World Ocean Atlas of Plankton Functional Types*. data set. DOI: 10.1594/PANGAEA.785501.

Ohman, MD (1990). "The Demographic Benefits of Diel Vertical Migration by Zooplankton". In: *Ecological Monographs* 60 (3), pp. 257–281. DOI: 10.2307/1943058. eprint: https://esajournals.onlinelibrary.wiley.com/doi/pdf/10.2307/1943058.

Oliveros-Ramos, R (2014). "End–to–end modelling for an ecosystem approach to fisheries in the Northern Humboldt Current Ecosystem". PhD thesis. University of Montpellier.

Oliveros-Ramos, R and YJ Shin (2016). "Calibrar: an R package for fitting complex ecological models". In: *arXiv*. URL: https://arxiv.org/abs/1603.03141 (visited on May 19, 2022).

Oliveros-Ramos, R, P Verley, V Echevin, and YJ Shin (2017). "A sequential approach to calibrate ecosystem models with multiple time series data". In: *Progress in Oceanography* 151, pp. 227–244.

O'Reilly, JE, S Maritorena, BG Mitchell, DA Siegel, KL Carder, SA Garver, M Kahru, and C McClain (1998). "Ocean color chlorophyll algorithms for SeaWiFS". In: *Journal of Geophysical Research: Oceans* 103 (C11), pp. 24937–24953. DOI: 10.1029/98JC02160.

Paredes, CE and ME Gutierrez (2008). "The Peruvian Anchovy Sector: Costs and Benefits. An analysis of recent behavior and future challenges". In: *Proceedings of the Fourteenth Biennial Conference of the International Institute of Fisheries Economics & Trade, July 22-25, 2008, Nha Trang, Vietnam: Achieving a Sustainable Future: Managing Aquaculture, Fishing, Trade and Development*. Ed. by AL Shriver. Corvallis, Oregon, USA: International Institute of Fisheries Economics & Trade, p. 10. URL: https://ir.library.oregonstate.edu/concern/conference_proceedings_or_journals/6682x476j (visited on May 19, 2022).

Pauly, D, A Jarre, S Luna, V Sambilay, JB Rojas de Mendiola, and A Alamo (1989). "On the quantity and types of food ingested by Peruvian anchoveta, 1953–1982". In: *The Peruvian upwelling ecosystem: dynamics and interactions. ICLARM Conference Proceedings 18*. Ed. by D Pauly, P Muck, J Mendo, and I Tsukayama. Manila: Instituto del Mar del Peru (IMARPE) Callao, Peru; Deutsche Gesellschaft fuer Technische Zusammenarbeit (GIZ), GmbH, Eschbom, Federal Republic of Germany; and International Center for Living Aquatic Resources Management (ICLARM), Manila Philippines., pp. 109–124.

Pauly, D and M Soriano (1987). "Monthly Spawning Stock and Egg Production of Peruvian Anchoveta (Engraulis ringens), 1953 to 1982". In: *The Peruvian anchoveta and its upwelling ecosystem: three decades of change. ICLARM Studies and Reviews 15*. Ed. by D Pauly and I Tsukayama. Instituto del Mar del Peru (IMARPE) Callao, Peru; Deutsche Gesellschaft fuer Technische Zusammenarbeit (GIZ), GmbH, Eschbom, Federal Republic of Germany; and International Center for Living Aquatic Resources Management (ICLARM), Manila Philippines., pp. 167–178.

Pauly, D and I Tsukayama (1987a). "On the Implementation of Management-Oriented Fishery Research: the Case of the Peruvian Anchoveta". In: *The Peruvian anchoveta and its upwelling ecosystem: three decades of change. ICLARM Studies and Reviews 15*. Ed. by D Pauly and I Tsukayama. Instituto del Mar del Peru (IMARPE) Callao, Peru; Deutsche Gesellschaft fuer Technische Zusammenarbeit (GIZ), GmbH, Eschbom, Federal Republic of Germany; and International Center for Living Aquatic Resources Management (ICLARM), Manila Philippines., pp. 1–13.

Pauly, D, AC Vildoso, J Mejia, M Samame, and ML Palomares (1987). "Population Dynamics and Estimated Anchoveta Consumption of Bonito (Sarda chiliensis) off Peru". In: *The Peruvian anchoveta and its upwelling ecosystem: three decades of change. ICLARM Studies and Reviews 15*. Ed. by D Pauly and I Tsukayama. Instituto del Mar del Peru (IMARPE) Callao, Peru; Deutsche Gesellschaft fuer Technische Zusammenarbeit (GIZ), GmbH, Eschbom, Federal Republic of Germany; and International Center for Living Aquatic Resources Management (ICLARM), Manila Philippines., pp. 325–342.

Pauly, D and I Tsukayama, eds. (1987b). *The Peruvian anchoveta and its upwelling ecosystem: three decades of change. ICLARM Studies and Reviews 15*. Instituto del Mar del Peru (IMARPE) Callao, Peru; Deutsche Gesellschaft fuer Technische Zusammenarbeit (GIZ), GmbH, Eschbom, Federal Republic of Germany; and International Center for Living Aquatic Resources Management (ICLARM), Manila Philippines.

Penven, P, V Echevin, J Pasapera, F Colas, and J Tam (2005). "Average circulation, seasonal cycle, and mesoscale dynamics of the Peru Current System: A modeling approach". In: *Journal of Geophysical Research: Oceans* 110 (C10021), pp. 1–21. DOI: 10.1029/2005JC002945.

Penven, P (2019). *Croco Tools*. Version 1.1. URL: https://gitlab.inria.fr/croco-ocean/croco_tools/-/blob/master/Visualization_tools/ (visited on Oct. 28, 2021).

Penven, P, C Roy, G Brundrit, AC De Verdière, P Fréon, A Johnson, J Lutjeharms, and F Shillington (2001). "A regional hydrodynamic model of upwelling in the Southern Benguela". In: *South African Journal of Science* 97 (11-12), pp. 472–475.

Péron, G, J François Mittaine, and B Le Gallic (2010). "Where do fishmeal and fish oil products come from? An analysis of the conversion ratios in the global fish-

meal industry". In: *Marine Policy* 34 (4). Coping with global change in marine social-ecological systems, pp. 815–820. ISSN: 0308-597X. DOI: 10.1016/j.marpol.2010.01.027.

Pikitch, EK, C Santora, EA Babcock, A Bakun, R Bonfil, DO Conover, P Dayton, P Doukakis, D Fluharty, B Heneman, ED Houde, J Link, PA Livingston, M Mangel, MK McAllister, J Pope, and KJ Sainsbury (2004). "Ecosystem-Based Fishery Management". In: *Science* 305 (5682), pp. 346–347. ISSN: 0036-8075. DOI: 10.1126/science.1098222. eprint: https://science.sciencemag.org/content/305/5682/346.full.pdf.

Pizarro, J (2015). "Interacción del hombre con la fauna marina en la Región Tacna". In: *Foro "Día nacional de la biodiversidad: diversas opciones hoy para un mañana sostenible"*.

Pizarro, J, F Docmac, and C Harrod (2019). "Clarifying a trophic black box: stable isotope analysis reveals unexpected dietary variation in the Peruvian anchovy *Engraulis ringens*". In: *PeerJ* 7, e6968. ISSN: 2167-8359. DOI: 10.7717/peerj.6968.

PRODUCE (2013). *Anuario Estadístico Pesquero y Acuicola 2012*. Lima, Peru: Ministerio de la Producción - PRODUCE. URL: https://sinia.minam.gob.pe/documentos/anuario-estadistico-pesquero-acuicola-2012 (visited on May 19, 2022).

Prosekov, AY and SA Ivanova (2018). "Food security: The challenge of the present". In: *Geoforum* 91, pp. 73–77. ISSN: 0016-7185. DOI: 10.1016/j.geoforum.2018.02.030.

Prowe, AF, M Pahlow, S Dutkiewicz, M Follows, and A Oschlies (2012). "Top-down control of marine phytoplankton diversity in a global ecosystem model". In: *Progress in Oceanography* 101 (1), pp. 1–13. ISSN: 0079-6611. DOI: 10.1016/j.pocean.2011.11.016.

Remsen, A, TL Hopkins, and S Samson (2004). "What you see is not what you catch: a comparison of concurrently collected net, Optical Plankton Counter, and Shadowed Image Particle Profiling Evaluation Recorder data from the northeast Gulf of Mexico". In: *Deep Sea Research Part I: Oceanographic Research Papers* 51 (1), pp. 129–151. ISSN: 0967-0637. DOI: [10.1016/j.dsr.2003.09.008](10.1016/j.dsr.2003.09.008).

Reyes, JC, JG Mead, and KV Waerebeek (1991). "A new species of beaked whales *Mesoplodon peruvianus* sp. n. (cetacea: ziphiidae) from Peru". In: *Marine Mammal Science* 7 (1), pp. 1–24. DOI: [10.1111/j.1748-7692.1991.tb00546.x](10.1111/j.1748-7692.1991.tb00546.x).

Ridgway, K, J Dunn, and J Wilkin (2002). "Ocean interpolation by four-dimensional weighted least squares—Application to the waters around Australasia". In: *Journal of*

atmospheric and oceanic technology 19 (9), pp. 1357–1375. DOI: 10.1175/1520-0426(2002) 019⟨1357:OIBFDW⟩2.0.CO;2.

Rose, KA, JI Allen, Y Artioli, M Barange, J Blackford, F Carlotti, R Cropp, U Daewel, K Edwards, K Flynn, SL Hill, R HilleRisLambers, G Huse, S Mackinson, B Megrey, A Moll, R Rivkin, B Salihoglu, C Schrum, L Shannon, YJ Shin, SL Smith, C Smith, C Solidoro, MS John, and M Zhou (2010). "End-To-End Models for the Analysis of Marine Ecosystems: Challenges, Issues, and Next Steps". In: *Marine and Coastal Fisheries* 2 (1), pp. 115–130. DOI: 10.1577/C09-059.1.

Rose, KA, J Fiechter, EN Curchitser, K Hedstrom, M Bernal, S Creekmore, A Haynie, S ichi Ito, S Lluch-Cota, BA Megrey, CA Edwards, D Checkley, T Koslow, S McClatchie, F Werner, A MacCall, and V Agostini (2015). "Demonstration of a fully-coupled end-to-end model for small pelagic fish using sardine and anchovy in the California Current". In: *Progress in Oceanography* 138. Combining Modeling and Observations to Better Understand Marine Ecosystem Dynamics, pp. 348–380. ISSN: 0079-6611. DOI: 10.1016/j.pocean.2015.01.012.

Rossi, V, C López, E Hernández-García, J Sudre, V Garçon, and Y Morel (2009). "Surface mixing and biological activity in the four Eastern Boundary Upwelling Systems". In: *Nonlinear Processes in Geophysics* 16 (4), pp. 557–568. DOI: 10.5194/npg-16-557-2009.

Roy, C (1993). "The optimal environmental window hypothesis: A non linear environmental process affecting recruitment success". In: *ICES Journal of Marine Science* 76, pp. 1–13.

Rykaczewski, RR and DM Checkley (2008). "Influence of ocean winds on the pelagic ecosystem in upwelling regions". In: *Proceedings of the National Academy of Sciences* 105 (6), pp. 1965–1970. ISSN: 0027-8424. DOI: 10.1073/pnas.0711777105. eprint: https://www.pnas.org/content/105/6/1965.full.pdf.

Ryther, JH (1969). "Photosynthesis and fish production in the sea". In: *Science* 166 (3901), pp. 72–76.

Saha, S, S Moorthi, HL Pan, X Wu, J Wang, S Nadiga, P Tripp, R Kistler, J Woollen, D Behringer, H Liu, D Stokes, R Grumbine, G Gayno, J Wang, YT Hou, H ya Chuang, HMH Juang, J Sela, M Iredell, R Treadon, D Kleist, PV Delst, D Keyser, J Derber, M Ek, J Meng, H Wei, R Yang, S Lord, H van den Dool, A Kumar, W Wang, C Long,

M Chelliah, Y Xue, B Huang, JK Schemm, W Ebisuzaki, R Lin, P Xie, M Chen, S Zhou, W Higgins, CZ Zou, Q Liu, Y Chen, Y Han, L Cucurull, RW Reynolds, G Rutledge, and M Goldberg (2010). "The NCEP Climate Forecast System Reanalysis". In: *Bulletin of the American Meteorological Society* 91 (8), pp. 1015–1058. DOI: 10.1175/2010BAMS3001.1.

Salvatteci, R and J Mendo (2005). "Estimación de las pérdidas bio-económicas causadas por la captura de juveniles de anchoveta (Engraulis ringens, J.) en la costa peruana". es. In: *EcologÃa Aplicada* 4, pp. 113–120. ISSN: 1726-2216. URL: http://www.scielo.org.pe/scielo.php?script=sci_arttext&pid=S1726-22162005000100015&nrm=iso (visited on May 19, 2022).

Salvatteci, R, RR Schneider, E Galbraith, D Field, T Blanz, T Bauersachs, X Crosta, P Martinez, V Echevin, F Scholz, and A Bertrand (2022). "Smaller fish species in a warm and oxygen-poor Humboldt Current system". In: *Science* 375 (6576), pp. 101–104. DOI: 10.1126/science.abj0270.

Saunders, RA, SL Hill, GA Tarling, and EJ Murphy (2019). "Myctophid Fish (Family Myctophidae) Are Central Consumers in the Food Web of the Scotia Sea (Southern Ocean)". In: *Frontiers in Marine Science* 6. ISSN: 2296-7745. DOI: 10.3389/fmars.2019.00530.

Scheffer, M, S Carpenter, and B de Young (2005). "Cascading effects of overfishing marine systems". In: *Trends in Ecology Evolution* 20 (11), pp. 579–581. ISSN: 0169-5347. DOI: 10.1016/j.tree.2005.08.018.

Schwartzlose, RA, J Alheit, A Bakun, TR Baumgartner, R Cloete, RJM Crawford, WJ Fletcher, Y Green-Ruiz, E Hagen, T Kawasaki, D Lluch-Belda, SE Lluch-Cota, AD MacCall, Y Matsuura, MO Nevárez-Martínez, RH Parrish, C Roy, R Serra, KV Shust, MN Ward, and JZ Zuzunaga (1999). "Worldwide large-scale fluctuations of sardine and anchovy populations". In: *South African Journal of Marine Science* 21 (1), pp. 289–347. DOI: 10.2989/025776199784125962.

Shannon, LJ, KL Cochrane, CL Moloney, and P Fréon (2004). "Ecosystem approach to fisheries management in the southern Benguela: a workshop overview". In: *African Journal of Marine Science* 26, pp. 1–8. ISSN: 1814-232X. DOI: 10.2989/18142320409504046.

Shchepetkin, AF and JC McWilliams (2005). "The regional oceanic modeling system (ROMS): a split-explicit, free-surface, topography-following-coordinate oceanic model". In: *Ocean modelling* 9 (4), pp. 347–404. DOI: 10.1016/j.ocemod.2004.08.002.

Shepherd, CJ and AJ Jackson (2013). "Global fishmeal and fish-oil supply: inputs, outputs and marketsa". In: *Journal of Fish Biology* 83 (4), pp. 1046–1066. DOI: 10.1111/jfb.12224.

Shimoda, AF and GB Arhonditsis (2016). "Phytoplankton functional type modelling: Running before we can walk? A critical evaluation of the current state of knowledge". In: *Ecological Modelling* 320, pp. 29–43. DOI: 10.1016/j.ecolmodel.2015.08.029.

Shin, YJ and P Cury (2001). "Exploring fish community dynamics through size-dependent trophic interactions using a spatialized individual-based model". In: *Aquatic Living Resources* 14 (2), pp. 65–80. DOI: 10.1016/S0990-7440(01)01106-8.

– (2004). "Using an individual-based model of fish assemblages to study the response of size spectra to changes in fishing". In: *Canadian Journal of Fisheries and Aquatic Sciences* 61 (3), pp. 414–431. DOI: 10.1139/f03-154.

Smith, ADM, CJ Brown, CM Bulman, EA Fulton, P Johnson, IC Kaplan, H Lozano-Montes, S Mackinson, M Marzloff, LJ Shannon, YJ Shin, and J Tam (2011). "Impacts of Fishing Low–Trophic Level Species on Marine Ecosystems". In: *Science* 333 (6046), pp. 1147–1150. ISSN: 0036-8075, 1095-9203. DOI: 10.1126/science.1209395.

Smith, VH and DW Schindler (2009). "Eutrophication science: where do we go from here?" In: *Trends in Ecology Evolution* 24 (4), pp. 201–207. ISSN: 0169-5347. DOI: 10.1016/j.tree.2008.11.009.

St. John, MA, A Borja, G Chust, M Heath, I Grigorov, P Mariani, AP Martin, and RS Santos (2016). "A Dark Hole in Our Understanding of Marine Ecosystems and Their Services: Perspectives from the Mesopelagic Community". In: *Frontiers in Marine Science* 3, p. 31. ISSN: 2296-7745. DOI: 10.3389/fmars.2016.00031.

Steele, JH and EW Henderson (1992). "The role of predation in plankton models". In: *Journal of Plankton Research* 14 (1), pp. 157–172. DOI: 10.1093/plankt/14.1.157.

Stock, CA, JP Dunne, and JG John (2014). "Global-scale carbon and energy flows through the marine planktonic food web: An analysis with a coupled physical–

biological model". In: *Progress in Oceanography* 120, pp. 1–28. ISSN: 0079-6611. DOI: 10.1016/j.pocean.2013.07.001.

Sueyoshi, EG, CR Moreno, DV Petre, MAM Torres, and DV Valencia (2016). *Aves marinas en el Perú*. Callao, Peru: Instituto del Mar del Perú. Serie de Divulgación Científica vol. 2.2.

Suntharalingam, P, J Sarmiento, and J Toggweiler (2000). "Global significance of nitrous-oxide production and transport from oceanic low-oxygen zones: A modeling study". In: *Global Biogeochemical Cycles* 14 (4), pp. 1353–1370. DOI: 10.1029/1999GB900100.

Suntharalingam, P, E Buitenhuis, C Le Quéré, F Dentener, C Nevison, JH Butler, HW Bange, and G Forster (2012). "Quantifying the impact of anthropogenic nitrogen deposition on oceanic nitrous oxide". In: *Geophysical Research Letters* 39 (7), p. L07605. DOI: 10.1029/2011GL050778.

Tacon, AGJ and M Metian (2009). "Fishing for Feed or Fishing for Food: Increasing Global Competition for Small Pelagic Forage Fish". In: *Ambio* 38 (6), pp. 294–302. ISSN: 00447447, 16547209. URL: http://www.jstor.org/stable/40390239 (visited on May 19, 2022).

Tam, J, MH Taylor, V Blaskovic, P Espinoza, R Michael Ballón, E Díaz, C Wosnitza-Mendo, J Argüelles, S Purca, P Ayón, L Quipuzcoa, D Gutiérrez, E Goya, N Ochoa, and M Wolff (2008). "Trophic modeling of the Northern Humboldt Current Ecosystem, Part I: Comparing trophic linkages under La Niña and El Niño conditions". In: *Progress in Oceanography* 79 (2). The Northern Humboldt Current System: Ocean Dynamics, Ecosystem Processes, and Fisheries, pp. 352–365. ISSN: 0079-6611. DOI: 10.1016/j.pocean.2008.10.007.

Tarazona, J and W Arntz (2001). "The Peruvian Coastal Upwelling System". In: *Coastal Marine Ecosystems of Latin America*. Ed. by U Seeliger and B Kjerfve. Berlin, Heidelberg: Springer Berlin Heidelberg, pp. 229–244. ISBN: 978-3-662-04482-7. DOI: 10.1007/978-3-662-04482-7_17.

Thomsen, S, T Kanzow, F Colas, V Echevin, G Krahmann, and A Engel (2016). "Do submesoscale frontal processes ventilate the oxygen minimum zone off Peru?" In: *Geophysical Research Letters* 43 (15), pp. 8133–8142. DOI: 10.1002/2016GL070548.

Tian, R, A Vézina, L Legendre, R Ingram, B Klein, T Packard, S Roy, C Savenkoff, N Silverberg, J Therriault, et al. (2000). "Effects of pelagic food-web interactions and nutrient remineralization on the biogeochemical cycling of carbon: a modeling approach". In: *Deep Sea Research Part II: Topical Studies in Oceanography* 47 (3-4), pp. 637–662. DOI: [10.1016/S0967-0645(99)00121-6](10.1016/S0967-0645(99)00121-6).

Tian, RC, AF Vézina, M Starr, and F Saucier (2001). "Seasonal dynamics of coastal ecosystems and export production at high latitudes: a modeling study". In: *Limnology and Oceanography* 46 (8), pp. 1845–1859. DOI: [10.4319/lo.2001.46.8.1845](10.4319/lo.2001.46.8.1845).

Tittensor, DP, TD Eddy, HK Lotze, ED Galbraith, W Cheung, M Barange, JL Blanchard, L Bopp, A Bryndum-Buchholz, M Büchner, C Bulman, D Carozza, V Christensen, M Coll, J Dunne, J Fernandes, E Fulton, A Hobday, V Huber, S Jennings, M Jones, P Lehodey, J Link, S Mackinson, O Maury, S Niiranen, R Oliveros-Ramos, T Roy, J Schewe, YJ Shin, T Silva, C Stock, J Steenbeek, P Underwood, J Volkholz, J Watson, and N Walker (2018). "A protocol for the intercomparison of marine fishery and ecosystem models: Fish-MIP v1. 0". In: *Geoscientific Model Development* 11 (4), pp. 1421–1442. DOI: [10.5194/gmd-11-1421-2018](10.5194/gmd-11-1421-2018).

Torrejón-Magallanes, J, D Grados, and W Lau-Medrano (2019). "Spatio-temporal distribution modeling of dolphinfish (*Coryphaena hippurus*) in the Pacific Ocean off Peru using artisanal longline fishery data". In: *Deep Sea Research Part II: Topical Studies in Oceanography* 169–170. Understanding changes in transitional areas of the Pacific Ocean, p. 104665. ISSN: 0967-0645. DOI: [10.1016/j.dsr2.2019.104665](10.1016/j.dsr2.2019.104665).

Tovar, H, V Guillen, and ME Nakama (1987). "Monthly Population Size of Three Guano Bird Species off Peru, 1953 to 1982". In: *The Peruvian anchoveta and its upwelling ecosystem: three decades of change. ICLARM Studies and Reviews 15*. Ed. by D Pauly and I Tsukayama. Instituto del Mar del Peru (IMARPE) Callao, Peru; Deutsche Gesellschaft fuer Technische Zusammenarbeit (GIZ), GmbH, Eschbom, Federal Republic of Germany; and International Center for Living Aquatic Resources Management (ICLARM), Manila Philippines., pp. 208–218.

Travers, M and YJ Shin (2010). "Spatio-temporal variability in fish-induced predation mortality on plankton: A simulation approach using a coupled trophic model of the Benguela ecosystem". In: *Progress in Oceanography* 84 (1). Special Issue: Parameterisation of Trophic Interactions in Ecosystem Modelling, pp. 118–120. ISSN: 0079-6611. DOI: 10.1016/j.pocean.2009.09.014.

Travers, M, YJ Shin, S Jennings, and P Cury (2007). "Towards end-to-end models for investigating the effects of climate and fishing in marine ecosystems". In: *Progress in Oceanography* 75 (4), pp. 751–770. ISSN: 0079-6611. DOI: 10.1016/j.pocean.2007.08.001.

Travers, M, YJ Shin, S Jennings, E Machu, J Huggett, J Field, and P Cury (2009). "Two-way coupling versus one-way forcing of plankton and fish models to predict ecosystem changes in the Benguela". In: *Ecological Modelling* 220 (21). Selected Papers from the Sixth European Conference on Ecological Modelling - ECEM '07, on Challenges for ecological modelling in a changing world: Global Changes, Sustainability and Ecosystem Based Management, November 27-30, 2007, Trieste, Italy, pp. 3089 –3099. ISSN: 0304-3800. DOI: 10.1016/j.ecolmodel.2009.08.016.

Travers, M (2009). "Couplage de modèles trophiques et effets combinés de la pêche et du climat, Coupling trophodynamic models for assessing the combined effects of fishing and climate". PhD thesis. Université Pierre et Marie Curie. URL: https://archimer.ifremer.fr/doc/00003/11445/ (visited on May 19, 2022).

Travers, M, YJ Shin, L Shannon, and P Cury (2006). "Simulating and testing the sensitivity of ecosystem-based indicators to fishing in the southern Benguela ecosystem". In: *Canadian Journal of Fisheries and Aquatic Sciences* 63 (4), pp. 943–956. DOI: 10.1139/f06-003. eprint: https://doi.org/10.1139/f06-003.

Travers-Trolet, M, Y Shin, and J Field (2014). "An end-to-end coupled model ROMS–N2P2Z2D2–OSMOSE of the southern Benguela foodweb: parameterisation, calibration and pattern-oriented validation". In: *African Journal of Marine Science* 36 (1), pp. 11–29. DOI: 10.2989/1814232X.2014.883326.

Travers-Trolet, M, YJ Shin, LJ Shannon, CL Moloney, and JG Field (2014). "Combined fishing and climate forcing in the southern Benguela upwelling ecosystem: an end-to-end modelling approach reveals dampened effects". In: *PloS one* 9 (4), e94286. DOI: 10.1371/journal.pone.0094286.

Tsikliras, AC and R Froese (2019). "Maximum Sustainable Yield". In: *Encyclopedia of Ecology*. Ed. by BD Fath. 2nd ed. Vol. 1. Elsevier, pp. 108–115. ISBN: 9780444641304. DOI: 10.1016/B978-0-12-409548-9.10601-3.

Varpe, Ø, Ø Fiksen, and A Slotte (2005). "Meta-ecosystems and biological energy transport from ocean to coast: the ecological importance of herring migration". In: *Oecologia* 146 (3), pp. 443–451. DOI: 10.1007/s00442-005-0219-9.

Vergnon, R, YJ Shin, and P Cury (2008). "Cultivation, Allee effect and resilience of large demersal fish populations". In: *Aquatic Living Resources* 21 (03), pp. 287–295. DOI: 10.1051/alr:2008042.

Watson, JR, CA Stock, and JL Sarmiento (2015). "Exploring the role of movement in determining the global distribution of marine biomass using a coupled hydrodynamic – Size-based ecosystem model, journal = Progress in Oceanography". In: 138. Combining Modeling and Observations to Better Understand Marine Ecosystem Dynamics, pp. 521–532. ISSN: 0079-6611. DOI: 10.1016/j.pocean.2014.09.001.

Williams, JJ, YP Papastamatiou, JE Caselle, D Bradley, and DMP Jacoby (2018). "Mobile marine predators: an understudied source of nutrients to coral reefs in an unfished atoll". In: *Proceedings of the Royal Society B: Biological Sciences* 285 (1875), p. 20172456. DOI: 10.1098/rspb.2017.2456.

Worley, SJ, SD Woodruff, RW Reynolds, SJ Lubker, and N Lott (2005). "ICOADS release 2.1 data and products". In: *International Journal of Climatology* 25 (7), pp. 823–842. DOI: 10.1002/joc.1166.

Worm, B, R Hilborn, JK Baum, TA Branch, JS Collie, C Costello, MJ Fogarty, EA Fulton, JA Hutchings, S Jennings, OP Jensen, HK Lotze, PM Mace, TR McClanahan, C Minto, SR Palumbi, AM Parma, D Ricard, AA Rosenberg, R Watson, and D Zeller (2009). "Rebuilding Global Fisheries". In: *Science* 325 (5940), pp. 578–585. DOI: 10.1126/science.1173146.

Worm, B and RA Myers (2003). "Meta-analysis of cod–shrimp interactions reveals top–down control in ocean food webs". In: *Ecology* 84 (1), pp. 162–173. DOI: 10.1890/0012-9658(2003)084[0162:MAOCSI]2.0.CO;2.

Xing, L, Z Chongliang, Y Chen, YJ Shin, P Verley, H Yu, and Y Ren (2017). "An individual-based model for simulating the ecosystem dynamics of Jiaozhou Bay, China". In: *Ecological Modelling* 360, pp. 120–131. DOI: 10.1016/j.ecolmodel.2017.06.010.

Xue, T, I Frenger, AEF Prowe, YS José, and A Oschlies (2021). "Mixed layer depth dominates over upwelling in regulating the seasonality of ecosystem functioning in the Peruvian Upwelling System". In: *Biogeosciences Discussions* 2021, pp. 1–29. DOI: 10.5194/bg-2021-113.

Yakushev, E, F Pollehne, G Jost, I Kuznetsov, B Schneider, and L Umlauf (2007). "Analysis of the water column oxic/anoxic interface in the Black and Baltic seas with a numerical model". In: *Marine Chemistry* 107 (3), pp. 388–410. DOI: 10.1016/j.marchem. 2007.06.003.

Yoshida, HO (1980). *Synopsis of Biological Data on Bonitos of the Genus Sarda*. U.S. Department of Commerce, National Oceanic and Atmospheric Administration, National Marine Fisheries Service. NOAA Technical Report NMFS Circular 432.

Web references

https://www.myroms.org (visited on Apr. 22, 2021)

http://www.sfb754.de (visited on May 3, 2021)

https://osmose-model.org (visited on Oct. 28, 2021)

https://github.com/osmose-model/osmose/tree/master/java (visited on Oct. 28, 2021)

http://documentation.osmose-model.org/index.html (visited on Oct. 28, 2021)

List of Figures

List of Tables

Abbreviation

AC	plankton accessibility coefficient parameter
APECOSM	Apex Predators ECOSystem Model
bgc	biogeochemical model(s)
BioEBUS	Biogeochemical model developed for Eastern Boundary Upwelling Systems
CROCO	Coastal and Regional Ocean COmmunity model
EBUS	eastern boundary upwelling systems
ENSO	El Niño–Southern Oscillation
ETSP	eastern tropical South Pacific
Gt	gigatonne
HTL	higher trophic levels (e.i., fish, macroinvertebrates and large marine predators)
IPCC	Intergovernmental Panel on Climate Change
LM	larval mortality parameter
LTL	lower trophic levels (e.i., plankton)
Mt	million tonnes
NHCS	northern-Humboldt Current System
OMZ	oxygen minimum zone
OSMOSE	Object-oriented Simulator of Marine Ecosystems
PISCES	Pelagic Interactions Scheme for Carbon and Ecosystem Studies
ROMS	Regional Ocean Modeling System
SST	sea surface temperature
WW	wet weight
yr	year

Glossary

benthic
located on the ocean floor

bottom–up effect
effect of a species or the environment on the trophic levels above. In a bottom–up controlled ecosystem, the environment and its impact on lower trophic levels drive the dynamics of the ecosystem

boundary conditions
fields used to force physical–biogeochemical models at their boundaries, for example, at the ocean–atmosphere interface or, in the case of regional models, at the edges of the model

dynamic model
model that simulates processes in a mechanistic way with a set of equations

end-to-end model
model of the marine ecosystem that includes from the plankton, affected by environmental drivers, to higher trophic levels such as fish

epipelagic
upper layer of the ocean between 0 and 200 m

higher trophic levels
organisms larger than zooplankton and up to whales that feed on plankton or any trophic level above. These include fish, macroinvertebrates and top predators.

landings
amount of fish in wet weight extracted from the system by fishing

lower trophic levels

plankton

mesopelagic

located in the region between 200 and 1000 m depth, also called the "twilight zone", below the epipelagic region

NPZD–type model

biogeochemical model simulating fluxes between nutrients (N), phytoplankton (P), zooplankton (Z) and detritus (D)

pelagic

floating in the water column. In contrast, benthic organisms sit on the ocean floor.

top–down effect

effect of a predator on the trophic levels below. In an ecosystem that is top–down controlled, top predators control the dynamics of the ecosystem

Mariana Hill Cruz

E-mail: mhill-cruz@geomar.de ⋄ LinkedIn: mariana-hill
ORCID: 0000-0001-7766-3492 ⋄ Personal website: oceanlizard.wordpress.com

Education and prizes

Doctorate in Natural Sciences *2018–2022*

Christian-Albrechts Universitat zu Kiel, *Germany*

MSc: Biological Oceanography *2016–2018*

Christian-Albrechts Universitat zu Kiel, *Germany*

Final grade: 1.1 (German scale), ECTS: A

BSc: Marine Science *2014–2015*

University of Western Australia, *Perth, Australia*

GPA: 6.877, WAM: 83.375 (Australian scale)

BMT Oceanica Consulting Marine Science Prize *2015*

Employment

GEOMAR Helmholtz Centre for Ocean Research Kiel *2018–2022*

Doctoral researcher

- Research on end-to-end modelling of marine ecosystems
- Coupling biogeochemical and fish models

Deutsche Gesellschaft fur Meeresforschung e.V. (DGM) *2020*

Member of the organisation team of the YOUMARES11 conference

GEOMAR Helmholtz Centre for Ocean Research Kiel *2017–2018*

Student job as Research Assistant "HiWi"

- Data analysis of a glider
- Compiling a database on bacteria growth efficiency

Languages

Spanish	mother tongue
English	fluent
German	B2

Computer skills

Basic tools and text processing	MS Office, LaTex, Markdown
Data analysis and visualisation	Python, R, Ferret, ArcGIS
Design and art	Affinity Photo and Designer, Lightroom, Final Cut Pro, Scribus, Procreate

Additional training

PADI Open Water Scuba Diver ◇ Whale sharks photo identification
Naturalistic illustration ◇ Written and visual science communication ◇ Leadership
Horseback riding ◇ Deep learning (AI)

Volunteering and fieldwork

Volunteering at NGOs including:

- CoalitionWILD	*2018–2019*
- Marine Mammals Research Association	*2018*
- Large Marine Vertebrates Research Institute Philippines	*2016*

Participation in research cruises to the Baltic Sea	*2016, 2017*

Fish sampling with BRUVs in Albany, Australia	*2015*

Public speaking

Scientific conferences:

- Ocean Sciences Meeting (OSM)	*2019, 2022*
- Advances in Marine Ecosystem Modelling Research (AMEMR)	*2021*
- ICES Working Group on Integrated Physical-biological and Ecological Modelling (WGIPEM) annual meeting	*2021*
- YOUMARES11 (organisation team and hosting the open session)	*2020*
- Australasian Conference of Undergraduate Research (ACUR)	*2015*

Simulations:

- KielMUN	*2020*
- Model Arctic Council	*2016, 2018*
- 2do Congreso Juvenil de las Américas	*2011*

Erklärung

Hiermit erkläre ich, dass die vorliegende Arbeit mit dem Titel: "From biogeochemistry to fisheries and back again: Modelling the upwelling ecosystem off Peru" von mir selbstständig angefertigt wurde. Bis auf zitierte Referenzen und Beratung meiner Betreuer wurden keine weiteren Quellen verwendet. Diese Arbeit ist unter Einhaltung der Regeln guter wissenschaftlicher Praxis der Deutschen Forschungsgemeinschaft entstanden. Sie wurde weder im Rahmen eines Prüfungsverfahrens an anderer Stelle vorgelegt noch veröffentlicht. Ich erkläre mich einverstanden, dass diese Arbeit an die Bibliothek des GEOMAR und die Universitätsbibliothek der CAU weitergeleitet wird.

Kiel, Mai 2022

_____

Mariana Hill Cruz